THERMODYNAMICS OF TERNARY SYSTEMS MgO-FeO-SiO_2 AND MgO-FeO-CaO AT 1000 K

A THESIS

submitted in fulfilment of the requirements
for the award of the degree
of
DOCTOR OF PHILOSOPHY
in
METALLURGICAL ENGINEERING

By

K. C. SHARMA

DEPARTMENT OF METALLURGICAL ENGINEERING
UNIVERSITY OF ROORKEE
ROORKEE-247667 (INDIA)

AUGUST, 1984

CANDIDATE'S DECLARATION

I hereby certify that the work which is being presented in the thesis entitled, "THERMODYNAMICS OF TERNARY SYSTEMS $MgO-FeO-SiO_2$ AND $MgO-FeO-CaO$ AT 1000 K", in fulfilment of the requirement for the award of the Degree of Doctor of Philosophy, submitted in the Department of Metallurgical Engineering of the University is an authentic record of my own work carried out during a period from ~~October 1980~~ Jan. 1979 to August 1984 under the supervision of Dr. M.L.Kapoor and Dr. R.D.Agrawal.

The matter embodied in this thesis has not been submitted by me for the award of any other degree.

KcSharma

(KRISHAN CHANDRA SHARMA)

This is to certify that the above statement made by the candidate is correct to the best of our knowledge.

Mlkapoor

(M.L.KAPOOR)
Professor
Department of Met. Engg.
University of Roorkee,
Roorkee (INDIA).

Agrawal

(R.D.AGRAWAL)
Reader
Department of Met. Engg.
University of Roorkee,
Roorkee (INDIA).

Dated: Aug. 16 , 1984.

ABSTRACT

Several natural and technological reactive and non-reactive multi-component systems such as slags encountered in different metal extraction or refining processes, refractories and building materials, dispersed phases of composite materials and molten magma, the parent rock material of the earth's crust constitute oxides like FeO, MgO, CaO, SiO_2 etc. Mutual interactions controlling the chemical reactivity and equilibrium phase assemblages among oxides, therefore, control the different slag-metal reactions involved in metal extraction and refining, behaviour of different type of refractories and mineralisation of rocks formed. Thermodynamic properties of oxide and silicate systems have, therefore, been extensively studied by metallurgists, materials scientists, geologists, ceramists and chemists.

The ternary systems MgO-FeO-SiO_2 and MgO-FeO-CaO and their corresponding binaries have special relevance to ferrous metallurgy. A survey of available literature reveals that although the binary FeO-MgO and FeO-CaO systems have been extensively studied for determination of thermodynamic properties and analysis of phase equilibria, the ternary systems FeO-MgO-SiO_2 and FeO-MgO-CaO have mostly been studied for phase equilibria.

In the present investigation, therefore, thermodynamic properties of the binary systems FeO-MgO, FeO-CaO and

$FeO-SiO_2$ and the ternary systems $FeO-MgO-SiO_2$ and $FeO-MgO-CaO$ are studied at 1000 K employing a calcia-stabilized zirconia solid electrolyte cell. For this purpose, a solid electrolyte cell operated in an inert atmosphere of dry, purified nitrogen, with the following cell scheme was locally fabricated,

$$Pt/\ Fe,\ \begin{matrix}\text{FeO containing}\\ \text{oxide System}\end{matrix}\ //\ (ZrO_2)_{0.85}(CaO)_{0.15}\ //Fe,FeO/\ Pt$$

From emf data, values of activity of FeO are calculated at different concentrations for slag samples studied. Using standard thermodynamic relationships, activities of other components and also the ΔG_{mix} and ΔG^{ex}_{mix} are calculated. Emf studies on the system $FeO-SiO_2$ permitted the calculation of standard free energy of formation of Fe_2SiO_4 from its component oxides. Lines of constant activity of FeO and other component oxides in different phase regions are drawn for the ternary systems studied. Properties of binary systems $FeSiO_3$-$MgSiO_3$ and Fe_2SiO_4-Mg_2SiO_4 are also computed and the values of standard free energy of formation for the compounds "$FeSiO_3$" and Fe_2SiO_4 are determined at 1000 K from the emf data on the ternary system $MgO-FeO-SiO_2$. In case of the ternary system MgO-FeO-CaO, isothermal section of phase diagram at 1000 K is drawn.

The entire text of the dissertation has been divided into six chapters.

Chapter 1 has been devoted to the brief introduction

to the problem, critical review of literature comprising of different techniques used to study the thermodynamic properties of alloy, oxide, silicate and other systems with emphasis on solid electrolyte technique, survey of available literature on various binary and ternary oxide and silicate systems and finally formulation of the problem.

Chapter 2 deals with the experimental set-up, materials used, sample preparation and technique adopted for experimentation for determination of thermodynamic properties of binary and ternary oxide systems.

Chapter 3 deals with the experimental results for the binary systems FeO-MgO, FeO-CaO and FeO-SiO_2. Activity and other thermodynamic properties are calculated from emf data and the present results are compared with the relevant data available in literature.

Chapter 4 deals with the experimental results for the ternary systems FeO-MgO-SiO_2 and FeO-MgO-CaO. Thermodynamic properties, calculated from emf data, are presented and compared, wherever possible, with the relevant data in literature.

Chapter 5 deals with the discussion of the results on binary and ternary oxide systems. Results on other similar systems from literature are presented for a comparison.

Finally, Chapter 6 lists the major conclusions drawn from the present investigation.

Assistance rendered by the technical and laboratory staff, Sarvasri S.R.Kaushik, S.B.Sharma, Rakesh Misra, B.D.Sharma, Abdul Razak and Rishipal during fabrication of experimental set-up and actual runs is also gratefully acknowledged.

But for the excellent draftsmanship of Sri M.C.Vaish and Sri Atma Prakash and meticulous typewriting of Sri U.K.Mishra and Sri Ram Gopal, the present shape of this thesis could not have been possible. The author expresses his very sincere appreciation of their efforts.

He would also like to record very sincerely and most humbly the continuous encouragement and kind support in all possible ways, he received from his parents during the entire period of research work and preparation of this dissertation.

Last, but not the least, the author would also express his sincere gratitude to several other friends and authors of research publications, who made available reprints of the papers not available locally.

KcSharma

(K.C.SHARMA)

Roorkee
Aug. 16 , 1984.

CONTENTS

ACKNOWLEDGEMENTS

The author wishes to record his deep sense of gratitude and indebtedness to Dr. M.L.Kapoor, Professor of Extractive Metallurgy, University of Roorkee, Roorkee, for not only suggesting the problem of the present investigation but also his timely, relentless and untiring assistance, able guidance as also the fruitful and constructive criticism during the entire period of experimentation and preparation of this dissertation. He would also like to record very sincerely and most humbly the valuable suggestions and fruitful discussions and criticism, he received from his co-supervisor, Dr. R.D.Agrawal, Reader, at this Department, to enable him to complete his investigation and prepare the dissertation in the form, it is presented now. The author also wishes to record his heartfelt indebtedness for the help rendered from time to time by Dr. V.N.S.Mathur, Reader in this Department, in preparation of the manuscript.

He is also thankful to Dr. M.L.Mehta, former Head of the Department and Dr. D.B.Goel, present Head of the Department, for providing necessary facilities to carry out the experimental work.

My friends Sarvasri S.K.Gupta, Sahab Prasad, N.C.Jain, S.K. Nath and Dr. K.S.Pandey have been source of constant encouragement due to their ready availability and all the help rendered at the different stages of preparation of this dissertation. The author expresses his gratefulness to all of them.

LIST OF FIGURES

LIST OF TABLES

CHAPTER-1

GENERAL

1.1 INTRODUCTION

Studies in properties of solutions have been a common concern of chemists, physicists, geologists, metallurgists and material scientists, although the systems studied by these different groups of scientists vary widely due to their diversified interests. Aqueous and fused salt solutions of oxide, sulphide and halide have been of special interest to the process metallurgists using different hydro-, electro- and pyrometallurgical processes for extraction and refining of metals. Thus silicate slags from smelting and refining furnaces consist of the ionic solutions of different oxides such as CaO, MgO, FeO, MnO, Al_2O_3, SiO_2, P_2O_5 etc. Matte, in copper or nickel smelting operations, consists of Cu_2S, FeS, Ni_2S_3, As_2S_3, Sb_2S_3, Bi_2S_3, precious metals etc. Igneous melts in fused salt electrolysis and slags from metallothermic reduction of rare and reactive metals also consist of solutions of halides such as chlorides or fluorides. Similarly different aqueous phases encountered in leaching, purification and recovery stages in hydrometallurgical extraction of metallic values contain solutions of their compounds. Fundamental thermodynamic properties of the different constituents present in such solutions affect essentially the feasibility and extent of different reactions used and, therefore, primarily control their behaviours during the metal extraction and

refining from their primary or secondary sources. These are, therefore, significant from the view-point of optimisation and control of existing processes and for the development of newer techniques.

Solutions of metal oxides are of considerable interest to process metallurgists and the importance of a knowledge of their thermodynamic properties cannot be overemphasized. Therefore, in the recent past, properties of such systems have been extensively studied experimentally to collect a host of selected data, compiled specially on binary oxide systems. In the absence of such data, the metallurgists is faced with the problem of making estimates of these properties which are so very important in understanding of the nature of many reactions. However, because of the limitations of such experimental studies, due to either their being tedious, time-consuming and costly, especially in the entire composition range of binary and higher component solvents or the dilute solution range of solutes or due to the requirements of precisely controlled elevated temperatures and other experimental conditions and also stringent requirements of high purity of materials used, several attempts have been simultaneously made, especially in the recent past to derive solution models which would permit a theoretical evaluation of such data and prediction of properties of such solutions. Theoretical progress has been slow even for the simpler kind of solutions and much work has yet to be done for arriving at models suitable for multi-component systems of interest to practical metallurgists.

The binary iso-structural solid solutions are of interest because they form the starting point for the understanding of more complex oxide systems met with in practice. Many attempts have been made in the recent past to measure the thermodynamic properties of these systems. The different methods used and important studies made as revealed by a survey of the available literature and Metal Abstracts will therefore be reviewed in the following section.

1.2 LITERATURE REVIEW

1.2.1 Experimental Techniques

Several methods [1,2,3] have been used for the measurement of thermodynamic properties of oxide and alloy systems. Selection of method to study a system primarily depends upon the properties to be investigated. Enthalpy change associated with the process under study can be determined by calorimetry as well as from the temperature derivative of free energy. Calorimetry is preferred for enthalpy studies, as it is a direct method and hence uncertainities and errors in the results are of lesser magnitude. For determination of activity-composition relationship at a given temperature, there is a choice of many methods. A method which is easier, rapid and more reliable is preferred over others. These techniques are briefly reviewed in the following sub-sections, with greater emphasis on emf technique, which is selected for the present investigation.

1.2.1.1 Calorimetry

Calorimetry measures "heat capacity" or enthalpy changes associated with any physical or chemical process by measuring accurately the temperature changes of a thermal system called "calorimeter", of known or calibrated heat capacity. The small changes in temperature of calorimeters associated with the process under study are measured accurately by either making use of special mercury-in glass thermometers such as Beckmann thermometers or platnnum resistance thermometers, thermocouples and more recently using thermisters, optical pyrometers etc. depending upon the range of temperature under study. Adequate corrections for the 'heat losses' are made to compute 'corrected changes in temperature'.

Various calorimeters used in practice for thermodynamic studies are described in literature [1,2,3] . 'Direct reaction calorimetry' and 'solution calorimetry' involve thermo-chemical study of chemical reactions and dissolution processes respectively, conducted directly in the calorimeter. 'Differential solution calorimetry' may be adopted for determining 'heat of formation' of alloys. High temperature calorimetry involving study at elevated temperatures poses special design, construction and operation problems due to requirements of special construction materials, higher rates of heat transfer or losses by radiation and on-set of thermionic emission.

Several sources of error affect results of calorimetry and adequate precautions must be taken to compensate for their adverse effects. The physical or statistical errors

include errors in measurement of temperature change and water-equivalent of calorimeter due to either inadequate control or compensation of heat losses. Systematic errors are chemical in nature, have more serious effects and involve either incomplete reactions, occurrence of simultaneous side reactions or due to presence of impurities in the calorimeter interfering with the process under study. Precision chemical analysis of reactants and products of reaction is an essential pre-requisite for accurate determination of temperature changes due to reaction under study and compensation and correction for errors introduced due to 'incomplete' or 'side' reactions. Impurities present, if reacting exothermically, can result in serious errors in study of low endothermic reactions and need proper accounting. Violent reactions, similarly, need careful study to prevent dispersion or associated errors. Thus, necessary precautions should be taken to yield reliable and reproducible results.

1.2.1.2 Equilibrium techniques

These involve either (i) a physical equilibrium between a condensed phase and its vapour in non-reactive systems and therefore, make the use of measurement of vapour pressure of the desired component for computation of thermodynamic properties based on clausius-clapeyron equation or (ii) a chemical equilibria between two phases-generally involving one gaseous phase and the other condensed phase-either solid or liquid or occasionally (iii) a liquid-liquid system

involving two immiscible phases for study of distribution of a solute between them. Under equilibrium condition, the chemical potential or activity of the component under study is the same between the equilibrated phases and hence 'solubility', 'partitioning' or 'chemical reaction' occurring in the system can be studied.

1.2.1.2.1 Vapour pressure method

These involve three groups - 'static', 'dynamic' and 'effusiom' methods for study.

If the vapour pressure is high, it can be measured by static methods like the rise of liquid manometer column or stretching of a flexible diaphragm etc. For measurement of low pressures, special techniques e.g., 'absorption spectrum', 'ionisation manometers' or 'dew-point method' have been used. 'Dynamic method' involve study of boiling point as best method of this group, which uses either a 'weight loss technique' for systems reflecting sharp boiling points or a modified method using constant temperature and variable external pressure for others. The most important indirect method for measuring vapour pressure greater than 10^{-3} atm. is transportation method [2] using an inert carrier gas . Reliable results can be obtained by this method if the correction for diffusion of sample molecules in the gas phase are made and adequate precautions are taken. In the pressure range of 10^{-9} to 10^{-3} atm, two principal effusion techniques - the 'Knudsen method' and 'Langmuir method' are used based on

rate of evaporation. Knudsen method involves the loss of molecules from a closed cell. For accurate measurements, the temperature of the orifice and other parts of the cell should be equal and area of sample should be much larger than the orifice area. Langmuir method involves the escape of molecules from a surface - 'free evaporation technique'. Interpretation of results from either method requires a knowledge of the species in the vapour. For complex vapours of uncertain compositions, use of mass-spectrometer is made.

Of the different vapour pressure methods, boiling point method using either varying pressure rather than varying temperatures or condensation technique is quick and accurate. Knudsen method yields best results and is more reliable than Langmuir's method,provided suitable cell material, non-reactive to the vapour under study is available, but need precise knowledge of molecular weight of the vapour. 'Transportation method' suffers from errors due to graphical technique. Thermal diffusion causes error in systems with mixture of vapours and very finely,powdered samples cause error due to the effect of surface energy.

1.2.1.2.2 Chemical equilibria

In systems involving gas-condensed phase equilibria, the desired component is transferred from the gaseous phase of known chemical potential of the component for equilibration in both reactive systems for study of desired chemical reaction and non-reactive systems for study of 'solubility'

or 'partition coefficient'. Gaseous mixtures of specified chemical potentials are prepared for this purpose either by mechanically mixing the constituent gases at constant flow rates and pressures or through a 'chemical equilibria'. Typical gaseous mixtures used for study include H_2-CH_4 mixture (for C- and H- chemical potential), H_2-H_2O or CO-CO_2 mixtures (for O-potential), SO_2-O_2 mixture (for S- and O- potential), H_2-NH_3 mixture (for N-potential), HCl-H_2 mixture (for H- and Cl- potential) etc. and choice of any specific mixture for use depends upon the chemical potential desired, the temperature of study, availability and ease of development of the desired gaseous mixture, simple apparatus design, ease of transport of gaseous mixture to the reaction zone and attainment of equilibrium in a reasonable period of time.

Major problems and sources of error include, (i) evolution of occluded gases from the material of construction of apparatus, necessitating few blank determinations to compensate for error and use of especially prepared materials only,

ii) thermal diffusion due to difference in densities of constituents of the gaseous mixture leading to seggregation of lighter component in high temperature zones and vice-versa. This effect is compensated by faster flow rates and dilution of the gas mixtures with an inert gas,

iii) non-availability or limited availability of material of construction for high temperature work including gas-tight and leak-proof joints. Induction heating using water cooled elements offers advantage in equilibrium studies involving metals.

In these studies it must be ensured that the equilibrium measured is independent of time and can be attained from both the sides. Due to uncertainity regarding the attainment of true equilibrium, 'equilibrium results' are not much reliable.

1.2.1.3 E.M.F. method

Of the various techniques used for the experimental determination of the thermodynamic data, the emf technique is the most suitable, convenient and yields most reliable results. It has, therefore, been extensively used for estimation of free energy change of different chemical reactions in reactive systems and activity of solutes in non-reactive systems. The necessary condition for its usage, however, is that the process under study must be such that its energy is capable of generating a reversible emf either in a galvanic cell for estimation of free energy of chemical reaction or in a concentration cell for determination of activity of a component in binary or higher component systems.

A simple consideration of energy conversion provides the relationship between the reversible cell potential, E

(in millivolts) and the Gibb's free energy change, ΔG(in joules) for the virtual chemical reaction of the cell,

$$\Delta G = - nF E = - 96.466\ nE \qquad ..(1.1)$$

where,

n is the equivalents of the charge passed through the external circuit and F is the Faraday's constant. Application of the Gibbs-Helmholtz relations to the temperature dependence of the cell voltage provides values for enthalpy change, ΔH, and entropy change, ΔS, for the virtual cell reaction.

1.2.1.3.1 Pre-requisities of cell design

Since the basis of emf method is the development of the reversible emf due only to the cell reaction under study, hence it must be ensured that electrical energy in the cell is generated only by the process under study. This process must be completed reversibly in the cell and no other process- chemical reaction , physical or physico-chemical phenomenon, nor any external source should contribute, directly or in-directly, to the emf so produced and measured. The 'cell-feasibility' should therefore, be studied adequately before designing such cells for emf measurement. This 'cell feasibility' is analysed in terms of the differences between free energies of formation of different compounds used as electrolytes in the cell and also due to their reactions with the construction material of the cell, the electrodes or the lead wires connecting the electrodes with the emf measuring units. This difference

should be sufficient to eliminate possibility of any side-reactions in the cell. Stability of different compounds measured in terms of the standard free energy, ΔG^{o}, and enthalpy ΔH^{o}, of formation and possibilities of their mutual exchange reactions, indicated by the difference, $\Delta (\Delta G^{o})$, between their standard free energies of formation are the best data guiding such cell designs. Differences in electronegativities, $\Delta\varepsilon$, and position in electrochemical series of the components of the alloy also are measures of their mutual reactivities. Systems with small $\Delta (\Delta G^{o})$ and $\Delta\varepsilon$ are susceptible to side reactions and need adequate precautions and/or compensation for accurate results.

1.2.1.3.2 Sources of error and precautions

1) No external emf, either due to thermo-electric or eddy current effects, should be allowed to be produced in the cell. For this, cell should be located in the constant temperature zone of the furnace, preferably surrounded by an earthed metallic tube of high thermal conductivity to enlarge uniform temperature zone and neutralise any interfering eddy-current emf. Non-inductive winding, with closely wound heating element near the ends of the furnace is to be used in the furnace construction. Absence of any stray emf is reflected by no change in the value of the cell-emf measured on momentarily switching-off the furnace.

2) No current should flow in the cell, otherwise the concentration at the two electrodes will change leading to production of local concentration cells and associated intermediate emf, interfering with cell-emf, developed due to the primary cell reaction. This reflects to the necessity of keeping external circuit open most of the time and preferred use of potentiometer-type instruments for measurement of emf.

3) Electrodes should be of pure materials of uniform composition for the same reason as impurities present will also lead to the formation of localised concentration cells and associated errors in emf measurement.

4) Studies must preferably be conducted with liquid electrodes for high diffusion rates and total homogenisation in electrodes. However, for cells using solid electrodes, sufficient time should be allowed for this reason.

5) Attainment of equilibrium in the cell must be ensured for development of reversible cell emf and hence measurement must be made only after the emf developed attains a constant value with reference to time.

6) Cell reversibility must be ensured. Necessary conditions for this include

   i) the electrolyte used should be pure and of constant composition and must have only ionic and no electronic conductivity, with a constant valence ion-transferred in the cell rather than mixture of

ions of different valence values. Formation of 'fog' or 'emulsion' of metals in the fused electrolyte contributes to electronic conductivity and hence must be avoided. Similar errors result from evaporation of electrode or electrolyte, which must be avoided.

ii) no reaction between the cell material, electrodes, electrolyte or lead wires except for slight etch, should be allowed, as any displacement or exchange reaction, especially when using fused electrolytes will generate corresponding intermediate emf and associated error. The ion transferred in the cell for the same reason should be least electronegative in the melt, thus necessitiating -

a) proper selection of electrolyte in relation to electrode and other cell materials. Affinity of anion of the electrolyte to the more electropositive metal of the alloy should be much less than its affinity for other constituents of the alloy.

b) Adequate and careful preparation of the electrolyte, especially of the hygroscopic fused salts to eliminate moisture etc.

c) cell should be free of air, oxygen or any other reactive gas, necessitating either use of vacuum or inert gas (exception being use of a gas as one of the electrode).

These requirements necessitate proper study of 'cell-feasibility' before design of cell. Any side-reaction, occuring in cell must be adequately compensated as demonstrated by Warner [4] for correction in the measured value, of emf.

iii) Constancy of cell emf with respect to time and on disturbing the equilibrium momentarily by either raising or lowering its temperature and again bringing back to the initial value.

iv) the different materials used in the cell construction must be in their most stable state to avoid occurence of unidentified transitions during experimentation and associated emf effects.

1.2.1.3.3 Development of the electrolytes

For many years, beginning in the last century, chemists have tried to avoid the limitations of aqueous electrolyte by attempting to use organic solvents, such as NaI and KI in ethylamine in study of certain alkali-amalgams [3,5] and there have been number of advances using this technique. However, organic non-aqueous solvents have their darker side. They decompose, particularly on electrodes. They also are characterised by low conductivity and often absorb moisture unless the apparatus is carefully protected. In view of this situation and their limited applicability to studies near room temperatures only, many technologists turned away from aqueous and non-aqueous field to use of molten salt or liquid

electrolyte and the nineteenth century saw the dawn of molten salt technology. Molten salt mixtures of appropriate melting points and high ionic conductivity are used for study of both solid and liquid systems at elevated temperatures. Generally eutectic mixtures have been used, e.g. potassium acetate - sodium acetate (M.P. 233°C) used below 300°C, beyond which it burns and decomposes with charring [6]. Lithium chloride-rubidium chloride (M.P. 312°C) [7] and Lithium chloride-potassium chloride eutectic (M.P. 359°C) have been extensively used [8-23]. For higher temperature works upto 1200°C, occassionally other salt-mixtures [24-46] have been used. However, because of the problems associated with the fused salts - such as absorption of water, interaction of the solvent with the cell materials, relatively towards electrodes and lead, evaporation loss, problem of formation of 'metal-fog' or emulsion, attempts were made to use various solid electrolytes in different types of galvanic cells for the measurement of the thermodynamic properties. Among them mention may be made of the galvanic cell.

$$CO_2\text{-}CO/\text{Thuringer glass}/O_2 \qquad ..(1.2)$$

used by Haber and Moser [47] in 1905 involving Thuringer glass to measure the oxygen partial pressures in CO_2-CO gas mixtures. In 1908, Katayama [48] used solid halide electrolytes in galvanic cells of type

$$Pb/Pb\ Br_2/Br_2 \qquad ..(1.3)$$

$$Pb/Pb\ Br_2/Ag\ Br/Ag \qquad ..(1.4)$$

to get the free-energies of the reactions

$$Pb + Br_2 = Pb\,Br_2 \qquad ..(1.5)$$

$$Pb + 2Ag\,Br = Pb\,Br_2 + 2Ag \qquad ..(1.6)$$

Porcelain was used as a solid electrolyte by Treadwell [49] in 1916 to measure the free energy of formation of various metal oxides in galvanic cells of the type

$$Cu, Cu_2O/\text{Borate melt}/\text{Porcelain}/O_2 \qquad ..(1.7)$$

Watcher [25] used pure solid silver chloride, being a pure ionic conductor for study of Ag-Au alloys. Ure [50] demonstrated the pure ionic conductivity of CaF_2 in 1957. Following this, a number of investigations have been made with galvanic cells involving CaF_2 and other refractory fluorides like $Sr\,F_2$ and $Mg\,F_2$ to measure the free energies of formation of a number of compounds like the silicates and titanates [51,52]. Recently this method has been adopted in the measurement of activities in the binary oxide systems. The application of oxides as solid electrolytes in galvanic cell measurements is restricted by the inherent electronic conduction of most of the oxides. Treadwell and Terebesi [53] used porcelain as a solid electrolyte in the cell

$$Al \,/\, \begin{matrix} Al_2O_3(S) \\ Na_3AlF_6 \end{matrix} \,/\, \text{Porcelain} \,/\, O_2 \qquad ..(1.8)$$

Hauffe [54] used glass as solid electrolyte in the electrochemical investigations of molten Na-Hg and Na-Cd alloy systems at 300-400°C, since Na^+ ions in glass carry

current. Lantratov [55] used K-glass for study of K-Pb alloys containing 5-90 % K. Aronson and Lemont [56] also used K-glass for study of K-Tl alloys between 623-723 K. Kubaschewski and Huchler [57] used silver glass to measure the activity in Ag-Au alloys. Virek [58] used tellurium glass as the electrolyte to measure the thermodynamic activity in Te-Sn system. Other attempts with copper halides and chalcogenides [6] failed due to their having both ionic and electronic conductivities. Ohtani and Sanbongi [59] used MgO as the solid electrolyte to determine the amount of dissolved oxygen in molten steel. But MgO have been found by Mitoff [60] to have very narrow limits of ionic conductivity with respect to temperature and oxygen partial pressure. The transport properties of MgO, by solid state galvanic cell measurements were studied by Pal'guev et al. [61] and Alcock [62]. However, with use of cells of the type

$$Ni, NiO/CaO\text{-}ZrO_2/Fe,FeO \qquad ..(1.9)$$

with solid electrolytes, first made by Kiukkola and Wagner [63], a new series of solid electrolytes have emerged out. This type of electrolyte, a solid solution of CaO in ZrO_2 having a stabilized fluorite structure, has the transport number of O^{2-} ions practically unity. Schmalzried [6,64] showed that below $P_{O_2} \simeq 10^{-18}$ atm at 1000°C it developes appreciable electronic conductivity. The application of various refractory oxides like MgO, ZrO_2-CaO and fused SiO_2 in solid state galvanic cells has been theoretically

dealt with by Schmalzried [65]. Other fluorite structured solid solutions based on ThO_2 with CaO, Y_2O_3 or LaO_2 additions, have also virtually unity O^{2-} ion transport number in the oxygen partial pressure range 10^{-6} - 10^{-28} atm. and minimum required conductivity of 10^{-6} mho cm^{-1} and are now extensively used. Sellars and Maak[66] used calcia stabilized zirconia for study of Au-Ni alloys between 775-935°C and Fruehan [67] used ZrO_2 (CaO) and ThO_2 (Y_2O_3) type electrolytes for study of Fe-Si alloys between 1500-1600°C. However, reducing atmospheres cause electronic conductivity in these and render them unsuitable for use. Delect and Egan [68] used solid CaF_2 electrolyte for study of Ca-Ag and Ca-In alloys. Fischboch [69] and Rievier and Pelton [70] used β-alumina solid electrolytes for study of Ag-Au alloys between 500-600°C and Na-Sn alloys in temperature range 250-450°C respectively.

Recently, open circuit emf measurements have been made by Choudhury [71] to demonstrate that a two-phase, polycrystalline mixture of β-alumina and α-alumina could be used as a solid electrolyte in galvanic cells with reversible electrodes fixing oxygen or aluminium chemical potentials. These measurements indicate that such a two-phase solid electrolyte could be used in galvanic cells to monitor oxygen levels as low as 10^{-47} atm. at 1000 K.

1.2.1.3.4 Comparison of the emf method with the gas-equilibrium method

Though the emf and gas-equilibrium techniques are used to measure the thermodynamic data in oxide, silicate and

spinel systems, there are conditions to their successful applications, for instance both techniques are not suitable for systems with very low oxygen partial pressures. The uncertainties involved in the two methods are given below.

An uncertainty of 1 % in the measurement of equilibrium constant in the gas-equilibrium technique leads to an uncertainty of 20 cals in the value of ΔG^{o} at 1000°C. On the other hand an uncertainty of 0.5 mV in the measured emf of a solid electrolyte cell will bring in an uncertainty of 11.5 n cals in the value of ΔG^{o}, where n is the number of Faradays to be passed across the cell to effect the reaction. Though the uncertainties involved in the two methods are comparable, emf technique has found wide applications in the last two decades, because of the simplicity of the method and the comparatively lower temperatures which can be used for the measurements.

1.2.2 Solid Electrolyte Galvanic Cells

1.2.2.1 Theoretical considerations

The emf of a solid electrolyte concentration cell, involving chemically identical electrodes at different chemical potentials, can be correlated with the free energy change of the cell reaction by the relationship.

$$\Delta G = - n E F \qquad ..(1.10)$$

Such a cell can be represented as

$$Pt', X_2(\mu'_{X_2}) / \overset{\text{Solid electrolyte}}{(L,M)\,X_2} / X_2(\mu''_{X_2}), Pt'' \quad ..(1.11)$$

where,

μ'_{X_2} and μ''_{X_2} are the chemical potentials at the two electrodes, of X_2, with respect to which the cell is reversible. In order to arrive at the conditions for the selection of suitable electrolyte for galvanic cell measurements, Steele [72] has made a thermodynamic analysis of the emf of such cell, in the light of the dissolution of electrode components in the electrolyte and the absence of total ionic conductivity of the electrolyte. A brief outline of the treatment is given here.

It can be assumed that μ'_{X_2} and μ''_{X_2} are established at the electrodes by condensed phase equilibria represented by the reactions : at the left hand electrode,

$$[A]_B + \tfrac{1}{2} X_2 = AX \quad ..(1.12)$$

and at the right hand electrode,

$$2C + \tfrac{1}{2} X_2 = [C_2X]_{DX} \quad ..(1.13)$$

where,

$[A]_B$ represents an alloy of the metals A and B and $[C_2X]_{DX}$, a solution of compounds C_2X and DX. The cations of these compounds, namely A^{2+}, B^{2+}, C^{+} and D^{2+} may be assumed to dissolve in the solid electrolyte. The cell can then be more correctly represented as :

$$\begin{array}{ccccc} Pt', X_2(\mu'_{X_2}) & \left|\begin{array}{l} AX \\ BX \\ (L,M)X_2 \end{array}\right. & (L,M)X_2 & \left|\begin{array}{l} C_2X \\ DX \\ (L,M)X_2 \end{array}\right. & X_2(\mu''_{X_2}), Pt'' \\ \alpha' & \beta' & & \beta'' & \alpha'' \end{array} \quad ..(1.14)$$

where,

α', β', α'' and β'' represent various phases in the two electrodes.

The electrons at the two platinum electrodes will be at two different chemical potentials $\bar{\mu}_e^{Pt'}$ and $\bar{\mu}_e^{Pt''}$ due to the electrochemical equilibria established at the two electrode - electrolyte interfaces. The emf, E, of the cell (1.14) is given by the relation

$$FE = F\ (\varphi^{\alpha''} - \varphi^{\alpha'}) \qquad ..(1.15)$$

where,

$\varphi^{\alpha''}$ and $\varphi^{\alpha'}$ are the electrochemical potentials in α'' and α' respectively. The electrical potentials can be related to chemical potentials as

$$F(\varphi^{\alpha''} - \varphi^{\alpha'}) = \left(\frac{1}{n}\right)(\bar{\mu}^{\alpha''} - \bar{\mu}^{\alpha'}) \qquad ..(1.16)$$

where,

$\bar{\mu}^{\alpha''}$ and $\bar{\mu}^{\alpha'}$ represent the corresponding chemical potentials and n is the number of Faradays involved in the reaction of interest. The chemical potentials can be related to those of the electrons as

$$FE = \left(\frac{1}{n}\right)(\bar{\mu}^{\alpha''} - \bar{\mu}^{\alpha'}) = -(\bar{\mu}_e^{Pt''} - \bar{\mu}_e^{Pt'}) \qquad ..(1.17)$$

At each electrode-electrolyte interface, the following equilibria are established assuming the cell to behave reversibly,

$$\frac{1}{2} X_2 + 2e = X^{2-} \qquad ..(1.18)$$

Hence,

$$\mu^{\alpha}_{X_2} + 4\,\bar{\mu}^{\alpha}_{e} = 2\,\bar{\mu}^{\alpha}_{X^{2-}} \qquad ..(1.19)$$

$$\bar{\mu}^{\alpha}_{e} = \frac{-1}{4}\left(\mu^{\alpha}_{X_2} - 2\bar{\mu}^{\alpha}_{X^{2-}}\right) \qquad ..(1.20)$$

Because of the equilibrium conditions in the galvanic cell

$$\bar{\mu}^{\alpha'}_{e} = \bar{\mu}^{Pt'}_{e} \quad \text{and} \quad \bar{\mu}^{\alpha''}_{e} = \bar{\mu}^{Pt''}_{e} \qquad ..(1.21)$$

Similarly,

$$\bar{\mu}^{\alpha'}_{X^{2-}} = \bar{\mu}^{\beta'}_{X^{2-}} \quad \text{and} \quad \bar{\mu}^{\alpha''}_{X^{2-}} = \bar{\mu}^{\beta''}_{X^{2-}} \qquad ..(1.22)$$

Substituting relations (1.20), (1.21) and (1.22) in relation (1.17), we get

$$FE = \frac{1}{4}\left(\mu^{\alpha''}_{X_2} - \mu^{\alpha'}_{X_2}\right) - \frac{1}{2}\left(\bar{\mu}^{\beta''}_{X^{2-}} - \bar{\mu}^{\beta'}_{X^{2-}}\right) \qquad ..(1.23)$$

Neglecting the second term the above relation simplifies to

$$FE = \frac{1}{4}\left(\mu^{\alpha''}_{X_2} - \mu^{\alpha'}_{X_2}\right) = \frac{1}{4}\Delta\mu_{X_2} \qquad ..(1.24)$$

which is identical to relation (1.10)

Thus, from relations (1.23) and (1.24) it is clear that, for the measurement of the free energy changes by the galvanic cell technique, the second germ, $-\frac{1}{2}\left(\bar{\mu}^{\beta''}_{X^{2-}} - \bar{\mu}^{\beta'}_{X^{2-}}\right)$, must be negligible. This term represents the difference in the electrochemical potentials of X^{2-} ionic species within the solid-

electrolyte phase β in contact with the two electrodes. Steele [72] points out that when the electrochemical potentials of the ionic species vary across the electrolyte phase, the irreversible diffusion processes involving the transfer of ionic species between the different concentration levels must be taken into consideration. Such processes result in a charge separations due to the different mobilities of the various ions which will oppose the flow of charged particles. At equilibrium, the steady state conditions characterize the existence of the diffusion potential.

The contribution to the diffusion potential alone cannot be measured separately, neither can an estimate be made of the chemical potential terms $\bar{\mu}^{\beta''}_{X^{2-}}$ and $\bar{\mu}^{\beta'}_{X^{2-}}$. For a concentration cell involving similar reversible electrodes and only one anion in the electrolyte, the following expression has been derived by irreversible thermodynamic considerations,

$$-\frac{1}{2}(\bar{\mu}^{\beta''}_{X^{2-}} - \bar{\mu}^{\beta'}_{X^{2-}}) = \int_{\beta'}^{\beta''} \sum_i t_i\left(-\frac{1}{z_i} d\bar{\mu}_i - \frac{1}{2} d\bar{\mu}_{X^{2-}}\right) \quad \ldots (1.25)$$

where,

z_i is the valence and t_i the transference number of the i^{th} ionic species with respect to an appropriate frame of reference such as the crystal lattice in the case of the solid electrolyte. Eq. (1.25) enables a linear combination of chemical potentials of the neutral molecules in the place of the chemical potentials of the ions. In the present context, considering the neutral species AX, BX, C_2X, DX and $(L,M)X_2$ along with electrons as a

seperate species, the term within the integral in Eq. (1.25) takes the form,

$$\int_{\beta'}^{\beta''} \Big[t_{A^{2+}} \left(-\tfrac{1}{2} d\,\bar{\mu}_{A^{2+}} - \tfrac{1}{2} d\,\bar{\mu}_{X^{2-}}\right) + t_{B^{2+}} \left(-\tfrac{1}{2} d\,\bar{\mu}_{B^{2+}} - \tfrac{1}{2} d\,\bar{\mu}_{X^{2-}}\right) + t_{C^{+}} \left(-d\,\bar{\mu}_{C^{+}} - d\,\bar{\mu}_{X^{2-}}\right) + t_{D^{2+}} \left(-\tfrac{1}{2} d\,\bar{\mu}_{D^{2+}} - \tfrac{1}{2} d\,\bar{\mu}_{X^{2-}}\right) + t_{L^{4+}} \left(-\tfrac{1}{4} d\,\bar{\mu}_{L^{4+}} - \tfrac{1}{2} d\,\bar{\mu}_{X^{2-}}\right) + t_{M^{2+}} \left(-\tfrac{1}{2} d\,\bar{\mu}_{M^{2+}} - \tfrac{1}{2} d\,\bar{\mu}_{X^{2-}}\right) + t_{e} \left(d\,\bar{\mu}_{e} - \tfrac{1}{2} d\,\bar{\mu}_{X^{2-}}\right) \Big]$$

$$= \int_{\beta'}^{\beta''} - \Big[\frac{t_{A^{2+}}}{2} d\,\mu_{AX} + \frac{t_{B^{2+}}}{2} d\,\mu_{BX} + \frac{t_{C^{+}}}{2} d\,\mu_{C_2X} + \frac{t_{D^{2+}}}{2} d\,\mu_{DX} + \frac{t_{L^{4+}}}{4} d\,\mu_{LX_2} + \frac{t_{M^{2+}}}{2} d\,\mu_{MX} + \frac{t_e}{4} d\,\mu_{X_2} \Big] \qquad ..(1.26)$$

From the above relation, it is seen that

1) In the absence of electronic conduction ($t_e = 0$),

   a) If there is no significant dissolution of the electrode components in the electrolyte then the electrolyte has constant composition and the

different terms vanish irrespective of the transference numbers.

b) If $t_{X^{2-}}$ is unity, then irrespective of the dissolution of the electrode components in the electrolyte, the diffusion terms vanish.

2) If $t_e \neq 0$,

a) Assuming the solubilities of the electrode components in the electrolyte and the non-stoichiometry of the electrolyte to be negligibly small, the diffusion term becomes

$$-\int_{\beta'}^{\beta''} \frac{t_e}{4} \, d\mu_{X_2} \qquad ..(1.27)$$

The cell emf is then given by substituting Eq. (1.27) in Eq. (1.23)

$$E = \frac{1}{4F}\left(\mu_{X_2}^{\alpha''} - \mu_{X_2}^{\alpha'}\right) - \frac{1}{4F}\int_{\mu_{X_2}^{\alpha'}}^{\mu_{X_2}^{\alpha''}} t_e \, d\mu_{X_2} \qquad ..(1.28)$$

$$= \frac{1}{4F}\int_{\mu_{X_2}^{\alpha'}}^{\mu_{X_2}^{\alpha''}} t_{ion} \, d\mu_{X_2} \qquad ..(1.29)$$

irrespective of the values of $t_{X^{2-}}$, $t_{L^{4+}}$ and $t_{M^{2+}}$ and

b) in case the electrode components dissolve in the electrolyte, but there is negligible transport of the A^{2+}, B^{2+} , C^{+} and D^{2+} ions (assuming $t_{\frac{}{A}2-} + t_e \simeq 1$),

Eq. (1.29) holds good for the emf of the cell. However, the integral in the Eq. (1.29) cannot be integrated accurately, because the variation of the electronic conductivity with composition and oxygen partial pressure is not known.

The dissolution of the electrodes in the electrolyte can affect the local thermodynamic equilibrium at the electrode-electrolyte interface due to changes in the relative concentration of the electrode constituents and modifications in the kinetics of the interfacial reactions. Precautions should be taken to detect such possibilities by testing the reversibility of the cell.

Intermediate compound formation is another phenomena that may affect the cell emf. In a typical galvanic cell used for the measurement of the free energy of formation of compound MX with an electrolyte LX_2 with pure anion condition

$$\text{Pt},(\text{M},\text{MX}) \;\Big|\; \begin{matrix}\text{Solid Electrolyte}\\ LX_2\\ t_{X^{2-}} = 1\end{matrix} \;\Big|\; X_2,\text{Pt} \qquad ..(1.30)$$

if a compound is formed between LX_2 and MX, the cell may then be represented as

$$\begin{matrix}\text{Pt},(\text{M},\text{MX}) \;\Big|\; (\text{L},\text{M})X_3 \;\Big|\; \text{Solid Electrolyte} \;\Big|\\ \qquad\qquad\qquad\qquad\quad LX_2 \qquad\qquad\quad X_2,\text{Pt}\\ p^{I}_{X_2} \qquad\quad p^{II}_{X_2}\end{matrix} \qquad ..(1.31)$$

where,

$p^{I}_{X_2}$ and $p^{II}_{X_2}$ are the equilibrium partial pressures of X_2 at the new interfaces created by the formation of $(L, M)X_3$.

In the absence of electronic conductivity, the emf of the cell has been shown by Steele [72] to be

$$E = \frac{1}{4F}\left[(\mu^{\alpha''}_{X_2} - \mu^{\alpha'}_{X_2}) + (t_L 4+ - 2t_A 2+)\,\Delta G^{o}_{(L,M)X_3}\right] \quad ..(1.32)$$

It is seen that $t_L 4+ - 2t_A 2+ \rightleftharpoons 0$ for the galvanic cell to give the true emf. Any electronic conductivity of the compound will further affect the cell emf.

Heyne [73] has examined the factors that make a solid a "good electrolyte" and has arrived at the following rules of thumb, which have general validity.

Rule I : the band gap of good solid electrolyte is larger than T/300 eV at any temperature T(in K).

Rule II : Good solid electrolytes are better at low than at high temperatures.

The ideal electrode material in all solid state elec chemical cells is characterised by the following three prc perties [73] :

i) it exhibits a high electronic conductivity,

ii) the diffusion coefficient for the mobile species in the electrode is of the same order of magnitude as it is in the electrolyte, and

iii) the range of homogeneity of the single phase is preferably broad.

1.2.2.2 Conductivity of the oxide electrolytes

From the theoretical treatment given above, it is clear that a chosen oxide electrolyte for galvanic cell measurements must be a pure ionic conductor and inert to the electrode. A detailed knowledge of the conductivities of the various refractory oxides is necessary for meeting the first condition. In the solid electrolytes, the energy gap between the valence and conduction bands is very large. Steele and Alcock [74] have represented the measured total conductivity, σ_T, as a sum of ionic conductivity, σ_{ionic}, conductivity due to p-type conduction, $\sigma_{\oplus}$, and conductivity due to n-type conduction, $\sigma_{\ominus}$:

$$\sigma_T = \sigma_{ionic} + \sigma_{\oplus} + \sigma_{\ominus} \qquad ..(1.33)$$

With large concentrations of ionic vacancies, the ionic conduction will not be a function of oxygen partial pressures. Steele and Alcock [74] suggest that any pressure independent electronic contribution to the conductivity may become significant only at very high temperatures.

From an oxide with p-type conduction, the reaction of the positive holes with the oxygen in the atmosphere may be written as :

$$n\ \oplus\ +\ \text{oxygen anions} = O_2(g) \qquad ..(1.34)$$

Thus $\sigma_{\oplus}$ will increase with increase in the partial pressure of oxygen and can be expressed as

$$\sigma_{\oplus} = K_1 (p_{O_2})^{1/n} \qquad ..(1.35)$$

The corresponding reaction, for an oxide with n-type of conduction may be

$$m_{\ominus} + O_2(g) = \text{oxygen anions} \qquad ..(1.36)$$

and the conductivity can be expressed as

$$\sigma_{\ominus} = K_2 \, p_{O_2}^{-1/m} \qquad ..(1.37)$$

Thus, the total conductivity is given by

$$\sigma_T = \sigma_{ionic} + K_1 \, p_{O_2}^{1/n} + K_2 \, p_{O_2}^{-1/m} \qquad ..(1.38)$$

Conductivity behaviours of various refractory oxides as a function of oxygen pressure is shown in Fig. (1.1). Four different types of behaviours have been observed:

1) A minimum in the conductivity - as observed in MgO.

2) An initial region of ionic conduction followed by n-type conduction at low partial pressures of oxygen. Zirconia based electrolytes show this type of conduction.

3) An initial region of p-type conduction followed by a pressure independent region where $t_{ionic} \simeq 1$. This type of behaviour is observed in thoria based electrolytes.

4) An initial p-type conduction region and a final n-type conduction region with an oxygen pressure independent region of conductivity in between.

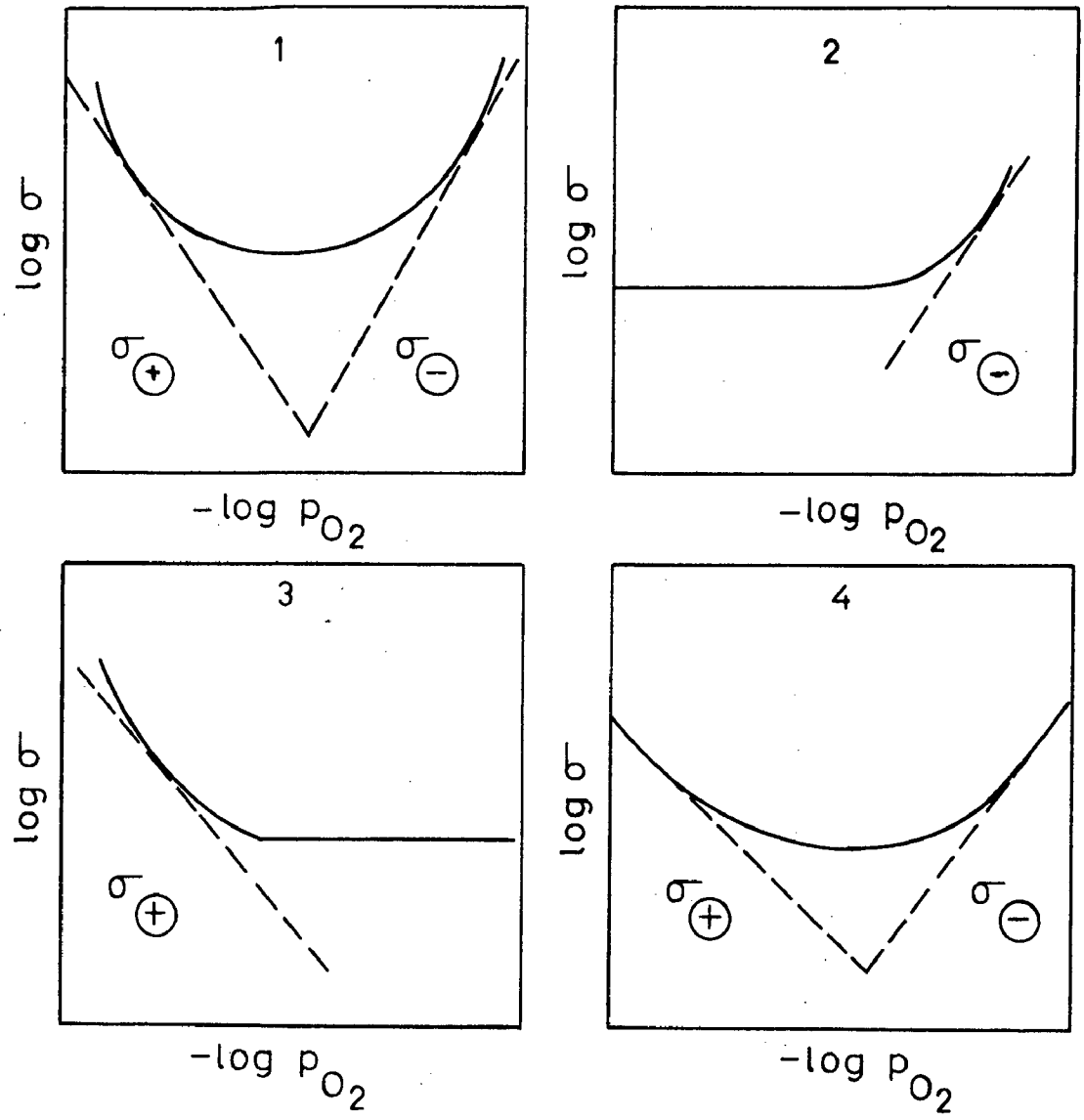

FIG. 1.1 TYPES OF CONDUCTIVITY BEHAVIOR AS A FUNCTION OF OXYGEN PRESSURE.

Schmalzried [64] has introduced the term $p_{\oplus}$ and $p_{\ominus}$ defined as the oxygen pressures at which σ_{ionic} equals $\sigma_{\oplus}$ and $\sigma_{\ominus}$ respectively and derived expressions for the t_{ion} as a function of oxygen pressure. These expressions and the corresponding equations for the emf for the first three types of conduction are given in Table-1.1.

1.2.2.2.1 Conductivity of ZrO_2-CaO solid electrolyte

These are most thoroughly studied and widely used solid electrolytes. Their first successful application for thermodynamic investigations was demonstrated by Kiukkola and Wagner [63] . Etsell et al [75] have given a detailed account of this system in their review paper. ZrO_2-CaO solid solutions are thermodynamically stable above 900°C and at least kinetically stable below this temperature. Theoretical considerations indicate that CaO should be the most effective stabilizing oxide for ZrO_2 [76] . Estell et al. [75] and Stocker [76] have measured the lattice parameters of the cubic solid solutions in the ZrO_2-CaO system. For the most widely used composition $Zr_{0.85}\ Ca_{0.15}\ O_{1.85}$ a lattice parameter of 5.131 A° agrees with most of the results. The lattice parameter increases linearly with CaO content due to the larger size of Ca^{2+} ion relative to Zr^{4+} ion. Density and X-ray intensity measurements have confirmed that anion vacancies are the predominant defects in these solid solutions [64,77-79] . Cation and anion vacancies are randomly distributed over the available lattice sites [64] . In samples

quenched from 1800°C at 1000°C/sec, Diness and Roy [80] found cation interstitials as the major defect.

Electrical conductivity data for various fluorite solid solutions at 1000°C are shown in Fig. (1.2). These values are interpolated from graphs, calculated from equation.

$$\sigma = A \exp(-\frac{\Delta H}{RT}) \qquad ..(1.39)$$

where,

A is approximately independent of temperature (ohm^{-1} cm^{-1}) and ΔH is the activation enthalpy (K.Cals/mole). In agreement with Eq. (1.39), Arrhenius plots are linear from 200-2000°C indicating that oxygen-ion vacancy migration is controlling the conductivity over this entire temperature range. Fig.(1.2) shows a decrease in conductivity with increase in CaO content and at 1000°C there is a conductivity maximum of about 5.5×10^{-2} ohm^{-1} cm^{-1} at 12-13 mole % CaO which coincides with the minimum amount of CaO necessary to stabilize ZrO_2. The ionic conductivity for the 15 mole % CaO is about 2.4×10^{-2} ohm^{-1} cm^{-1} at 1000°C. Activation energies for the 12-13 and 15 mole % CaO compositions are 25.2 and 29.0 K.Cal/mole respectively. The conductivity decreases across the cubic phase region despite the increase in the number of anion vacancies. With increase in CaO content, both log A and ΔH in Eq.(1.39) increase linearly due to rapid decrease in oxygen ion mobility. An increase in ΔH would reduce the mobility. This increase could result from lattice distortion, due to differences in the radii of the cations, the presence of Ca^{2+} ion-anion

TABLE-1.1 Theoretical expressions for t_{ion} and emf by Schmalzried [64]

Electrolyte System	t_{ion}	Electromotive force
Type (1)	$\left[1+\left(\frac{p_{O_2}}{p_{\oplus}}\right)^{1/n}+\left(\frac{p_{O_2}}{p_{\ominus}}\right)^{-1/n}\right]^{-1}$ assuming n=m in Eq.(1.38)	$\frac{nRT}{4F}\left[\ln\frac{p_{\oplus}^{1/n}+p'^{1/n}_{O_2}}{p_{\oplus}^{1/n}+p''^{1/n}_{O_2}}+\ln\frac{p_{\oplus}^{1/n}+p^{1/n}_{O_2}}{p_{\oplus}^{1/n}+p'^{1/n}_{O_2}}\right]$
Type (2)	$\left[1+\left(\frac{p_{O_2}}{p_{\ominus}}\right)^{-1/m}\right]^{-1}$	$\frac{mRT}{4F}\left[\ln\frac{p_{\ominus}^{1/m}+p''^{1/m}_{O_2}}{p_{\ominus}^{1/m}+p'^{1/m}_{O_2}}\right]$
Type (3)	$\left[1+\left(\frac{p_{O_2}}{p_{\oplus}}\right)^{1/n}\right]^{-1}$	$\frac{nRT}{4F}\left[\ln\frac{p''^{1/n}_{O_2}}{p'^{1/n}_{O_2}}+\ln\frac{p_{\oplus}^{1/n}+p'^{1/n}_{O_2}}{p_{\oplus}^{1/n}+p''^{1/n}_{O_2}}\right]$

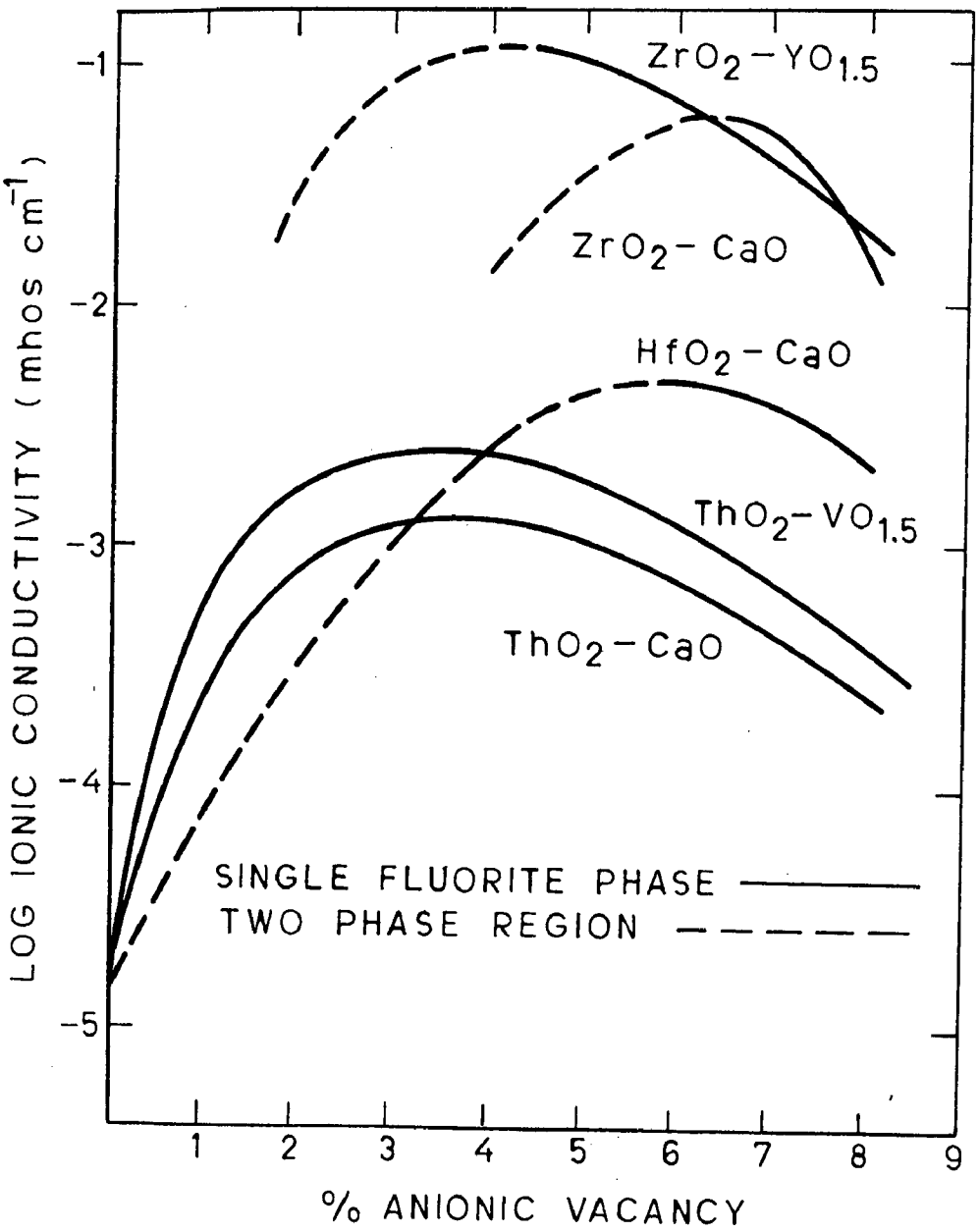

FIG.1.2 LOG IONIC CONDUCTIVITY vs. PERCENT ANIONIC VACANCIES FOR VARIOUS FLUORITE SOLID SOLUTIONS.[74]

vacancy complexes [81,82] or vacancy clustering [83]. Defect interactions or clustering will tend to reduce the number of available charge carriers to below the expected level. Vacancy ordering [79,83-86] will reduce the anion mobility by decreasing the activation entropy. Errors introduced by the grain boundaries [87] in the conductivity data are insignificant compared to the lack of reproducibility [75]. Carter and Roth [83] obtained identical results for single and polycrystalline specimens. Anion diffusion coefficients are at least five to six order of magnitude greater than cation diffusion coefficients at 1000°C [77,88-90]. In the Nernst-Einstein equation, the entire electrical conductivity can be accounted for by using anion diffusion coefficients,

$$\sigma_i = \frac{C_i D_i Z_i^2 F^2}{RT} \qquad ..(1.40)$$

where,

σ_i is partial ionic conductivity, C_i, the concentration, D_i diffusion coefficient and Z_i the valency of the species i. Schmalzried [64] and Patterson et al. [91] measured the conductivity of ZrO_2-CaO electrolyte as a function of oxygen partial pressure. Their results are shown in Fig. (1.3). There have been numerous investigations to determine the transport numbers for electrons and electron holes in ZrO_2-CaO electrolytes [63,64,74,92,93] using various experimental methods and the relations derived by Schmalzried [94]. Patterson [95,96] used a graphical method for the presentation of electrolytic domain data for solid electrolytes. The definition of the electrolytic domain is the region of

temperature and p_{X_2} where $t_{ion} \geq 0.99$. Fig. (1.4) shows a comprehensive plot of electrolytic domains in log p_{X_2} - $\frac{1}{T}$ space for selected halides and oxide electrolytes.

1.2.2.2.2 Conductivity of ThO_2-Y_2O_3 solid electrolyte

A number of investigators [63,97,98] have determined the conductivity of the system ThO_2-Y_2O_3. Peters and Mobius [98] found that the electronic conductivity of the thoria based electrolytes could be significant only at high oxygen pressures. Steele and Alcock [74] studied the conductivity and the ionic transport number of thoria based electrolytes in great detail and concluded that these are p-type conductors. The ionic transport was found to be more than 0.99 at oxygen partial pressures lower than 10^{-6} atm at 1000°C. Results of the conductivity measurements of Patterson et al. [91] and Steele and Alcock [74] are given in Fig. (1.5). Rao and Tare [99] concluded from their experimental investigations on thoria doped with 15 mole % Y_2O_3 that the safe lower limits of oxygen partial pressure for the use of doped thoria as solid electrolyte vary from $10^{-32.6}$ atm at 1200 K to $10^{-24.0}$ atm at 1448 K.

1.2.2.3 Applications of solid electrolyte galvanic cells with oxide electrolytes

The various applications of these cells are briefly described below:

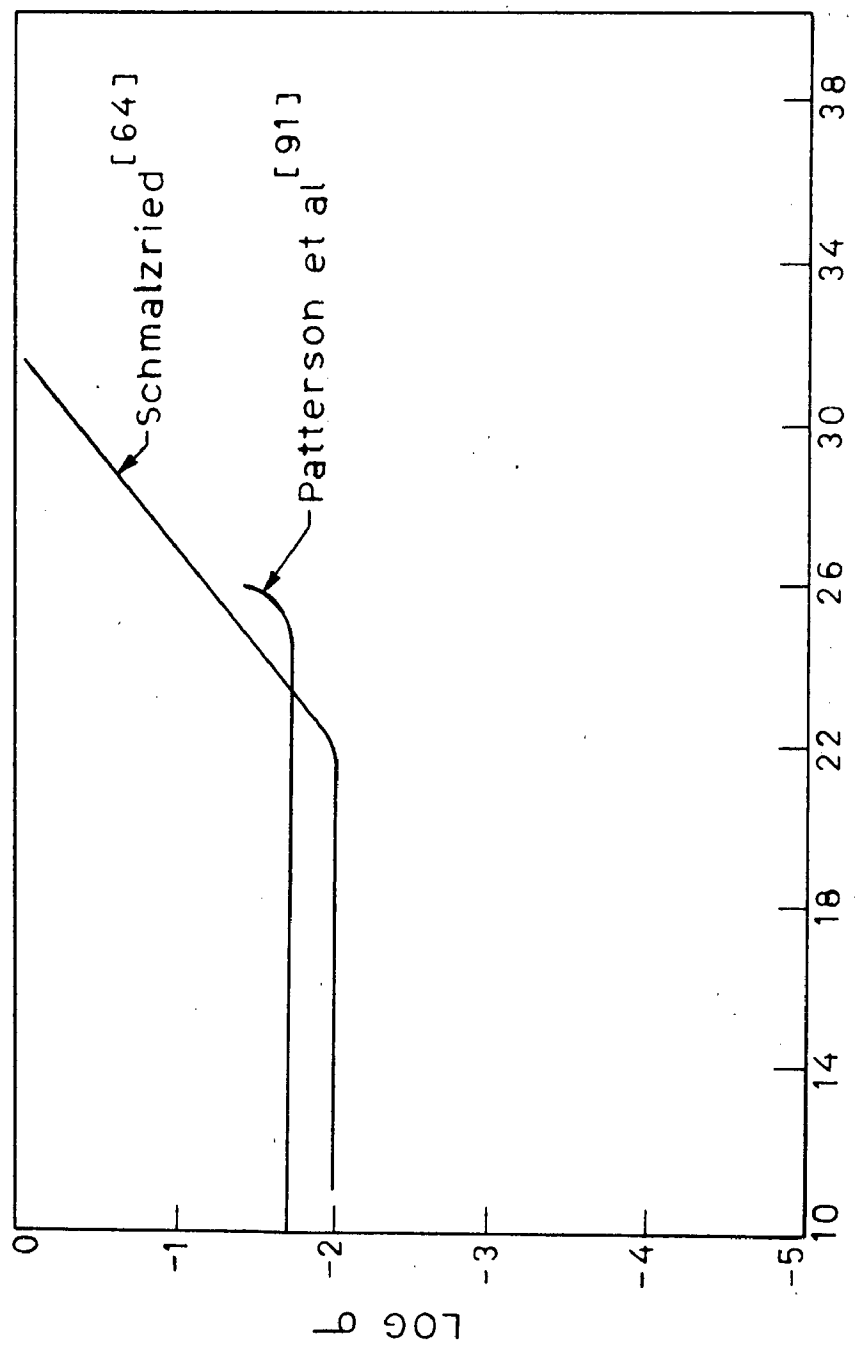

FIG. 1.3 LOG CONDUCTIVITY vs. OXYGEN PARTIAL PRESSURE FOR THE SYSTEM ZrO_2 - CaO AT 1000°C.

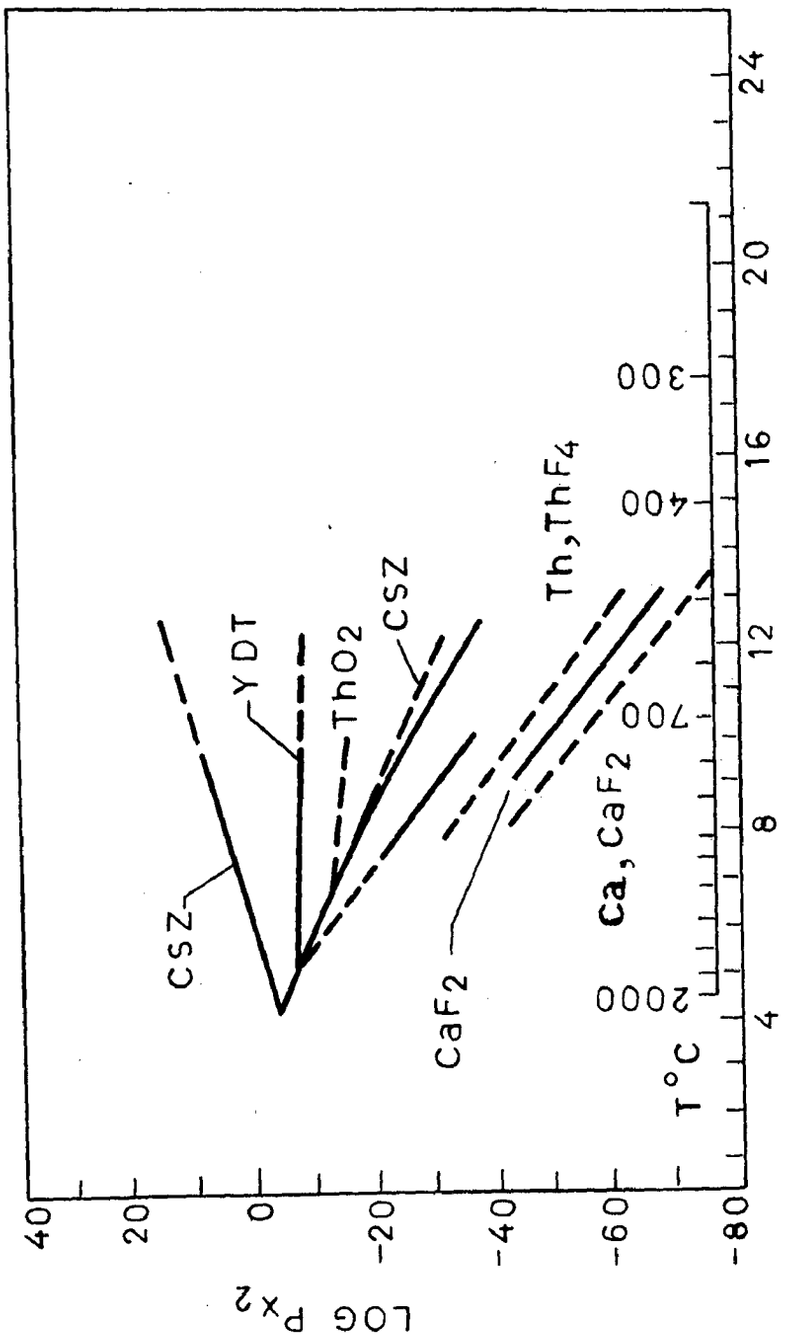

FIG.1.4 PLOT OF ELECTROLYTIC DOMAINS IN LOG P_{x_2} -1/T SPACE FOR SELECTED HALIDE AND OXIDE SOLID ELECTROLYTES.[96]

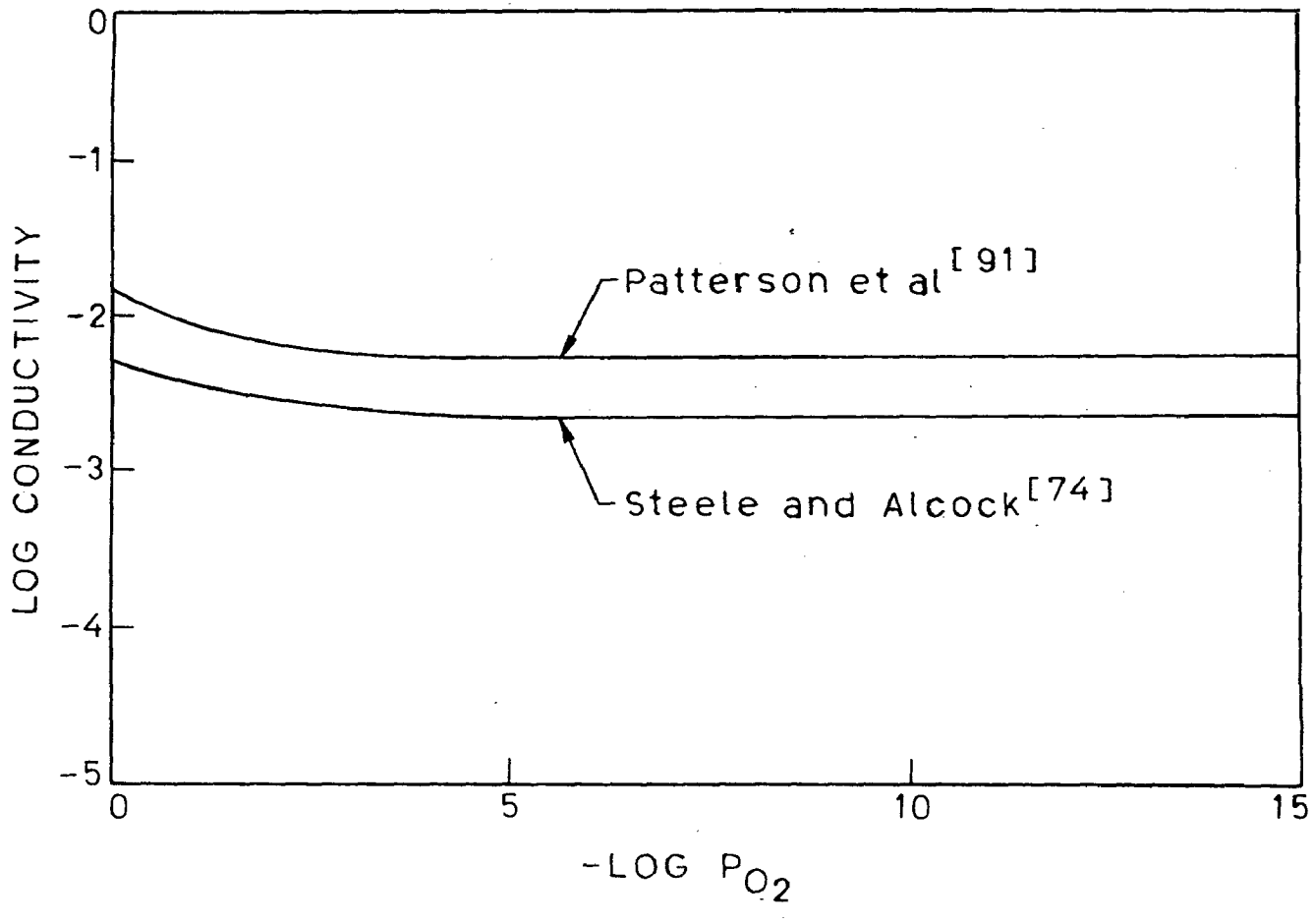

FIG. 1.5 LOG CONDUCTIVITY vs. OXYGEN PARTIAL PRESSURE FOR THE SYSTEM 0.85 ThO_2 - 0.15 $YO_{1.5}$ AT 1000 °C.

The standard free energy of formation of a number of metal oxides have been studied [63,100-102] by use of galvanic cells of the type

$$A, AO/\text{Solid Electrolyte}/BO, B \qquad ..(1.41)$$

involving the reaction

$$A + BO = AO + B \qquad ..(1.42)$$

The standard free energy of formation of a number of spinels, silicates, molybdates, tungstates, aluminates, chromates and stannates have been determined [103-106] using galvanic cells of the type

$$A, B_2O_3, AB_2O_4/\text{Solid Electrolyte}/A, AO \qquad ..(1.43)$$

with the cell reaction

$$AO + B_2O_3 = A\,B_2O_4 \qquad ..(1.44)$$

Activity in binary and ternary alloy systems has been determined [107,108] with the cell

$$A, AO/\text{Solid Electrolyte}/[A]_{alloy}, AO \qquad ..(1.45)$$

with the cell reaction

$$A = [A]_{alloy} \qquad ..(1.46)$$

Cell (1.45) has also been used in the determination of phase boundaries of alloy systems [109,110].

Measurement of activity in binary oxide systems can be carried out [111,112] using cells of the type

$$A, AO/\text{Solid Electrolyte}/(A,B)O, A \qquad ..(1.47)$$

the cell reaction being

$$AO = [AO]_{BO} \qquad ..(1.48)$$

Above cell has also been used for the determination of phase boundaries of oxide systems [113-115]. Measurement of activity of a metal oxide in ternary metal oxide systems has also been carried out with similar cells [116].

Simultaneous measurement of the range of non-stoichiometry and oxygen activity can be carried out by the solid electrolyte galvanic cell method. An elaborate treatment of the various methods of studying defect equilibria in oxide systems has been given by Wagner [117].

The activity of dissolved oxygen in molten metals and alloys [118,119] can be measured using cells of the type

$$[O]_{\text{liquid metal}}/\text{Solid Electrolyte}/A, AO \qquad ..(1.49)$$

the cell reaction being

$$\frac{1}{2} O_2 = [O]_{\text{liq.metal}} \qquad ..(1.50)$$

Oxygen probes for measuring the level of oxygen in liquid metals [120] are based on solid electrolyte.

Diffusivities of oxygen in solid metal can be measured [121] and the kinetics of various metallurgical reactions like oxidation processes can be studied [122] using the cell

$$[O]_{\text{metal}}/\text{Solid Electrolyte}/O_2, \text{air} \qquad ..(1.51)$$

The measurement of the oxygen content of gas mixtures can be carried out with the galvanic cells of the type

$$O_2(Air)/Solid\ Electrolyte/Gas\text{-}Mixture \qquad ..(1.52)$$

Solid electrolytes with oxygen ion conduction find potential application in high temperature fuel cells [123]

1.2.2.4 Fluoride electrolytes

Alkali and alkaline earth fluorides are stoichiometric. Due to the wide energy gap between the valence and conduction bands, the electronic conduction is negligible. Only intrinsic ionic defects due to thermal disorder can be envisaged in these fluorides. Fluoride ion conduction can be expected in fluorides with anti-Frenkel type defects. This would mean that the cationic radius must be large for the given crystal arrangement. The fluorides of calcium, magnesium, strontium and barium fall under this category.

A number of investigators [124-134] have measured the conductivity of CaF_2 solid electrolyte. Recently, Hinze and Patterson [135] measured A.C. conductivity of single crystals of CaF_2 from 550° to 880°C. Fig. (1.6) shows the variation of the total conductivity of CaF_2 as a function of log p_{F_2} for various temperatures. A.C. conductivity and galvanic cell emf measurements lead to the conclusion that the ionic transference number for CaF_2 is essentially unity. Croatto and Bruno [136] and Baris and Taylor [126] confirmed the total conductivity of pure SrF_2 and that doped with LaF_3.

Tubandt et al [137] confirmed that BaF_2 is a pure ionic conductor at 530°C. Baris and Taylor [126] measured the conductivity of pure BaF_2 as well as that doped with GdF_3 and KF. A number of investigators have studied the conductivity behaviour of MgF_2 [138-141]. Its electrical conductivity is much lower than that of the fluorite. β-PbF_2 is structurally similar to CaF_2 doped with BiF_2 and is an anion conductor [142]

1.2.2.5 Cell design

In the earliest form of the cell Kiukkola and Wagner [63] put the solid-electrolyte pellet sandwithched between the reference and test electrodes. The outer surface of the electrode in each case was kept in contact with a platinum foil connected to the two electrical leads of the galvanic cell, as shown in Fig. (1.7a). This type of cell assembly is adequate for systems with high equilibrium oxygen pressures. To ensure good electrical contact, surfaces of the electrodes and electrolyte are polished and spring loaded from the top and bottom. Gerasimov et al [143] devised another method to ensure good electrical contact. They used a clamp that can be tightened to give the best contact, insulated well from the electrodes as shown in Fig. (1.7b). Schmalzried [144,145] and Rapp [146], however, embeded the electrodes in the electrolyte as shown in Fig. (1.7c). In an attempt to isolate the two electrodes from each other with an object to avoid the transfer of any oxygen between the two electrodes via the gas

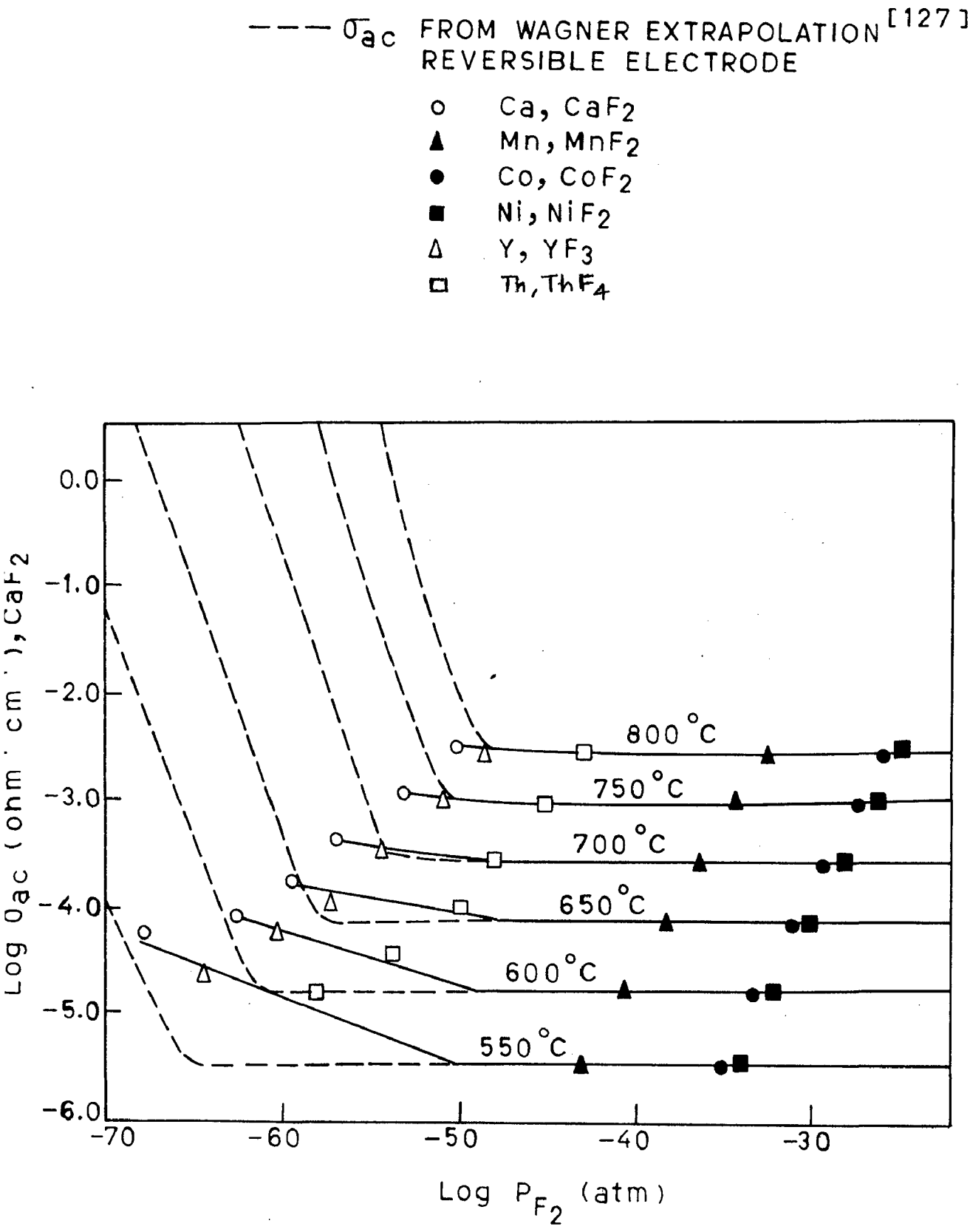

FIG.1.6 TOTAL CONDUCTIVITY OF CaF_2 AS A FUNCTION OF LOG P_{F_2} FOR VARIOUS TEMPERATURES.[135]

phase and thus to improve the accuracy of the data, Kubik and Alcock [109] and Charatte and Flengas [100] suggested the use of a cell with the provision for separate gas streams to each electrode. The electrodes of this cell design are separated by an electrolyte crucible and the cell is held together firmly on a support by spring pressure inside a gas tight reaction tube. The satisfactory operation of "open-cell" technique where both electrodes are exposed to the same gas atmosphere has been demonstrated by Bugden and Pratt [147]. A cell design of this type is shown in Fig. (1.8). It would appear that gas-phase oxygen transfer due to different equilibrium pressures at the two electrodes is minimised partly by the use of crucibles of the electrolyte material which separate the electrodes more effectively than a simple disc of electrolyte.

Charette and Flengas [100] devised a more sophisticated cell, which permits the isolation of the electrodes and the electrolyte. The cell design is shown in Fig. (1.9). Maintenance of the true thermodynamic equilibrium between the electrodes and their respective gaseous environments is ensured by keeping a static inert atmosphere in each of the sealed electrode compartments. The standard free energies of formation of various oxides reported by these authors have been widely accepted as highly reliable data. Taylor and Schmalzried [51] have devised a unique design of the cell assembly where the possible contamination of the electrolyte material can be prevented. In this design the test electrode

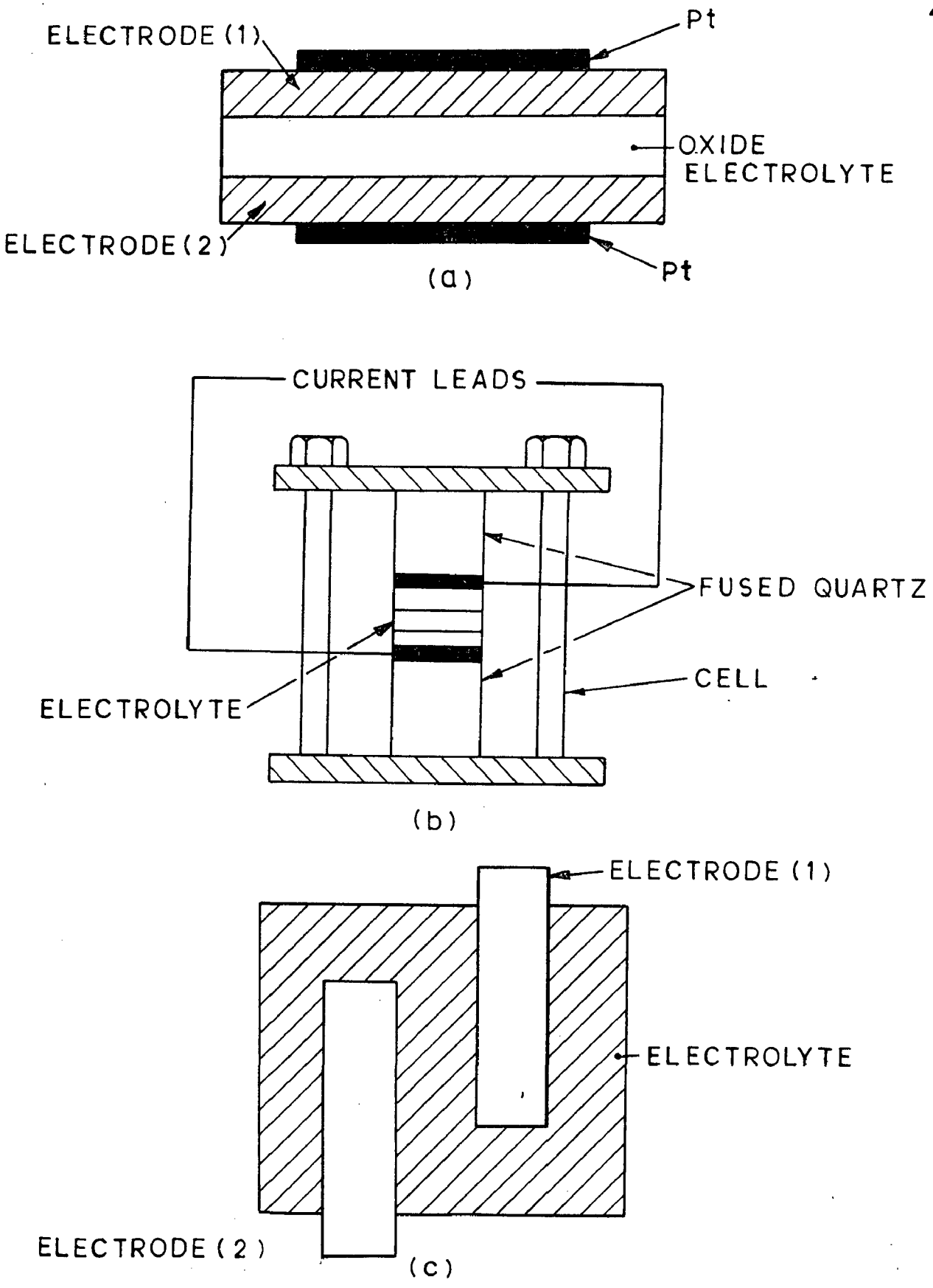

FIG.1.7 CELLS WITHOUT SEPARATE ELECTRODE COMPARTMENTS.

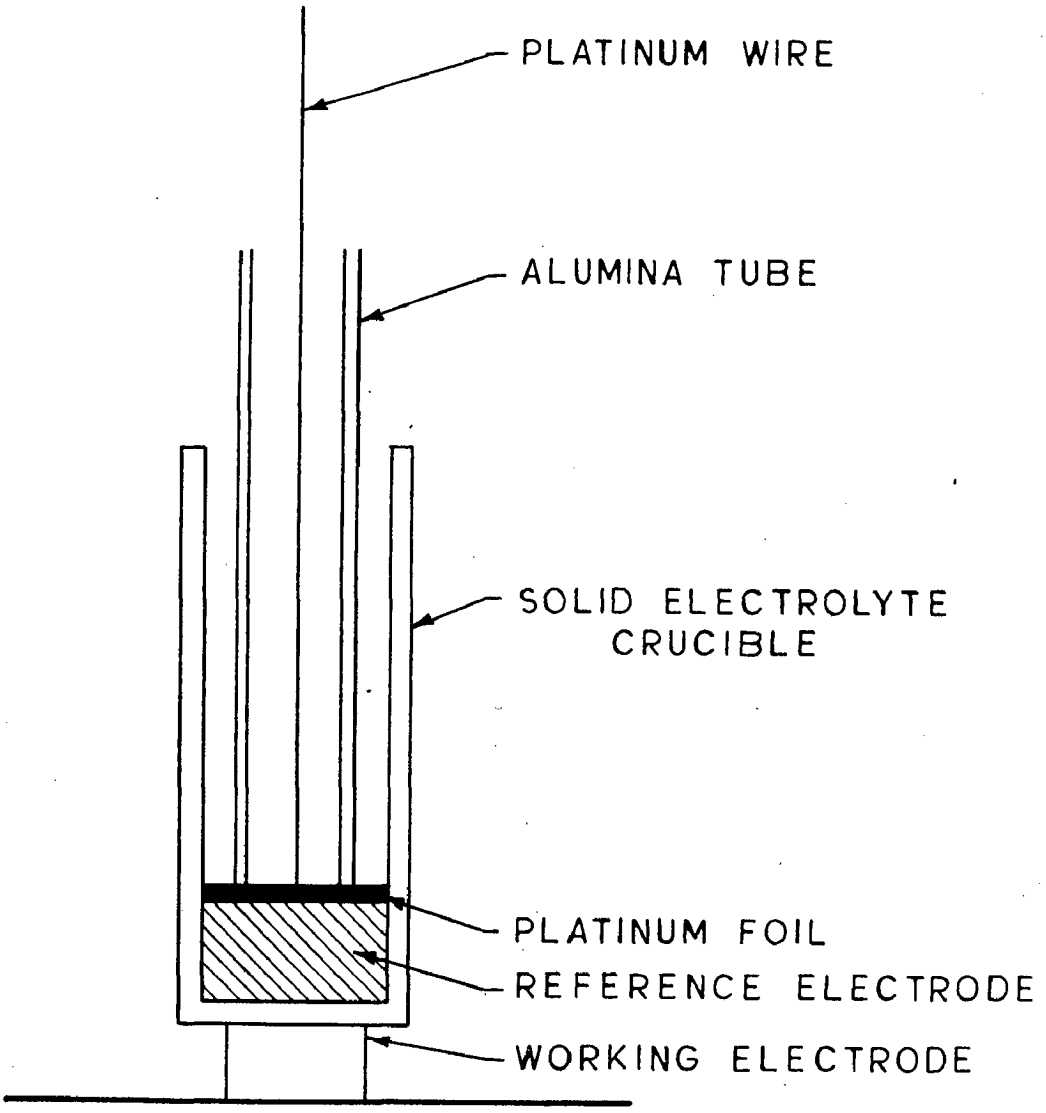

FIG.1.8 CELL DESIGN (Open-Cell Technique) [147]

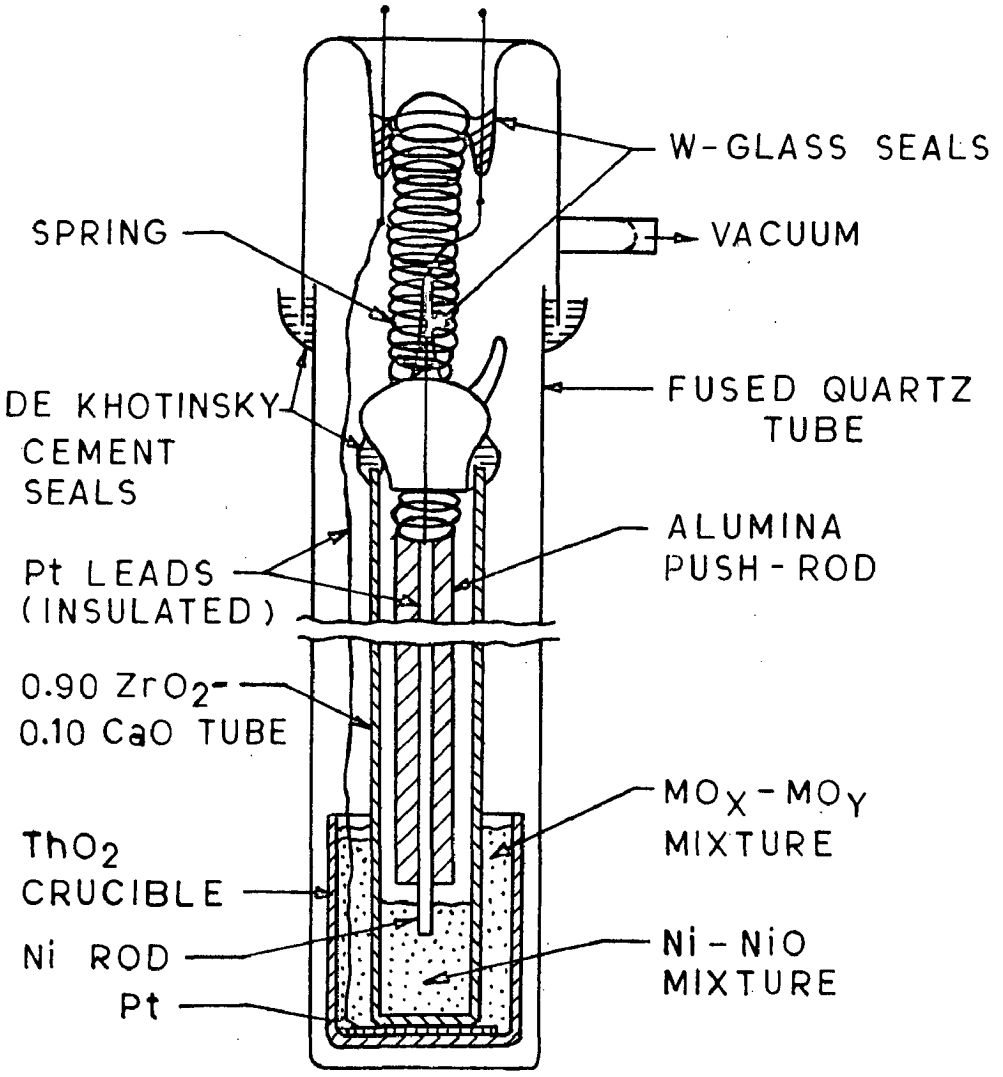

FIG. 1.9 CLOSED CELL FOR EMF MEASUREMENTS [100]

is equilibrated with a static gas phase which has an oxygen partial pressure very close to that of the electrode and the partial pressure of oxygen is measured by the galvanic cell. Though there are difficulties in measurement with this cell design, the advantages are obvious.

1.2.2.6 The cell environment

For the proper functioning of the oxygen concentration cell and to ensure that redox reactions do not occur at the electrode-electrolyte interface, the environment of the cell must be inert, either vacuum or a flowing stream of inert gas [148] . A flowing stream of inert gas has the advantage that the electrode-electrolyte contact can be checked by ascertaining the dependence of the cell emf on the gas flow rate. If the gas flow rate affects the cell emf, it can be concluded that the oxygen present in the inert gas is establishing a mixed potential at the electrode-electrolyte interface. In a discussion on the emf measurements held at Vienna [148] the importance of using a "getter" which can remove the last traces of oxygen in the vicinity of the electrolyte has been highly stressed. Gotto and Matsushita [149] recommended that the oxygen partial pressure of the gas phase should be very close to that of the two electrodes for successful measurement. If the difference between the oxygen pressures of the two electrodes is very large, separation of the electrodes into two compartments is recommended by using a solid-electrolyte tube. Too large a difference in oxygen

pressure would mean that the inert gas atmosphere may be oxidising to one electrode and reducing to the other. This difficulty can be avoided by choosing a reference electrode which establishes an oxygen pressure which is within 10^{-5} atm of the established equilibrium oxygen pressure of the test electrode. If the inert gas phase is purified to an oxygen pressure of 10^{-15} atm., the number of oxygen molecules from the gas phase striking the interface will be negligible and therefore, the inert gas should not influence the oxygen potential at the electrode interface.

1.2.2.7 Emf measuring device

A potentiometer is normally used for the measurement of emf developed by a cell. Petot et al. [150] recommended the use of an electrometer with input impedance of the order of 10^{14} ohms or more like the Vibron capillary electrometer. In the present investigation a servo-potentiometric type two-pen strip chart recorder, having internal resistance of one mega ohm and capable of measuring to 0.002 mV on the smallest range, was used.

1.2.2.8 Reversibility of the galvanic cells

The attainment of true thermodynamic equilibrium can be ascertained by checking the reversibility of the galvanic cells. For this, the galvanic cell is polarized by passing a definite amount of current in either direction and ascertaining that the

emf returns to initial value. The reversibility of the cell is also proved by measuring steady emf values of the cell at rising and falling temperatures.

1.2.3 Experimental Studies on Binary and Ternary Oxide Systems

Emf and gas-equilibrium techniques have been extensively used to measure the thermodynamic data in oxide, silicate and spinel systems. These are briefly reviewed in the following sub-sections :

1.2.3.1 Binary systems

1.2.3.1.1 System MgO-FeO

Solid solutions of wustite ('FeO') and periclase have simple sodium chloride structure. FeO-MgO phase diagram, Fig. (1.10), shows complete solid solubility between the end members [151]. Wustite has a defect structure and its composition varies from $Fe_{0.83}O$ to $Fe_{0.96}O$ within the stability range of this phase. Various thermodynamic investigations [152-158] on this system have led to the conclusion that the system shows considerable positive deviation from ideality. Shashkina and Gerasimov [152] studied the hydrogen reduction equilibria of FeO and solid solutions of FeO-MgO of different compositions at 860, 960 and 1060°C and noted that the system had a positive deviation from ideality. Schmahl et al [153] measured FeO activity by equilibrium of the solid solution

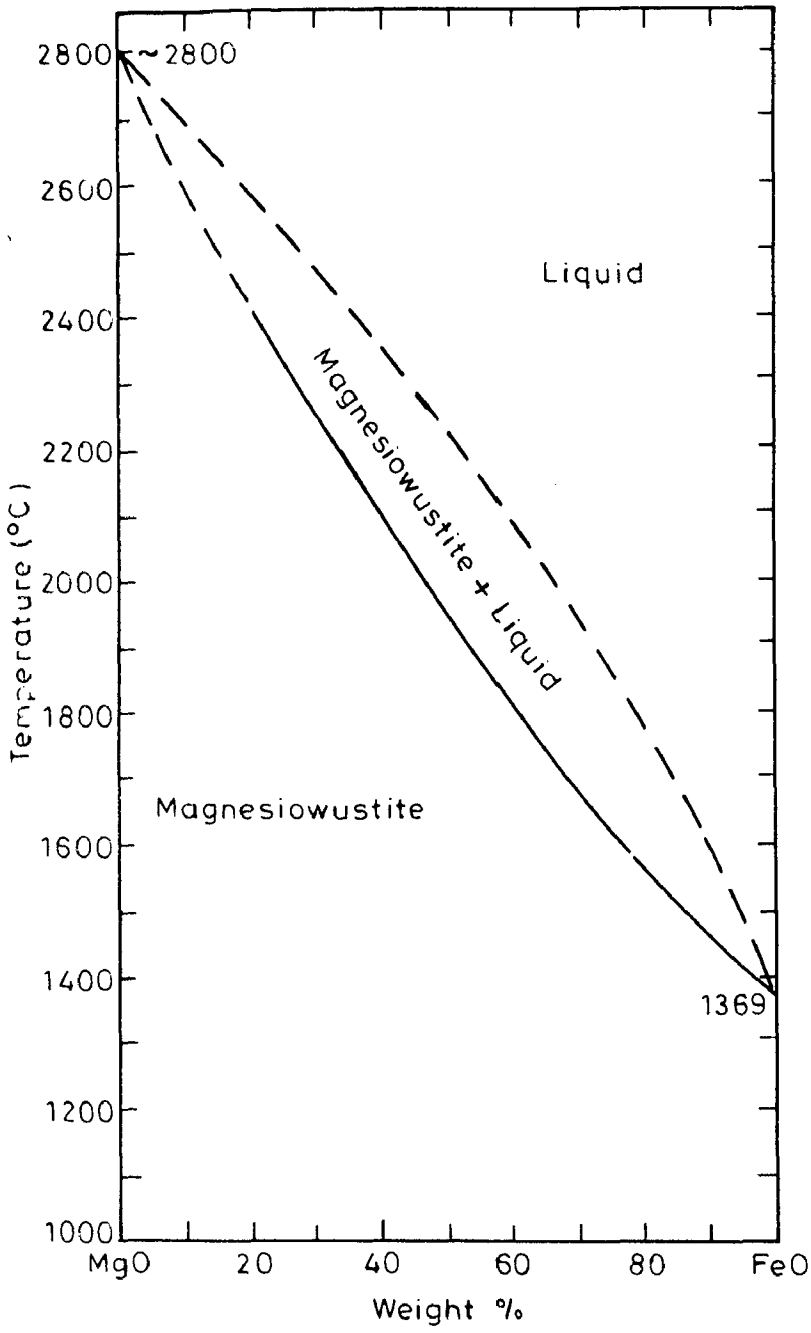

FIG.1.10. PHASE DIAGRAM FOR THE SYSTEM MgO–FeO [151]

with $CO-CO_2$ gas mixture at temperatures 800, 900 and 1000°C and reported a moderate positive deviation from Raoults law. Using CO_2-H_2 mixture to get an atmosphere of controlled oxygen partial pressure, Hahn and Muan [154] equilibrated the oxide samples with pure metallic iron and determined the values of activity of FeO in FeO-MgO solid solution in the range 1100 to 1300°C. They also reported a considerable positive deviation from Raoult's law. On the basis of the equilibrium data on the reduction of magnesium ferrochromites and ferroaluminates, Korneev et al [155] determined the thermodynamic characteristics of the $Mg_x Fe_{1-x}O$ solid solution formed during reduction in equilibrium with iron. Using statistical method for the determination of the dependence of the activity values of the components on the concentration of the solution FeO-MgO, they found that the values so obtained are in good agreement with the literature data obtained directly from experiments. Prasad [156] investigated this system using acid solution calorimetry. Gordeev et al [157] measured the emf of the cell.

$$Fe, (Fe,Mg)O/(ZrO_2)_{0.85}(CaO)_{0.15}/Fe,FeO \qquad ..(1.53)$$

in the temperature interval 900-1200°C and found that the system showed a positive deviation from ideality that increased with increasing temperature. Engell [158] determined the values of activity of FeO in the binary solid solution FeO-MgO by emf measurements with cells incorporating calcia stabilized zirconia electrolyte and reported high positive deviation from ideality for this system. Sakawa et al. [159] measured

the activity of FeO in the ternary system FeO-MgO-SiO_2 by means of the levitation method of an induction furnace at 1900°C. Their results on FeO-MgO system show slight positive deviation from ideality.

1.2.3.1.2 System CaO-FeO

Equilibrium relations in the system CaO-iron oxide at different levels of oxygen pressure have been studied in considerable detail. Fig. (1.11) shows the phases present in the system CaO-FeO as a function of temperature and total composition in contact with metallic iron [151]. Striking features of this diagram, as compared with the system FeO-MgO are (i) low liquidus and solidus temperatures prevailing in the central part of the system, and (ii) the presence of an intermediate phase (calcium ferrite). These features are largely reflections of the greater size difference between Ca^{2+} and Fe^{2+} as compared to the size difference between Mg^{2+} and Fe^{2+}. Both the oxides have limited solubility for each other and the solid solutions of CaO and FeO have simple sodium chloride structure. Johnson and Muan [160] studied the CaO-FeO-SiO_2 system in contact with metallic iron at 1080°C by equilibrating the samples with CO/CO_2 gas mixtures. They calculated activity-composition relations for CaO-FeO solid solutions along CaO-FeO join and reported a large positive deviation from ideality for this system. As reported by Muan et al [160], Hahn [161] investigated this system at 1090°C and he also reported a large positive deviation from Raoult's law. Lykasov et al [115]

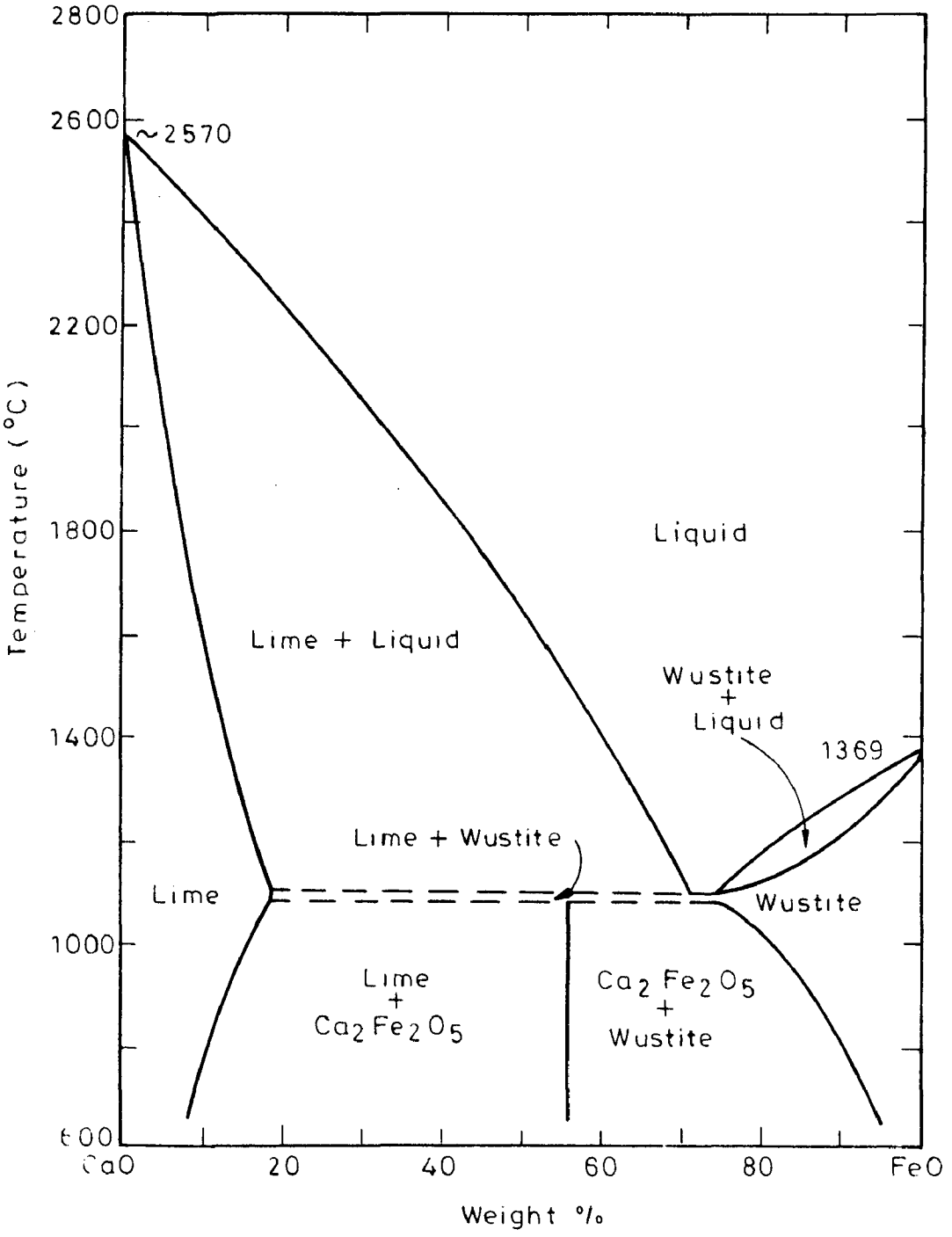

FIG.1.11. PHASE RELATIONS IN THE SYSTEM CaO-FeO IN CONTACT WITH METALLIC IRON [151]

determined the solubility of CaO in wustite in equilibrium with iron in the temperature interval 850-1050°C by measuring emf of the cell

$$Pt/Fe,(Fe,Ca)O//ZrO_2(CaO)//Fe,FeO/Pt \qquad ..(1.54)$$

They found that calciowustite is a regular ionic solution of wustite and CaO. Tare and Deo [114] also studied this system by emf method and determined solid solubility limits. Shiro Ban-ya et al [162] measured the equilibrium between H_2/H_2O gas mixture and liquid FeO-CaO, FeO-SiO_2, FeO-TiO_2 and FeO-Al_2O_3 slag samples at 1400°C. They calculated the activity of FeO and the ratio of Fe^{2+} and Fe^{3+} as a function of composition. To evaluate the thermodynamic properties of complex slags from those of binary slags, they applied a regular solution model for cations and expressed quantitatively the oxygen distribution between slag and metal over the wide range of slag composition.

1.2.3.1.3 Other binary isostructural metal oxide systems

The binary iso-structural solid solutions are of interest because they form the starting point for the understanding of more complex oxide systems met with in practice. Many attempts have been made in the past to measure the thermodynamic properties of these systems, which are briefly reviewed in the following lines:

Complete miscibility at high temperatures in the system FeO-MnO was established by Andrews et al. [163] , Jay and

Andrews [164] and Foster and Welch [165]. Conflicting results have been reported for the activities of component oxides in this system by various investigators. Foster and Welch [166] studied the system FeO-MnO by gas-equilibria technique in the temperature range 850-1150°C and found that this system behaved ideally, within the limits of error. Schenck et al [167] employed the same technique and reported moderate positive deviation of FeO activities from Raoult's law. Schwerdtfeger and Muan [168] too adopted gas-equilibria technique to study this system in the temperature range 1000-1300°C and confirmed the results of Schenck et al [167]. However, Engell [158] reported very high positive deviation from ideality, who studied this system by high temperature solid electrolyte galvanic cell technique. Engell's results indicate that the system FeO-MnO follows regular solution behaviour. Still higher positive deviations have been reported by Takenov et al. [169], who used gas-equilibria technique to study this system. Averbukh et al [170] have used equilibrium technique and have reported negative deviation in this system. Seetharaman [171] measured activities in this system using solid electrolyte galvanic cell and found FeO activities in rough agreement with those reported by Engell [158].

Aukrust and Muan [172] determined the activity-composition relationship in the system FeO-CaO at 1200°C by gas-equilibria technique and reported that the system showed a slight positive deviation from ideality. Seetharaman and Abraham [173] studied the system in the temperature range

800-1000°C employing a ThO_2-Y_2O_3 solid electrolyte galvanic cell and reported a positive deviation from ideality, which decreased with increasing temperature. Seetharaman [171] studied this system by acid solution calorimetry too.

The complete miscibility in the system CaO-CdO was established by Natta and Passerini [174]. Prasad [156] measured the CaO activities in this system by emf technique employing a fluoride solid electrolyte and found that the system CaO-CdO behaved ideally. Raghavan [175] also reported that this system behaved ideally, who studied this system by a modified cell arrangement in which solid solution electrode was separated from the CaF_2 electrolyte.

Passerini [176] and later Karlsson [177] established a complete solid solubility in the system NiO-MgO. Hahn and Muan [178] studied this system by gas-equilibria technique and reported the system to be ideal. On the other hand Seetharaman and Abraham [179] reported that the system NiO-MgO exhibited substantial positive deviation from ideality, who studied this system by emf technique. Petot et al [150] concluded from their studies that this system behaved ideally. Raghavan [175] using fluoride solide electrolyte, found the system to be regular, exhibiting considerable positive deviation.

Jay and Andrews [164] and Woermann and Muan [180] investigated the system MgO-MnO by X-ray studies and reported that the system had complete miscibility at 1150° and 1500°C. Woermann and Muan [180] and Hahn and Muan [181] inferred the

approximate activity-composition relations in this system and showed that the system displayed strong positive deviation from ideality at 1100, 1200 and 1300°C . Raghavan [175] investigated this system by emf technique in the temperature range 900-1050°C and reported a positive deviation from ideality.

Jay and Andrewes [164] and Glasser [182] made an X-ray study of the system CaO-MnO and found that the system exhibits complete miscibility in the temperature range of study, viz. 1000° - 1700°C. Tiberg and Muan [183] inferred the approximate activity-composition relations in this system and reported that the system displayed a considerable positive deviation from ideality at 1100°C. Raghavan [175] also arrived at the same conclusion from his emf studies on this system.

Aukrust and Muan [172] studied the system CoO-MgO by gas-equilibria technique at 1200°C and reported that the system was ideal. Seetharaman and Abraham [184] measured the activity of CoO in CoO-MgO solid solution in the temperature range 800-1000°C using ThO_2-Y_2O_3 solid electrolyte cell and reported that the system exhibited slight positive deviation and confirmed to a regular solution model. Prasad [156] and Rigand et al [111] have also studied CoO-MgO system using emf technique. System CoO-MnO is investigated by Aukrust and Muan [172] using gas-equilibria technique and by Seetharaman and Abraham [185] using ThO_2-Y_2O_3 solid electro-lyte cell. Cameron and Unger [112] studied the system NiO-MnO employing a solid electrolyte cell and reported that positive deviation

from ideal behaviour is exhibited by the system. Hahn and Muan [178] used gas equilibria technique and Seetharaman and Abraham [186] employed solid electrolyte cell technique to study this system. Raghavan [175] established the terminal solid solubilities in the system CaO-CoO in the temperature range 850-1050°C using emf technique.

1.2.3.2 Ternary systems

An understanding of the manner in which the activities of the metal oxides and silica vary with composition in ternary and complex silicates is of great importance to the extraction metallurgist. A knowledge of the thermodynamic properties of ternary and higher oxide systems in absence of silica is also useful to a metallurgist. Apart from phase diagram studies, measurements have been made of the thermodynamic properties of ternary oxide and silicate mixtures. These are reviewed in the following sub-sections.

1.2.3.2.1 System $MgO-FeO-SiO_2$

Experimental investigations of parts of the system $MgO-FeO-SiO_2$ were initiated some seventy years ago by Bowen and Andersen [187] and further investigations were followed by Greig [188] and Bowen and Schairer [189]. Bowen and Schairer [189] studied this system in detail and established a comprehensive knowledge and understanding of phase relations in this system. These authors showed that there is a complete

Solid-solution series extending from $MgSiO_3$ part-way towards $FeSiO_3$, the maximum content of the latter component being approximately 56 mole percent at solidus temperature. Fig.(1.12) shows a subsolidus isothermal section through the system MgO-FeO-SiO_2 in contact with metallic iron.

As mentioned by Richardson [190], Sahama and Torgeson [191] carried out calorimetric measurements on the crystalline solid solutions $MgSiO_3$+$FeSiO_3$ and Mg_2SiO_4+Fe_2SiO_4 and reported that heats of formation of these solid solutions were negligibly small at room temperature. Richardson [190] calculated the values of activity of $MgSiO_3$ in the pyroxene solid solution near the liquidus temperature over the range 0 to 54 %. $FeSiO_3$ and found that $MgSiO_3$ activities were almost ideal.

Kitayama and Katsura [192] determined the activity-composition relations in ortho-, and metasilicate solid solutions in the FeO-MgO-SiO_2 system at 1204°C on the basis of the measurement of equilibrium oxygen partial pressure and found that both the olivine and pyroxene solid solutions exhibited significant positive deviation from ideality.

Muan et al [193] determined the compositions of(Mg,Fe) SiO_3 solid solutions (20 to 60 mole percent $FeSiO_3$) in equilibrium with tridymite and metallic iron as a function of oxygen pressure (10^{-11}-10^{-13} atm) at 1250 and 1300°C. From their data, they calculated the standard free energy change for the following reactions:

$$x\ Fe+Fe_{1-x}O+SiO_2 = FeSiO_3 \qquad ..(1.55)$$

$$Fe_2SiO_4+SiO_2 = 2FeSiO_3 \qquad ..(1.56)$$

and found that $\Delta G^{o}_{(1.55)}$ is approximately -1 K.Cal and

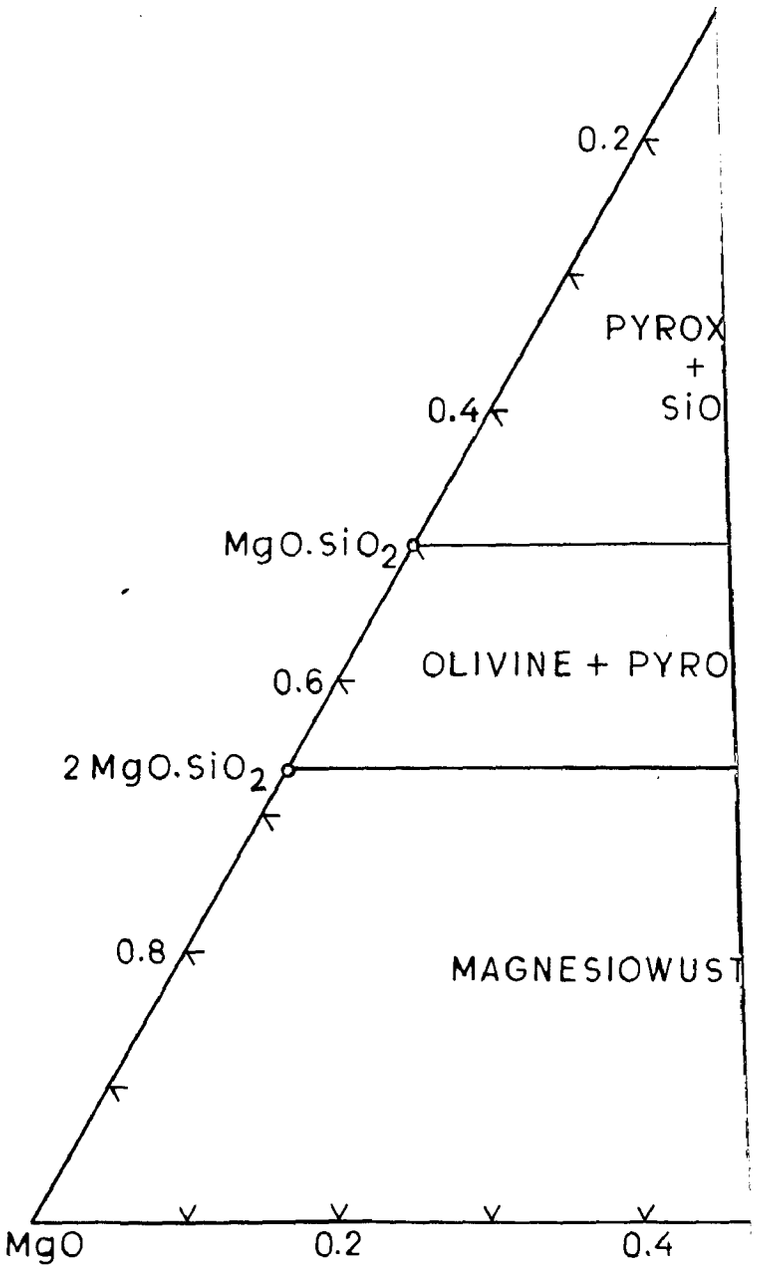

FIG. 1.12. SUBSOLIDUS ISOTHERMAL
MgO - FeO - SiO_2 IN CONTA

$\Delta G^{\circ}_{(1.56)}$ approximately ± 2 K.Cal at these temperatures.

Nafziger and Muan [194] determined the compositions of coexisting solid solution phases in the system $MgO-FeO-SiO_2$ under low oxygen partial pressures by equilibrating the samples with CO_2-H_2 gas mixtures at solidus and subsolidus temperatures. The data was used by them to derive activity-composition relations for the silicate solid solutions within the system and stability data for end-member compounds. Their studies revealed that olivine solid solution had a moderate positive deviation from ideality, whereas the pyroxene solid solution was practically ideal. They have reported the value of the standard free energy of formation of $FeSiO_3$ from its component oxides to be -0.9 K.Cal/mole at 1250°C and that of Mg_2SiO_4 to be -13.1 K.Cal/mole at 1200°C. Their data was helpful in dealing with problems of distribution of Fe^{2+} and Mg^{2+} among rock-forming minerals.

Kojima et al [195] determined the compositions of the $FeO-MgO-SiO_2$ slags in equilibrium with the liquid iron at 1600°C and determined the activity values of FeO. Slag composition determined by them were in good agreement with those estimated from the solidus line of the equilibrium diagram. The activity values of FeO showed a positive deviation from ideality. They have presented the isoactivity curves in this ternary system.

Sakawa et al [159] measured the activity of FeO in the ternary system $MgO-FeO-SiO_2$ by means of the levitation method of an induction furnace at 1900°C. Isoactivity lines of FeO

in this system have been drawn by them at this temperature. Activity values of FeO and MgO, calculated by these workers, for the binary system FeO-MgO show a slight deviation from ideality. They calculated the activity of MgO in the binary system $MgO-SiO_2$ from the activity of FeO in this ternary syste and applied the polymer theory to the $MgO-SiO_2$ system. The theoretical curve fitted the calculated values of activity of MgO in the system $MgO-SiO_2$ when the equilibrium constant of the polymer theory was 0.01. They reported that application of the polymer theory to the ternary system $MgO-FeO-SiO_2$ could be possible with several assumptions.

1.2.3.2.2 Other ternary silicate systems

Because of the metallurgical and geochemical importance of the oxides CaO, FeO and SiO_2, the system CaO-FeO-SiO2 has been the subject of several experimental studies during the past 50 years. Phase relations in the system $CaO-FeO-SiO_2$ in contact of metallic iron were determined by Bowen et al [196] and additional phase-equilibrium data for this system have been presented by Allen and Snow [197]. Chipman and associate [198,199] in early forties, determined activities of FeO in liquidus of this system. Since that time attempts have been made by Richardson [191,200] and by Flood and coworkers [201] to interpret the data of Chipman et al in terms of the constitution of the silicate liquids and the interaction parameters among the various constituents of the system. Results of Chipman et al [198,199] have been used by Elliott [202] to

calculate approximate values of the activities of CaO and SiO_2 by application of the Gibbs Duhem relationship. Ende et al [203] studied the saturation limits of $CaO-FeO-SiO_2$ slags by equilibrating these slags with iron melts at 1650°C. They determined the activity of FeO in the range of unsaturated slags and along the saturation isotherm and investigated the equilibrium of Mn, P, S and Cr reactions as a function of slag composition and temperature. Lavrov et al [204] studied the slags of the $FeO-CaO-SiO_2$ system at 1250,1300 and 1350°C by gas-equilibria technique. They reported an increase in FeO activity with an increase in temperature and also with an increase in basicity. Indyk and Bell [116] measured the activity of FeO in this system in the temperature range 700-1050°C by emf method and proposed few minor modifications to the phase diagram. Johnson and Muan [160] determined the equilibrium CO_2/CO ratios of a gas phase coexisting with selected oxide phase assemblages of the system $CaO-FeO-SiO_2$ and metallic iron. From the data obtained, they calculated the activity-composition relations for metasilicate, orthosilicate and CaO-FeO solid solutions and determined the value for the free energy of formation of $Ca_3Si_2O_7$. Floridis and Moser [205] determined the activity of ferrous oxide in ferromonticellite ($CaO.FeO.SiO_2$) at 920-1100°C gravimetrically by equilibrating the samples with atmospheres having controlled oxygen potential. Value of ferrous oxide activity increased from 0.62 at 920°C to 0.68 at 1100°C. Wanibe et al [206] measured the oxygen activity of a Ag melt in equilibrium with the liquid slags $FeO-CaO-SiO_2$ and $FeO-MnO-SiO_2$ between 1250

and 1350°C. The values of the activity of FeO were calculated from the experimental data and the isoactivity lines of FeO were plotted for the system $CaO-FeO-SiO_2$.

The general features of the sub-solidus phase relations in the system $FeO-MnO-SiO_2$ under strongly reducing conditions are known from the work of Riboud and Muan [207]. Schwerdtfeger and Muan [208] determined the equilibrium ratios CO/CO_2 of a gas phase coexisting with selected compositions of the system $FeO-MnO-SiO_2$ at 1150°C. From the data thus obtained, they derived the activity-composition relations for the various oxide components of the olivine and the pyroxenoid solid solutions. They also evaluated the standard free energies of formation of ferrosilite ($FeSiO_3$), tephroite (Mn_2SiO_4), and rhodonite ($MnSiO_3$) from their component oxides. Fujita and Maruhashi [209] performed the studies on equilibrium between $FeO-MnO-SiO_2$ slags and molten iron at 1560°C and constructed the iso-activity diagrams for the $FeO-MnO-SiO_2$ melts and iso-concentration diagrams for molten iron in equilibrium with these slags.

Kalyanram et al [210] studied the sulphur equilibrium between $CO-CO_2-SO_2$ gas mixtures and $CaO-MgO-SiO_2$ slags at 1500°C and used the results to assess the activity of lime in these slags. To survey the liquid field in the $CaO-MgO-SiO_2$ system, Henderson and Taylor [211] determined the activity values of SiO_2 in liquid oxide solution at 1500 and 1550 °C by measuring the equilibrium pressure for the reaction : $SiO_2+3C=SiC+2CO$. Sawamura [212] determined the activity of

CaO in the ternary systems CaO-MgO-SiO_2 and CaO-MnO-SiO_2 at 1600°C by measuring the emf of the double cell. Relations between the activity of CaO and basicity ratio of the slags were found from the experimental data and the diagrams of constant CaO activity were plotted for the system studied. Abraham et al [213] measured the activity of MnO at 1500-1650 °C in the CaO-MnO-SiO_2 melts by equilibrating the melts with a gas phase of controlled oxygen potential. Glasser [182] studied the system CaO-MnO-SiO_2 and presented the phase equilibrium data from quenching experiment. Pillay and Richardson [214] studied the system PbO-CaO-SiO_2 at 1200 °C and presented the isoactivity contours for PbO in this system. Kapoor and Frohberg [215] determined the activity values of PbO in the system Na_2O-PbO-SiO_2 by emf technique in the temperature range 800 to 1050 °C, plotted isoactivity curves for PbO at 1000 °C and explained their results in terms of positive cations interaction energies.

1.2.3.2.3 Ternary iso-structural oxide systems

A survey of literature reveals that very limited work has been done on the thermodynamic properties of ternary oxide systems, which have some relevance to extractive metallurgy. Some preliminary work on the system FeO-CaO-MgO was performed by Brisi and Burdese [216], who reported that a solid solution containing 90 % FeO and 10 % MgO could dissolve about 6 % CaO at 1000 °C and an increase of MgO decreased the solubility of CaO. A systematic study to determine the phase equilibrium

relations in the system FeO-CaO-MgO at 1500°C was carried out by Johnson and Muan [217], which had a bearing on the performance of tar-bonded dolomite refractories under conditions existing in a steelmaking vessel. The 1500°C isothermal section through this system at an oxygen pressure of 10^{-9} atm after Johnson and Muan [217] is shown in Fig. (1.13). However, no work could be found in literature on the study of thermodynamic properties of this system.

Like FeO-CaO-MgO system, component oxides of the ternary oxide system CaO-FeO-MnO are also iso-structural. Solid-liquid equilibria in the system CaO-FeO-MnO in contact with liquid iron was studied by Valla et al [218]. They found that solid miscibility gap between CaO and FeO in the system CaO-FeO in contact with metallic iron gradually closes as MnO is added as a third component. Activity-composition relations at 1100°C in this system in contact with metallic iron were experimentally determined by Tiberg and Muan [183] by using gas-equilibria technique. They determined the extent of the solid miscibility gap in this system and plotted the iso-activity curves for FeO, CaO and MnO at 1100°C and also calculated the activity values of CaO and MnO in the binary system CaO-MnO, which displayed considerable positive deviation from ideality at the temperature of study.

1.3 FORMULATION OF THE PROBLEM

Importance of systematic experimental and theoretical studies of thermodynamic properties of oxide and silicate

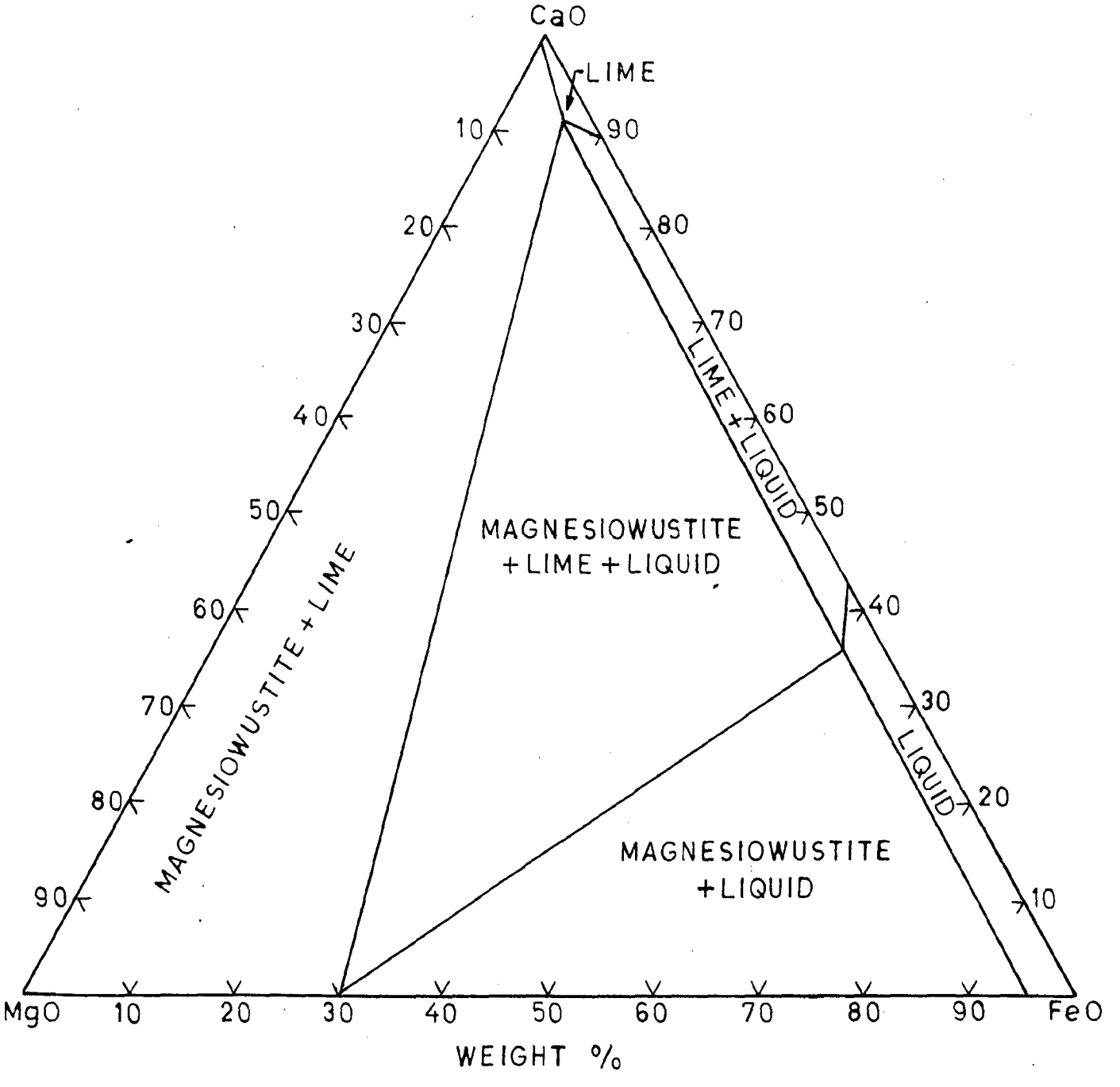

FIG. 1.13 PHASE RELATIONS IN THE SYSTEM CaO - MgO - FeO AT 1500 °C. After Johnson and Muan [217]

systems has been amply demonstrated in earlier sections. Preferred suitability of emf method over other experimental techniques for such experimental investigations has also been emphasized. It has been pointed out that the system FeO-MgO-SiO_2 has mostly been investigated for phase equilibria and no data on thermodynamic properties of the system FeO-MgO-CaO at any temperature is available in literature. Further, thermodynamic properties of the system FeO-MgO-SiO_2 have been experimentally investigated using gas-equilibria technique and only one systematic work [217] on the phase stability relations in the system FeO-MgO-CaO at 1500°C is reported in literature. Also, although several workers [152-158] have studied the system FeO-MgO using gas equilibria as well as emf technique, the data reported is not consistent. Activity-composition relations in binary system FeO-CaO were derived by Johnson and Muan [160] from the data obtained on the ternary system FeO-CaO-SiO_2 using gas-equilibria technique. Various workers have studied the binary system FeO-CaO [114,115,161,162] at different temperatures and as the solid solubility limits in this system change with temperature, experimentally determined activity-composition relationship are not meaningful at temperatures, which differ much from the temperature of study.

In the present investigation, therefore, thermodynamic properties of the ternary systems FeO-MgO-SiO_2 and FeO-MgO-CaO at 1000 K will be studied using emf technique employing solid electrolyte cell. For experimental runs, a suitable set-up using calcia-stabilized zirconia solid electrolyte cell working under an inert atmosphere of purified dry nitrogen will be

designed and locally fabricated. Experimental studies will initially be carried out on the relevant binary systems, viz. FeO-MgO, FeO-CaO and FeO-SiO_2, and then on the two ternary systems selected. The experimental data so obtained on binary systems will be compared with the existing data in literature. Further, the experimental data on the binary systems, coupled with that on the ternary systems will be utilized to calculate and interpret : (i) activity plots of component oxides as applicable to the isothermal section at 1000 K of the two ternary systems studied, (ii) standard free energy of formation of compounds $Ca_2Fe_2O_5$, $FeSiO_3$ and Fe_2SiO_4 from their component oxides, (iii) thermodynamic properties of the pyroxene and olivine solid solutions, and (iv) the phase stability relationships in the ternary system FeO-MgO-CaO at the temperature of study. Results obtained from the present investigation will be compared, wherever possible with the relevant data available in literature..

CHAPTER-2

EXPERIMENTAL

This chapter deals with the materials used and technique adopted for the present work. The electromotive force method employing calcia stabilized zirconia solid electrolyte was adopted to study the thermodynamic properties of different binary and ternary oxide systems. The different materials used, experimental set up, methods adopted for the preparation of samples and actual experimental runs are described in the following sections.

2.1 MATERIALS USED

Pure quartz lumps were picked up from a quarry near Delhi and Analar grade chemicals such as ammonium ferrous sulphate (Glaxo Laboratories (India) Ltd., Bombay), calcium oxide (Fisons, Philadelphia, U.S.A.), magnesium oxide (Thomas Baker and Co., London), electrolytic grade iron powder (Sarabhai Merck Limited, Baroda), electrolytic grade nickel powder (Sarabhai M.Chemicals Ltd., Baroda), nickel oxide (Narang Chemical Industries, India), conc. hydrochloric acid (Glaxo Laboratories (India) Ltd., Bombay)etc. were used for the present work. Calcia stabilized zirconia pellets, used as solid electrolyte, were procured from M/S Friedrichsfeld, W.Germany.

2.2 EXPERIMENTAL SET-UP

Figure (2.1) shows the block diagram of the experimental set-up used for the present studies. Essential features of the experimental set-up are: gas purification train, sample preparation unit and cell assembly with proper thermostatic control for maintaining the desired temperature.

2.2.1 Gas Purification Train

High purity nitrogen, made available from M/S Modi Gas and Chemicals Ltd., Modi Nagar, was further purified with the aim of removing moisture and lowering down the oxygen partial pressure of the gas. Nitrogen gas from cylinder was bubbled through conc. H_2SO_4 and alkaline pyrogallol solution contained in a series of bubblers (nine bubblers were connected in series such that first, fifth and ninth were empty, second, third and fourth contained sulfuric acid and sixth, seventh and eighth contained alkaline pyrogallol solution). Then the gas was passed through phosphorus penta oxide powder. Next, the gas was passed over copper turnings kept in a furnace at 480°C followed by iron turnings also maintained at 480°C. The gas was finally passed through the graphite pieces (1 to 2 mm size) kept in a furnace at 800°C before it was allowed to enter the cell assembly or sample preparation unit. Flow rate of the gas was measured with a capillary flow meter placed just after the gas purification train and was maintained at about 50 ml/min.

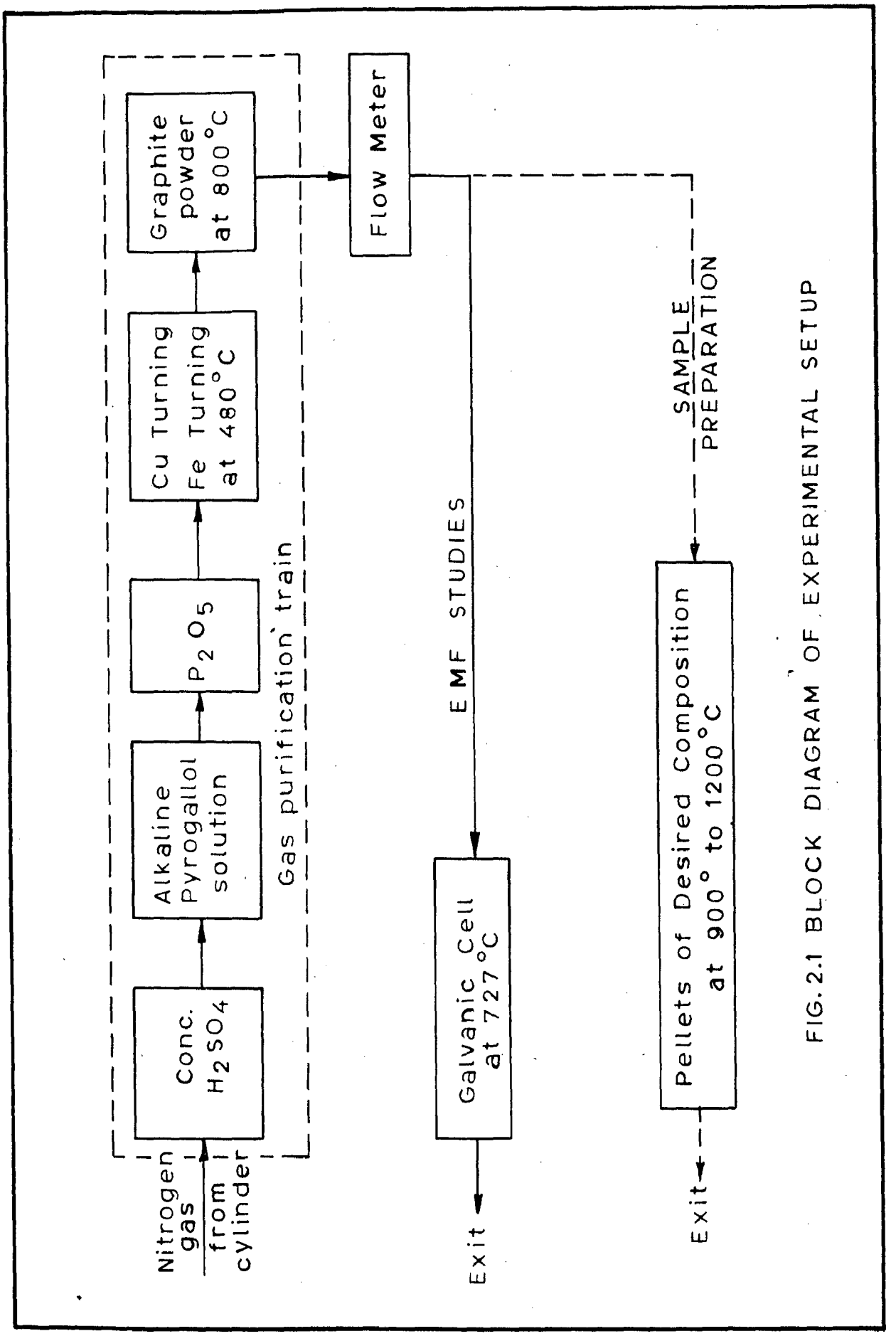

FIG. 2.1 BLOCK DIAGRAM OF EXPERIMENTAL SETUP

2.2.2 Sample Preparation Unit

A horizontal globar furnace employing silicon carbide rods as heating elements (M/S Bysakh and Co., Calcutta) was used for homogenisation of samples. Recrystallised alumina tube, cemented with B55 pyrex glass joints by means of araldite on both ends, was placed between the four silicon carbide rods. The ends of reaction tube were water cooled by means of copper cooling jackets. Temperature of the furnace was controlled by means of an electronic temperature controller (M/S Applied Electronics Ltd., Thana, India), employing a Pt/Pt-13 % Rh control thermocouple. All the samples investigated in the present work were prepared in an inert atmosphere of purified nitrogen using the furnace described above.

2.2.3 Cell Assembly

Details of the cell assembly used are shown in Fig.(2.2). The cell consists of three pellets : (i) (Fe+FeO) pellet as reference electrode, (ii) calcia stabilized zirconia pellet as solid electrolyte, and (iii) (Fe+oxide system containing FeO) pellet as test electrode. These three pellets were kept in a one-end closed recrystallised alumina tube (500 mm long, about 30 mm internal diameter and 2 mm uniform wall thickness) such that calcia stabilized zirconia electrolyte was sandwitched between the reference electrode and the test electrode. Thermocouple sheath, resting on test electrode was spring loaded to ensure good contact between the pellets. The whole assembly was supported closed end down by means of suitable

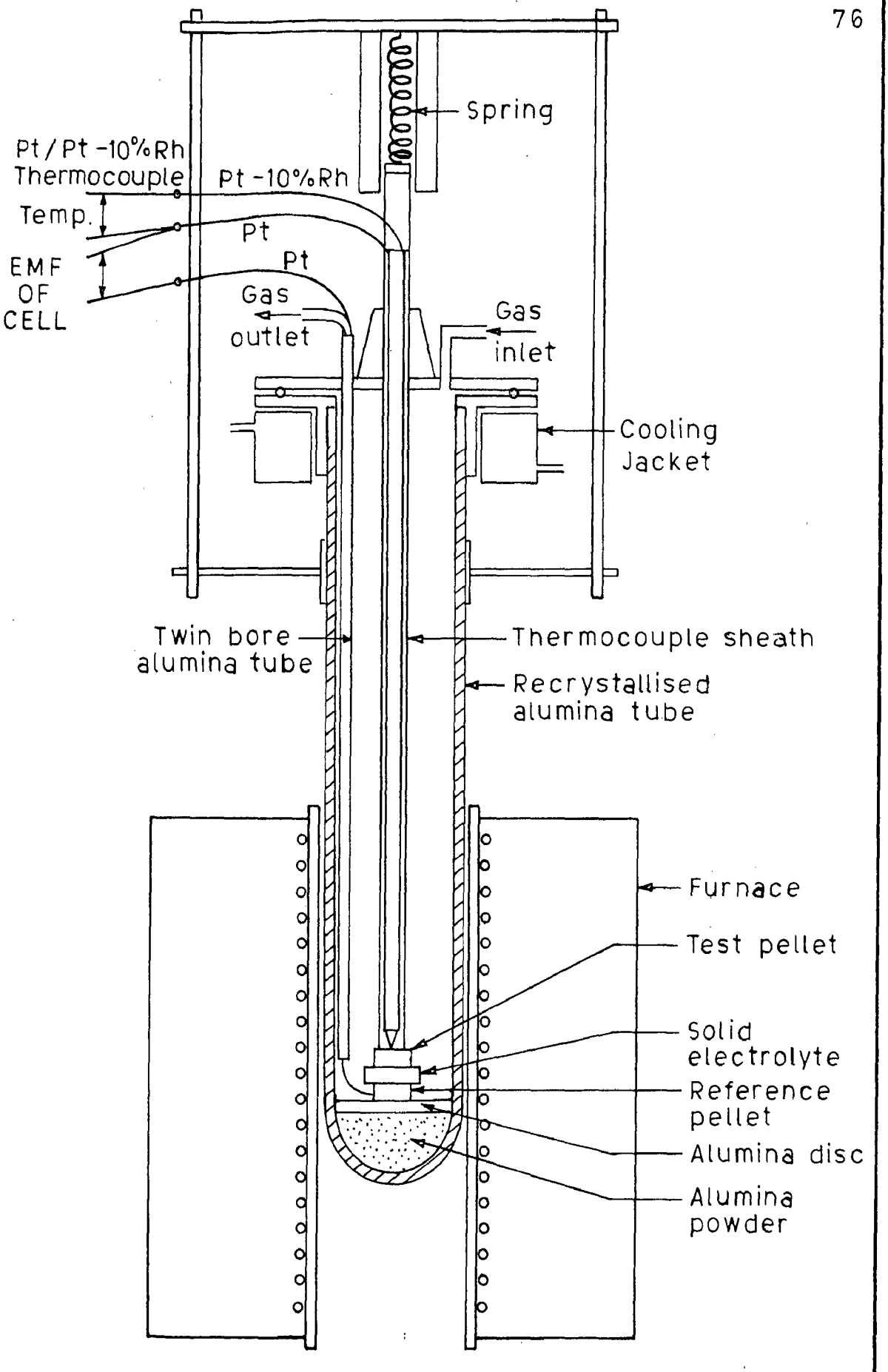

FIG. 2.2 THE CELL ASSEMBLY

clamps and introduced into the furnace tube with non-inductive winding and proper thermostatic control to obtain and maintain the desired temperature. The temperature of the furnace was controlled by means of an electronic temperature controller (M/S Applied Electronics Ltd., Thana, India) to an accuracy of $\pm$ 2°C. The temperature of the cell was measured with the help of a Pt/Pt-10 % Rh thermocouple in contact with the top electrode. Emf of the cell was measured by connecting two platinum leads, i.e. platinum lead of the thermocouple and a single platinum lead in contact with the bottom electrode, to a two-pen strip chart recorder (Houston Instruments Inc., U.S.A.).

2.3 PREPARATION OF SAMPLES

Basic oxides used for preparation of samples were wustite, silica, magnesia and calcia. This section deals with the preparation of wustite, purification of quartz and preparation of samples for study of binary and ternary oxide systems from pure oxides and also the preparation of electrodes for the cell.

2.3.1 Preparation of Wustite

To obtain wustite, first α -Fe_2O_3 was produced from analar ammonium ferrous sulphate by the thermal decomposition. Thermal decomposition was carried out in two stages-initially ammonium ferrous sulphate was heated at 900°C for 48 hours and the product obtained in the first stage was heated at

1150°C for 24 hours. Product thus obtained was confirmed to be α-Fe_2O_3 by X-ray diffraction analysis. Electrolytic grade iron powder, slightly in excess over the amount that was required to form wustite, was added to α-Fe_2O_3. This mixture was compacted in a die at a pressure of 440 MN m^{-2}. These compacts, (cylindrical pellets of 18 mm diameter and about 10 mm height) were placed in an iron boat and were heated at 1150°C for 8 hours in an inert atmosphere of purified nitrogen. These compacts were first furnace cooled upto 700°C and then rapidly cooled to room temperature by drawing the iron boat containing compacts in the colder region of the alumina tube (at this stage, flow rate of nitrogen was increased to facilitate the faster cooling). The resulting product, when investigated by X-ray diffraction analysis, revealed simple NaCl structure with d spacings corresponding to the structure of wustite.

2.3.2 Purification of Quartz

Quartz lumps picked up from quarry were crushed and ground to -48 mesh size. This silica powder was treated with conc. HCl several times and finally washed with distilled water and dried to render it free of any clay or other soluble impurities. The product analysed silica greater than 99 %.

2.3.3 Sintering of Oxide Mixtures

Various compositions were selected for studying binary and ternary oxide systems on the basis of their respective

phase diagrams. Compositions of these samples for binary systems are given in Chapter 3 and for that of ternary systems in Chapter 4, where experimental results and the properties derived from experimental data are presented.

Accurately weighed quantities of the component oxides were used for the preparation of samples of desired compositions. The weighed ingredients were mixed thoroughly in a hand mortar. These powdered mixtures were compacted into pellets at a pressure in the range of 340 to 440 MN m^{-2}. Maximum of five samples, placed in an iron boat and covered by a thin layer of iron powder, were sintered in an atmosphere of dry, purified nitrogen. Most of the samples were sintered at 1200°C. Sintering time of 8 days at 1200°C was found to be sufficient for obtaining equilibrium phases in the oxide-mixtures, as revealed by the X-ray diffraction analysis of the samples of the binary system FeO-MgO. However, sintering time for ternary oxide-mixtures was approximately doubled (samples were initially sintered for 8 days, quenched, ground to fine powder, compacted and resintered for another 10 days). Samples having compositions in the vicinity of the central region of FeO-CaO join in FeO-MgO-CaO system were sintered at 1050 °C. Samples corresponding to composition of low solidus in FeO-CaO system were sintered at 1070°C. All the samples, which were sintered below 1200°C, were initially sintered for 10 days, quenched, ground to fine

powder , compacted and resintered for another 10 days. Finally, all the samples were mixed with iron powder, compacted to pellets and sintered at 900°C for 4 hours.

2.3.4 Preparation of Pellets for the Cell

Sintered compacts of homogenised oxide-mixtures were broken into small pieces and then ground to fine powder in a hand mortar. To each of these ground mixtures, iron powder, about two and a half times the weight of the given mixture, was added and thoroughly mixed. These mixtures, containing about 70 wt percent metallic iron and about 30 wt percent oxide-mixture, were compacted in a die at a pressure of 440 MN m^{-2}. As it was not possible to polish the compacts in the green state, these compacts were sintered at 900°C, in an inert atmosphere of purified nitrogen for 4 hours. The resulting pellets were polished using fine grade emery papers (1/0 to 4/0) in the same way as metallographic specimens are polished. These pellets (18 mm dia and 4 to 6 mm thick) were used as samples or test electrodes.

Similarly, sufficient iron powder was added to wustite powder such that the resulting mixture contained about 30 wt percent wustite. Reference electrodes (18 mm dia and 6 mm thick) were made from these mixtures by following the same procedure, as was used to prepare the test electrodes.

Both the surfaces of calcia stabilized zirconia pellets (20 mm dia, 3 mm thick) were polished on fine grade emery papers to obtain smooth surfaces required to obtain good contact between the pellets of the solid state electrochemical cell.

2.4 EXPERIMENTAL RUNS

2.4.1 EMF Studies

The cell was assembled as shown in Fig. (2.2). Purified nitrogen gas was allowed to flush out the tube before the heating of the furnace was started. When the temperature of the cell reached 1000 K, recording of the emf and temperature of the cell was begun. Emf of the cell was recorded by a servo-potentiometric type two-pen strip chart recorder (Houston Instruments Inc., U.S.A.). This recorder has an input resistance of one mega ohm and is rated at better than $\pm$ 0.3 % accuracy, independent of line frequency and voltage and is capable of measuring to 0.002 mV on the smallest range.

The reversibility of the cell during the runs was checked by the following tests : (i) the equilibrium emf readings at the temperature of study were reproducible when the temperature was changed and brought back to its original value, (ii) the cell emf rapidly returned to its original value (in less than 5 minutes) on application of an external emf. To ensure that the electrode-electrolyte contacts were perfect, effect of gas flow rate, on the cell emf was checked during each run.

Once the equilibrium was attained, the cell emf was almost constant at the temperature of study and was reproducible to $\pm$ 0.5 mV.

2.4.2 Calibration of the Cell

Before starting the experiments the proper working condition of the equipment was checked with the following cell:

$$Pt/Fe,FeO//ZrO_2\text{-}CaO//Ni,NiO/Pt \qquad ..(2.1)$$

The emf values for the cell (2.1) were measured at 700, 750, 800, 850 and 900°C. The cell emf was measured at falling and rising temperatures as the cell was taken through a thermal cycle. Equilibrium emf values were observed for about 30 minutes to one hour at each temperature. Cell emf for falling and rising temperatures agreed within 0.5 mV. Observed values of reversible emf for the cell (2.1) at different temperatures are given in Table-2.1. Emf values for the same cell after Kiukkola and Wagner [63] and calculated from the data reported by Charette and Flengas [100] ($E = 154.13 + 0.104\ T$, E in mV, T in K) are also presented in this table. Table-2.1 shows that the present data on cell (2.1) are in good agreement, within the experimental error, with the data reported in literature.

TABLE 2.1 Emf values at different temperatures for calibration of the cell

Cell: Pt / Fe, FeO // ZrO_2 - CaO // Ni, NiO / Pt

Temperature (K)	Emf (mV)		
	Present Investigation	Kiukkola & Wagner [63]	Charette & Flengas [100]
973	255.0 ±0.5	-	255.3±0.9
1023	261.0± 0.5	261.0±2	260.5±0.9
1073	266.0±0.5	266.0±1	265.7±0.9
1123	271.0±0.5	271.0±1	270.9±0.9
1173	276.0±0.5	276.0±1	276.1±0.9

CHAPTER-3

RESULTS-BINARY SYSTEMS

The present chapter deals with the experimental results and the thermodynamic properties, derived from emf data, of the binary systems FeO-MgO, FeO-CaO and FeO-SiO_2 at 1000 K. Based on published data on the stability of different phases present in these systems at 1000 K, suitable compositions in each phase region were selected for the experimental study. To determine the activity of FeO* in a sample under study, a suitable solid electrolyte galvanic cell of the following cell scheme was constructed.

$$\text{Pt/Fe , } \begin{matrix}\text{Oxide System} \\ \text{Containing FeO}\end{matrix} // ZrO_2\text{-}CaO // \text{Fe,FeO/Pt} \quad ..(3.1)$$

The cell was operated in an inert atmosphere of purified nitrogen at 1000 K and all binary and ternary oxide systems investigated in the present work were studied using this cell scheme.

3.1 SYSTEM FeO-MgO

Complete miscibability in this system in solid state, Fig. (1.10), has been established by Bowen and Schairer

---

*Wustite has a defect structure in which the ratio of oxygen to iron varies and never has as low a value as 1:1 corresponding to the simplified formula FeO. In equilibrium with metallic iron, wustite has an oxygen content of approximately 23.2 wt pct, corresponding to the formula $FeO_{0.960}$. For sake of simplicity, the formula FeO is used to represent the wustite phase in this thesis.

[190]. Magnesiowustite, solid solution of FeO and MgO, has simple sodium chloride structure and is known to be continuous between the end members in strongly reducing conditions such as prevail in contact with metallic iron.

Samples with seven different mole fractions of FeO, viz. N_{FeO} equal to 0.1, 0.23, 0.36, 0.5, 0.64, 0.77 and 0.9, covering the whole composition range were prepared. Values of the reversible emf of the cell, as represented by Eq. (3.1), at different concentrations of FeO in the binary oxide solution are presented in Table-3.1. Values of activity of FeO, a^{*}_{FeO}, were calculated from emf data, using the following relationship,

$$a_{FeO} = \exp\left(-\frac{2F}{RT} \times E\right) \qquad ..(3.2)$$

which on substitution of relevant values of Faraday's constant, F; universal gas constant, R and temperature (1000 K) yields

$$a_{FeO} = \exp(-0.0232028 \times E) \qquad ..(3.3)$$

where,

E is the reversible emf of the cell (3.1) in mV.

Activity of MgO, a_{MgO}, was calculated from Gibbs Duhem equation by making use of Darken's Eq.[219] :

---

*Standard state of FeO, as usual, is taken as the wustite which is in equilibrium with metallic iron at 1000 K i.e. "FeO" of minimum oxygen content at the temperature of study.

$$\ell n\ \gamma_{MgO} = -\alpha_{FeO}\, N_{FeO}\, N_{MgO} - \int_{N_{MgO}=1}^{N_{MgO}=N_{MgO}} \alpha_{FeO}\, dN_{MgO} \qquad ..(3.4)$$

where,

α-function is defined by the relationship,

$\alpha_{FeO} = (\ell n\ \gamma_{FeO})/(1-N_{FeO})^2$. ($\gamma_i$ is activity coefficient of component i)

Calculated values of a_{FeO} and a_{MgO}, alongwith measured values of reversible emf, are presented in Table-3.1. Variations of a_{FeO} and a_{MgO} with composition at 1000 K are plotted in Fig. (3.1). Values of a_{FeO}, after Hahn and Muan [154] at 1373 K are also incorporated in this figure for a comparison.

As FeO and MgO are iso-structural and ionic radii of Fe^{2+} ion (0.76 A^o) and Mg^{2+} ion (0.65 A^o) are comparable, complete solid solubility is expected at subsolidus temperatures, but differences in sizes of ionic radii and other properties do not permit ideal mixing of these two oxides. As indicated by activity-composition plots in Fig. (3.1), this system exhibits, considerable positive deviation from ideality. Higher positive deviation shown in the present study-as compared to the work of Hahn and Muan [154]-is probably due to lower temperature of study.

Values of ΔG_{Mix} and ΔG^{Ex}_{Mix} for different compositions were calculated from activity data using the following relationships:

TABLE 3.1 : Emf and activity values for the system FeO-MgO at 1000K

Cell : Pt/Fe ,(FeO+MgO)//ZrO_2-CaO//Fe,FeO/Pt

N_{FeO}	Emf (mV)	a_{FeO}	a_{MgO}
0.10	47.6	0.3314	0.9153
0.23	24.8	0.5625	0.8324
0.36	17.1	0.6725	0.7730
0.50	11.6	0.7640	0.7007
0.64	8.7	0.8172	0.6390
0.77	6.3	0.8640	0.5593
0.90	3.2	0.9284	0.3802

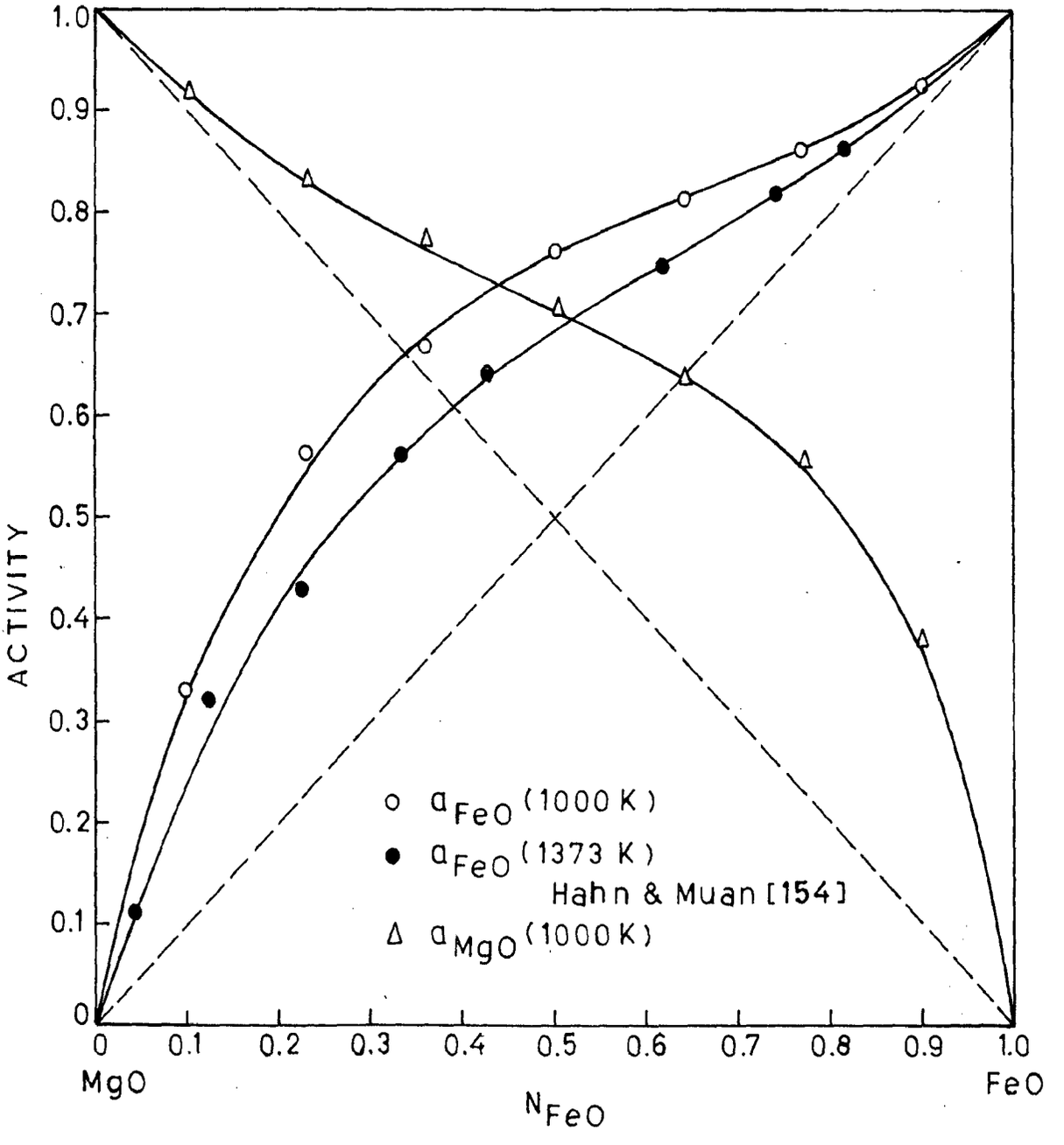

FIG. 3.1. ACTIVITIES OF FeO AND MgO AS A FUNCTION OF COMPOSITION IN THE SYSTEM FeO-MgO AT 1000 K.

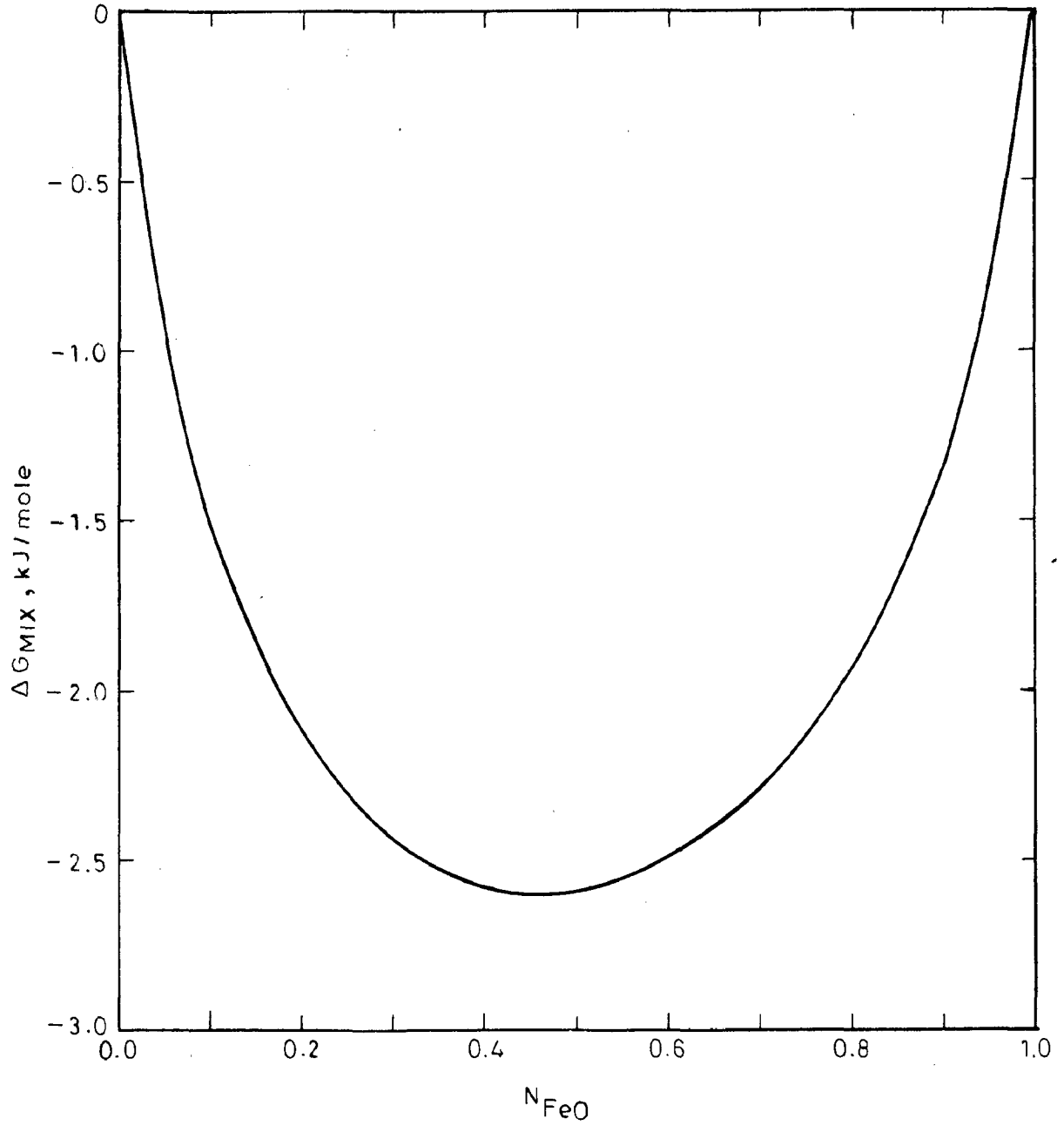

FIG.3.2. INTEGRAL FREE ENERGY OF MIXING FOR FeO-MgO SOLID SOLUTIONS AT 1000 K

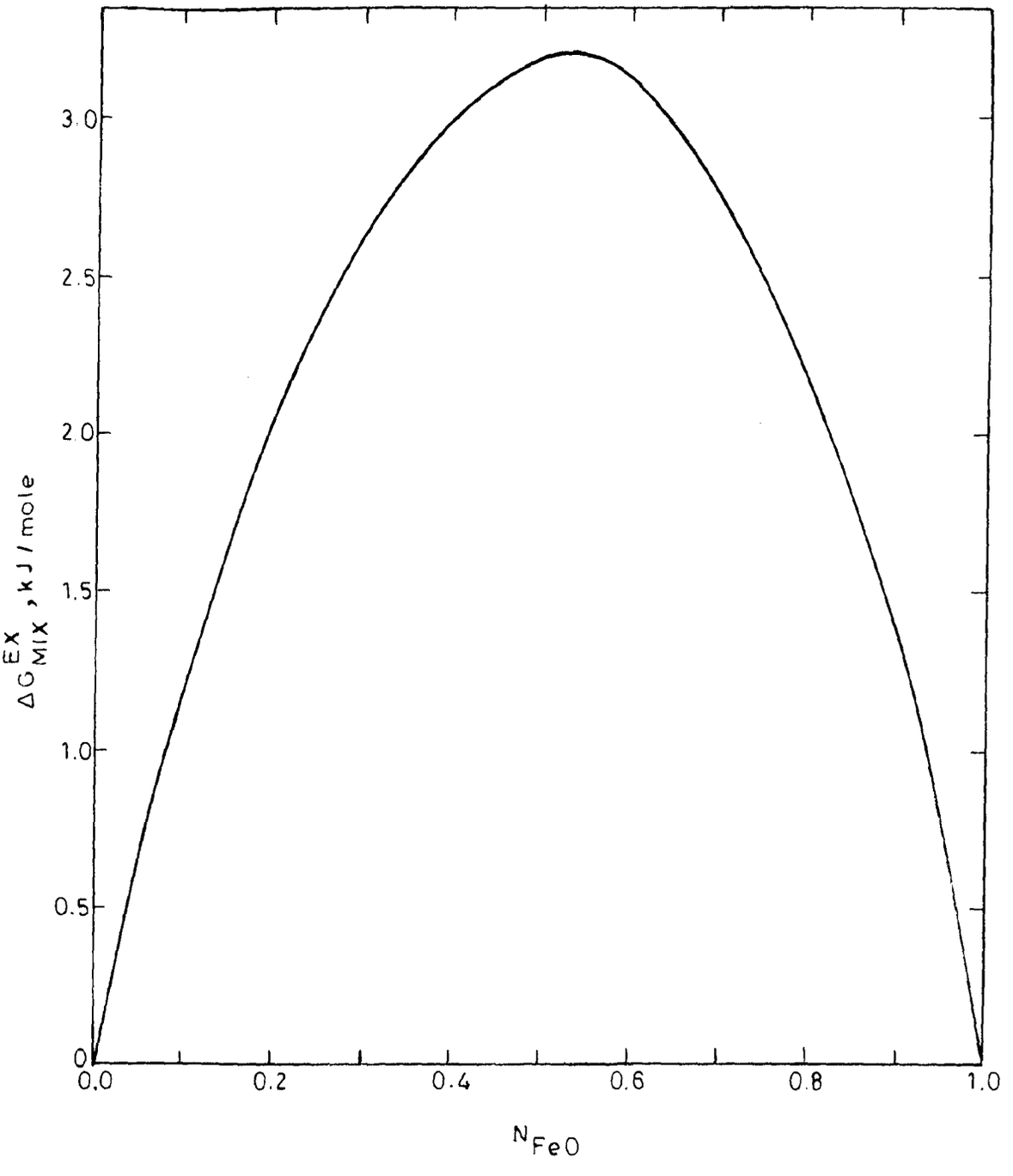

FIG.3.3. INTEGRAL EXCESS FREE ENERGY OF MIXING FOR FeO-MgO SOLID SOLUTIONS AT 1000 K

$$\Delta G_{Mix} = RT\ (N_{FeO}\ \ell n\ a_{FeO} + N_{MgO}\ \ell n\ a_{MgO}) \qquad ..(3.5)$$

$$\Delta G^{Ex}_{Mix} = RT\ (N_{FeO}\ \ell n\ \gamma_{FeO} + N_{MgO}\ \ell n\ \gamma_{MgO}) \qquad ..(3.6)$$

Calculated values of ΔG_{Mix} and ΔG^{Ex}_{Mix} for this binary solid solution are plotted against composition, N_{FeO}, in Figs. (3.2) and (3.3) respectively.

3.2 SYSTEM FeO-CaO

Equilibrium relations at different level of oxygen pressures have been studied in considerable detail in the system iron oxide-calcium oxide. Fig. (1.11) shows the phases present as a function of temperature and total composition for the system FeO-CaO in contact with metallic iron after Muan et al.[151]. A comparison of the diagrams for this system and FeO-MgO reveals the following main features:

i) low liquids and solidus temperature prevailing in the central part of the system, and

ii) presence of an intermediate compound, $Ca_2\ Fe_2O_5$, in the central region of the system.

These features are largely reflections of the greater ionic size difference between Ca^{2+} (0.99 A^o) and Fe^{2+}(0.76 A^o) as compared to that exists between Mg^{2+}(0.65 A^o) and Fe^{2+} ions. The ions Mg^{2+} and Fe^{2+}, therefore, readily substitute for each other in the crystalline phase, whereas limited substitution of Fe^{2+} and Ca^{2+} ions for each other results in limited solid solubility in CaO-FeO system. Formation of the

compound, $Ca_2 Fe_2O_5$, in this system may be attributed to the difference in the cation field strength of Ca^{2+} and Fe^{3+} ions (these two ions form the cation lattice of $Ca_2Fe_2O_5$). Cation field strength (defined as the cation charge divided by the square of the ionic diameter) for Ca^{2+} ion in 0.5102, whereas for Fe^{3+} ion (ionic radius, 0.64 A^o) it is 1.8311.

The CaO-FeO phase diagram shown in Fig. (1.11) indicates that the stable phases at 1000 K are as follows : Lime at $N_{FeO} < 0.075$, Lime + $Ca_2Fe_2O_5$ at $0.075 < N_{FeO} < 0.5$, $Ca_2Fe_2O_5$ + wustite at $0.5 < N_{FeO} < 0.94$, and wustite at $N_{FeO} > 0.94$. On the basis of known stability relations of these phases, samples of nine different compositions, viz. N_{FeO} = 0.02, 0.04, 0.06, 0.1, 0.3, 0.6, 0.8, 0.94 and 0.97 were prepared and studied at 1000 K using the solid electrolyte cell represented by Eq. (3.1). Values of activity of FeO, a_{FeO}, were calculated from the experimental values of reversible emf for the different samples using Eq. (3.3). Variation of activity of FeO with composition, N_{FeO}, is shown in Fig. (3.4). Solid solubility limits obtained from this figure are in good agreement with the values obtained from FeO-CaO phase diagram after Muan et al. [151] at 1000 K.

Values of activity of CaO at N_{FeO} equal to 0.02, 0.04, 0.06 and 0.075 were calculated from Gibbs -Duhem equation by making use of Darken's equation, i.e. Eq. (3.4) as applied to present system.

As Gibbs-Duhem equation applies to single phase region only and, therefore, is not valid in two phase regions,

activity of CaO at N_{FeO} equal to 0.94 was calculated from the equilibrium constant of the following reaction:

$$3FeO + 2CaO = Ca_2Fe_2O_5 + Fe^{*} \qquad ..(3.7)$$

Considering, $Ca_2Fe_2O_5$ and Fe to be present as pure phases, equilibrium constant, $K_{(3.7)}$, will be expressed by the following relationship;

$$K^{**}_{(3.7)} = \frac{1}{a^3_{FeO} \cdot a^2_{CaO}} \qquad ..(3.8)$$

If a^{I}_{FeO} and a^{II}_{FeO} are the values of activity of FeO at N_{FeO} equal to 0.075 and 0.94 respectively (these values of N_{FeO} refer to boundaries (lime)/(Lime+$Ca_2Fe_2O_5$) and ($Ca_2Fe_2O_5$+ Wustite)/(Wustite) respectively at 1000 K) and a^{I}_{CaO} and a^{II}_{CaO} are also expressed similarly, substitution of these values in Eq. (3.8) yields the following relationship:

$$\frac{1}{(a^{I}_{FeO})^3 (a^{I}_{CaO})^2} = \frac{1}{(a^{II}_{FeO})^3 (a^{II}_{CaO})^2} \qquad ..(3.9)$$

---

* As 'FeO' actually refers to $Fe_{1-x}O$, where x represents the nonstoichiometry of wustire, reaction(3.7) should be written as:

$$3xFe+3Fe_{1-x}O+2CaO=Ca_2Fe_2O_5+Fe \qquad ..(3.7a)$$

For sake of convenience term FeO is used for ($xFe+Fe_{1-x}O$) to represent chemical reactions involving wustite phase throughout this thesis.

** Equilibrium constant of a reaction, Eq.(3.7) in this case, is represented by the symbol $K_{(3.7)}$, where subscript 3.7 refers to the reaction represented by Eq.(3.7). Similarly standard free energy of formation for the reaction(3.7) is represented as $\Delta G^{o}_{(3.7)}$. This practice is followed throughout the thesis.

From the known values of a^{I}_{FeO}, a^{II}_{FeO}, and a^{I}_{CaO}, activity of calcium oxide at N_{FeO} equal to 0.94, a^{II}_{CaO}, was calculated by making use of Eq. (3.9). (a^{I}_{FeO} and a^{II}_{FeO} were experimentally determined and a^{I}_{CaO} was obtained from Gibbs Duham equation). As the phase region beyond N_{FeO} equal to 0.94 is a single phase region of wustite at 1000 K, activity of CaO at N_{FeO} equal to 0.97 was calculated from Gibbs Duhem equation.

Calculated values of a_{FeO} and a_{CaO} along with measured values of emf in mV, for different compositions, are presented in Table 3.2. a_{FeO} and a_{CaO} as a function of composition, N_{FeO}, are plotted in Fig. (3.4). Activity-composition relations after Johnson and Muan [160] at 1353 K are also included in this figure. A very high positive deviation from ideality as revealed by Fig. (3.4) is expected in a system like FeO-CaO on account of limited solubility and large miscibility gap. Sudden change in the values of a_{FeO} and a_{CaO} at N_{FeO} equal to 0.5 may be explained on the basis of formation of a compound at this composition, which separates the regions of (lime + $Ca_2Fe_2O_5$) and ($Ca_2Fe_2O_5$ + wustite). Equilibrium constant, $K_{(3.7)}$, for the reaction (3.7), calculated from a^{I}_{FeO} and a^{I}_{CaO} values was found to be 3.5. Standard free energy change for reacion (3.7), from $K_{(3.7)}$ equal to 3.5, was calculated to be -10.4 kJ/mole.

Elliott, Gleiser and Ramakrishna [220] have reported the data on free energy of formation of $Ca_2Fe_2O_5$ according to the following reaction:

TABLE-3.2 : Emf and activity values for the system FeO-CaO at 1000 K

Cell : $Pt/Fe,(FeO+CaO)//ZrO_2 - CaO//Fe,FeO/Pt$

N_{FeO}	Emf (mV)	a_{FeO}	a_{CaO}
0.02	54.1	0.2850	0.9812
0.04	27.8	0.5246	0.9628
0.06	18.5	0.6510	0.9512
0.10	16.1	0.6883	0.9477
0.30	16.1	0.6883	0.9477
0.60	2.6	0.9415	0.5860
0.80	2.6	0.9415	0.5860
0.94	2.6	0.9415	0.5860
0.97	1.3	0.9703	0.2961

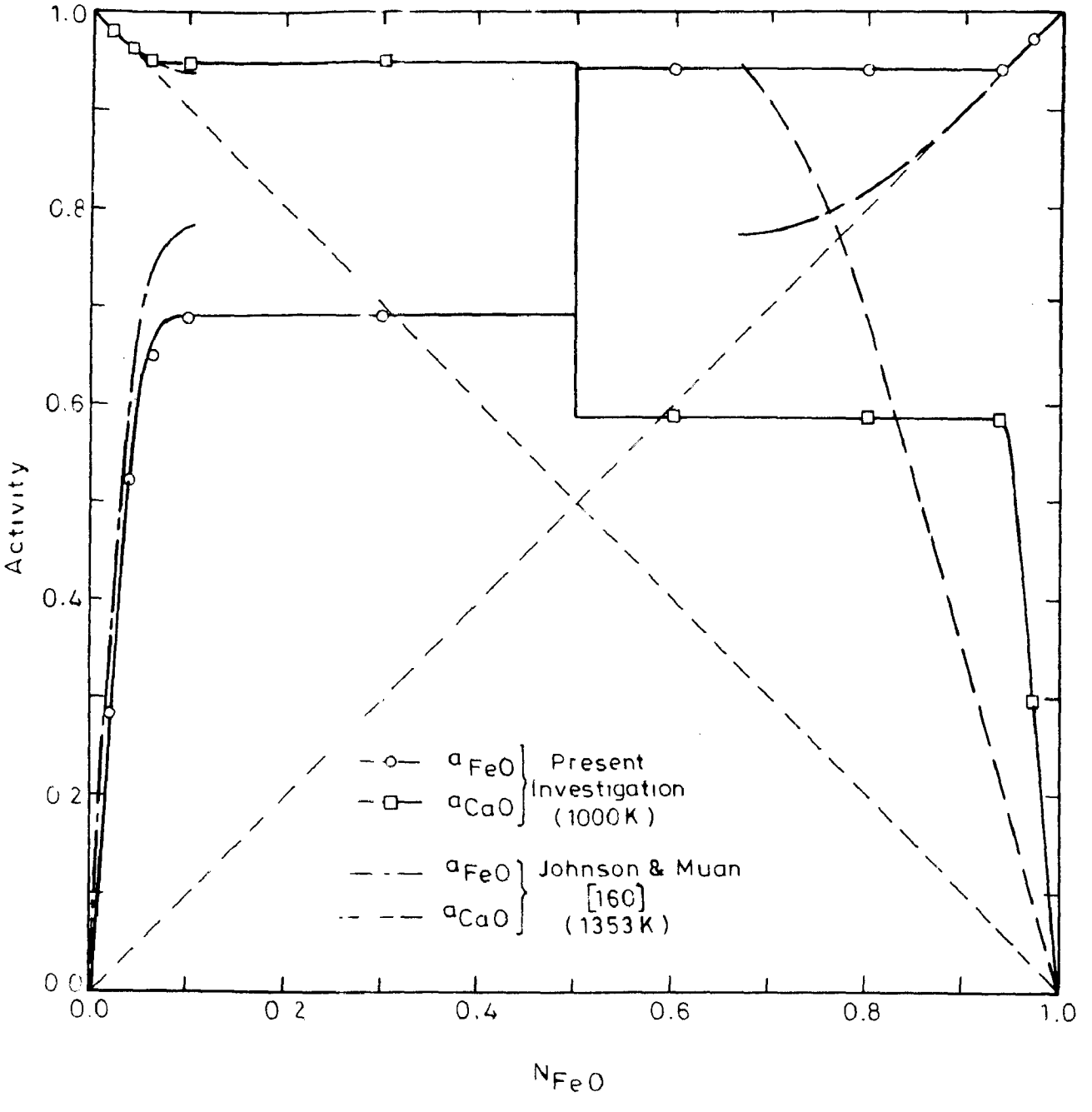

FIG.3.4. ACTIVITIES OF FeO AND CaO AS A FUNCTION OF COMPOSITION IN THE SYSTEM FeO – CaO AT 1000 K

$$2CaO + Fe_2O_3 = Ca_2Fe_2O_5 \qquad ..(3.10)$$

at 298.15 K and at temperatures above 1200 K upto melting point (1750 K) of $Ca_2Fe_2O_5$ at 100 K temperature intervals. Plot of these values of $\Delta G^{o}_{(3.10)}$ as a function of temperature, on interpolation to 1000 K yields the value of $\Delta G^{o}_{(3.10)}$ at this temperature to be -47.8 kJ/mole.

Value of $\Delta G^{o}_{(3.10)}$ can be calculated using present data on $\Delta G^{o}_{(3.7)}$ with the help of relevant data after Kubaschewski et al. [11] for the following reactions:

$$FeO = Fe + \frac{1}{2} O_2 \qquad \ldots\ldots \quad I$$

$$\Delta G^{o}_{I} = 62050 - 14.95\ T \qquad \ldots\ldots \quad (3.11)$$

$$Fe_3O_4 = 3FeO + \frac{1}{2} O_2 \qquad \ldots\ldots \quad II$$

$$\Delta G^{o}_{II} = 74620 - 29.9T \qquad \ldots\ldots \quad (3.12)$$

$$3Fe_2O_3 = 2Fe_3O_4 + \frac{1}{2} O_2 \qquad \ldots\ldots \quad III$$

$$\Delta G^{o}_{III} = 59620 - 33.62\ T \qquad \ldots\ldots \quad (3.13)$$

where,

T is absolute temperature in K and ΔG^{o} values are in calories.

Combination of chemical reactions expressed by Eqs.(3.7) and I,II, and III above yields the following relationship for calculation of $\Delta G^{o}_{(3.10)}$.

$$\Delta G^{o}_{(3.10)} = \Delta G^{o}_{(3.7)} - \Delta G^{o}_{I} + \frac{2}{3}\Delta G^{o}_{II} + \frac{1}{3}\Delta G^{o}_{III} \qquad ..(3.14)$$

Substitution of relevant values of ΔG^{o}_{I}, ΔG^{o}_{II} and ΔG^{o}_{III} calculated at 1000 K and $\Delta G^{o}_{(3.7)}$ equal to -10.4 kJ/mole yields

the value of $\Delta G^{\circ}_{(3.10)}$ equal to -46.4 kJ/mole, which is in very good agreement with the value of $\Delta G^{\circ}_{(3.10)}$ equal to -47.8 kJ/mole obtained above graphically using published data [220].

3.3 SYSTEM FeO-SiO_2

Fig. (3.5) represents the phase diagram for the system FeO-SiO_2 in contact with metallic iron after Bowen and Schairer [189]. As is evident the oxides, FeO and SiO_2, have no mutual solubility and an intermediate compound, Fayalite (Fe_2SiO_4) is formed at N_{FeO} equal to 0.667.

To determine the standard free energy of formation, $\Delta G^{\circ}_{Fe_2SiO_4}$, three samples in the two phase region of SiO_2 + Fe_2SiO_4 having N_{FeO} equal to 0.4, 0.45, and 0.5 were prepared and values of reversible emf of the solid electrolyte cell with cell scheme (3.1) were measured. Standard free energy of formation, $\Delta G^{\circ}_{Fe_2SiO_4}$, was calculated from these emf values as follows:

The cell reaction, for the cell employed for studying properties of (SiO_2+Fe_2SiO_4) phase assemblage, viz.

$$Pt/Fe, (SiO_2+Fe_2SiO_4)//ZrO_2\text{-}CaO//Fe,FeO/Pt \qquad ..(3.15)$$

may be represented by the following equation:

$$2FeO + SiO_2 = Fe_2SiO_4 \qquad ..(3.16)$$

Free energy of reaction for the above reaction will be

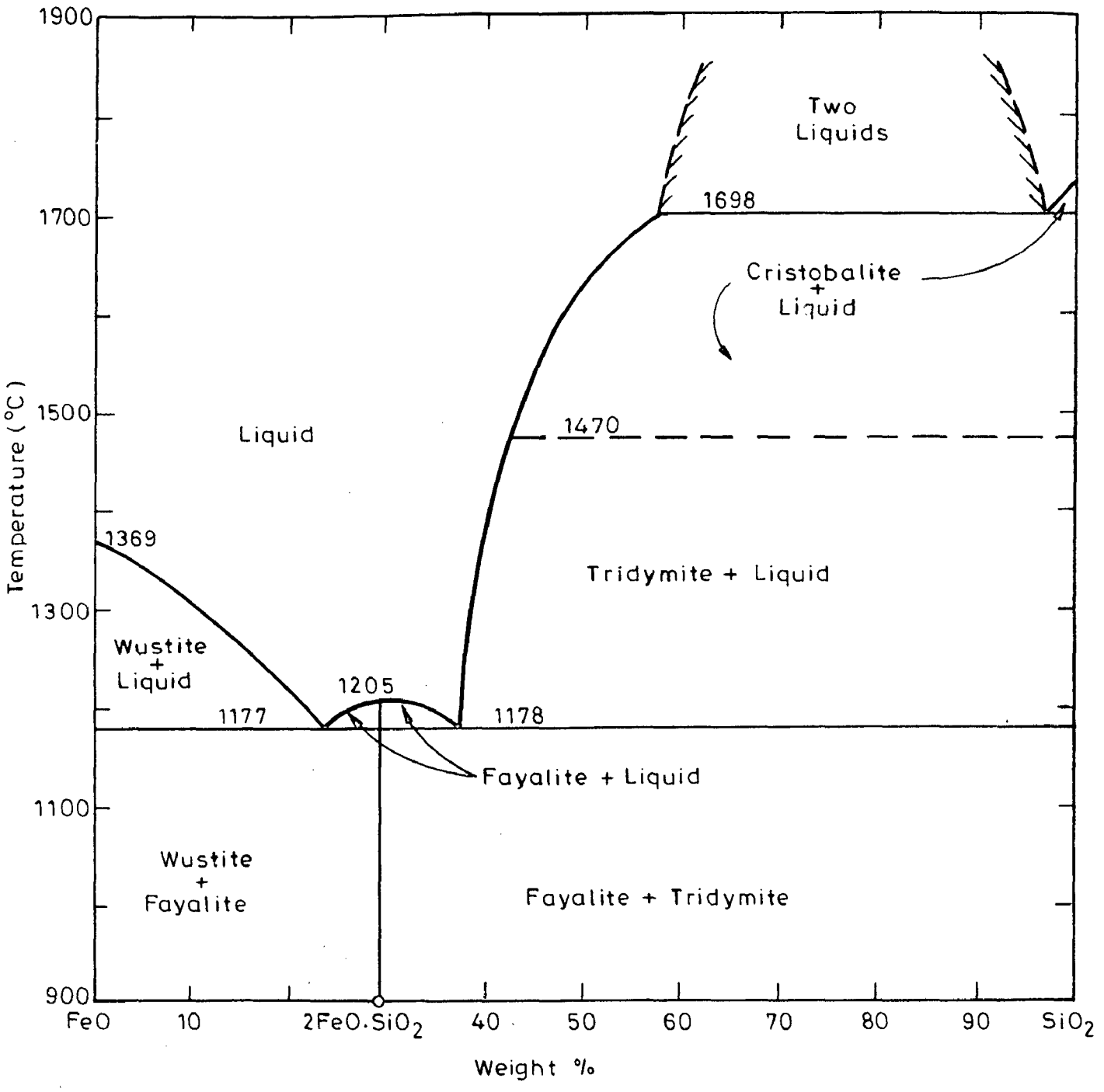

FIG.3.5. PHASE DIAGRAM FOR THE SYSTEM $FeO-SiO_2$ [151]

equal to standard free energy of formation, $\Delta G^{o}_{Fe_2SiO_4}$, of Fe_2SiO_4 from compoment oxides FeO and SiO_2 and is related to the emf, E, of the cell by the following relationship

$$\Delta G^{o}_{Fe_2SiO_4} = -2n\ F\ E \qquad ..(3.17)$$

Eq. (3.17) on substitution of relevant value of Faraday's constant, F and n equal to 2 yields the following relationship:

$$\Delta G^{o}_{Fe_2SiO_4} = -0.3856 \times E \qquad ..(3.18)$$

where,

E is in mV and $\Delta G^{o}_{Fe_2SiO_4}$ in kJ/mole.

The measured values of reversible emf of the cell (3.15) for the three samples studied having N_{FeO} equal to 0.4, 0.45, and 0.5 were found to be 35.7, 35.5 and 35.6 mV respectively. As stable phases in the three samples are same (viz. Silica and Fayalite), a small fluctuation in emf values are on account of experimental errors. An average of the three values of emf, 35.6 mV, was used to calculate the value of $\Delta G^{o}_{Fe_2SiO_4}$ from its component oxides at 1000 K was found to be equal to -13.7 kJ/mole. Several workers have determined the value of standard free energy of formation of Fe_2SiO_4 from component oxides FeO and SiO_2 and the values reported by them are as follows: -18 kJ/mole at 1353 K by Johnson and Muan [160], -16.7 kJ/mole at 1353 K by Schwerdtfeger and Muan [208], -16.7 kJ/mole at 1523 K and 1573 K by Muan et al. [193], -11.1 kJ/mole at 1200 K by Elliott et al. [220], -24.7 kJ/mole at 1000 K by Richardson et al. [221], -17.6 kJ/mole at 1173 K by Taylor et al. [222] and -13.8 kJ/mole at 1402 -1447 K by Kitayama and Katsura [223]. All these values

except that reported by Richardson et al. [221], are in good agreement with the value of $\Delta G^{\circ}_{Fe_2SiO_4}$ found in the present work. For a direct comparison, value of $\Delta G^{\circ}_{Fe_2SiO_4}$ at 1000 K was determined from the data reported by Elliott, Gleiser and Ramakrishna [220] at 298.15, 1200, 1300, 1400 and 1490 K. Value of $\Delta G^{\circ}_{Fe_2SiO_4}$ at 1000 K obtained graphically from the plot of above values of $\Delta G^{\circ}_{Fe_2SiO_4}$ vs. temperature was found to be -15.1 kJ/mole, which is in excellent agreement with the value of -13.7 kJ/mole obtained in the present work.

CHAPTER-4

RESULTS-TERNARY SYSTEMS

The present chapter deals with the thermodynamic properties of the ternary systems $MgO-FeO-SiO_2$ and $MgO-FeO-CaO$ derived from the experimental emf data at 1000 K. Compositions of samples for experimental studies were selected on the basis of known stable phases in the system $MgO-FeO-SiO_2$ at 1000 K, such that all the important phase regions were covered. As the stable phases in the system $MgO-FeO-CaO$ are not known at or near 1000 K, a number of compositions were selected for experimental study in order to derive complete information regarding 1000 K-isothermal section through this system.

4.1 SYSTEM $MgO-FeO-SiO_2$

It was the work of Bowen and Schairer [189] which established a comprehensive knowledge and understanding of phase relations in the system $MgO-FeO-SiO_2$. Any subsolidus isothermal section through this system is divided in five phase regions, viz. I-Silica + Pyroxene, II-Pyroxene + Olivine, III-Olivine + Magnesiowustite, IV-Silica + Pyroxene + Olivine, and V-Silica + Olivine. Based on the phase boundaries determined by Bowen and Schairer [189] at 1523, 1423, 1323 and 1228 K, an isothermal section through the system $MgO-FeO-SiO_2$ in contact with metallic iron at 1000 K is shown in Fig. (4.1).

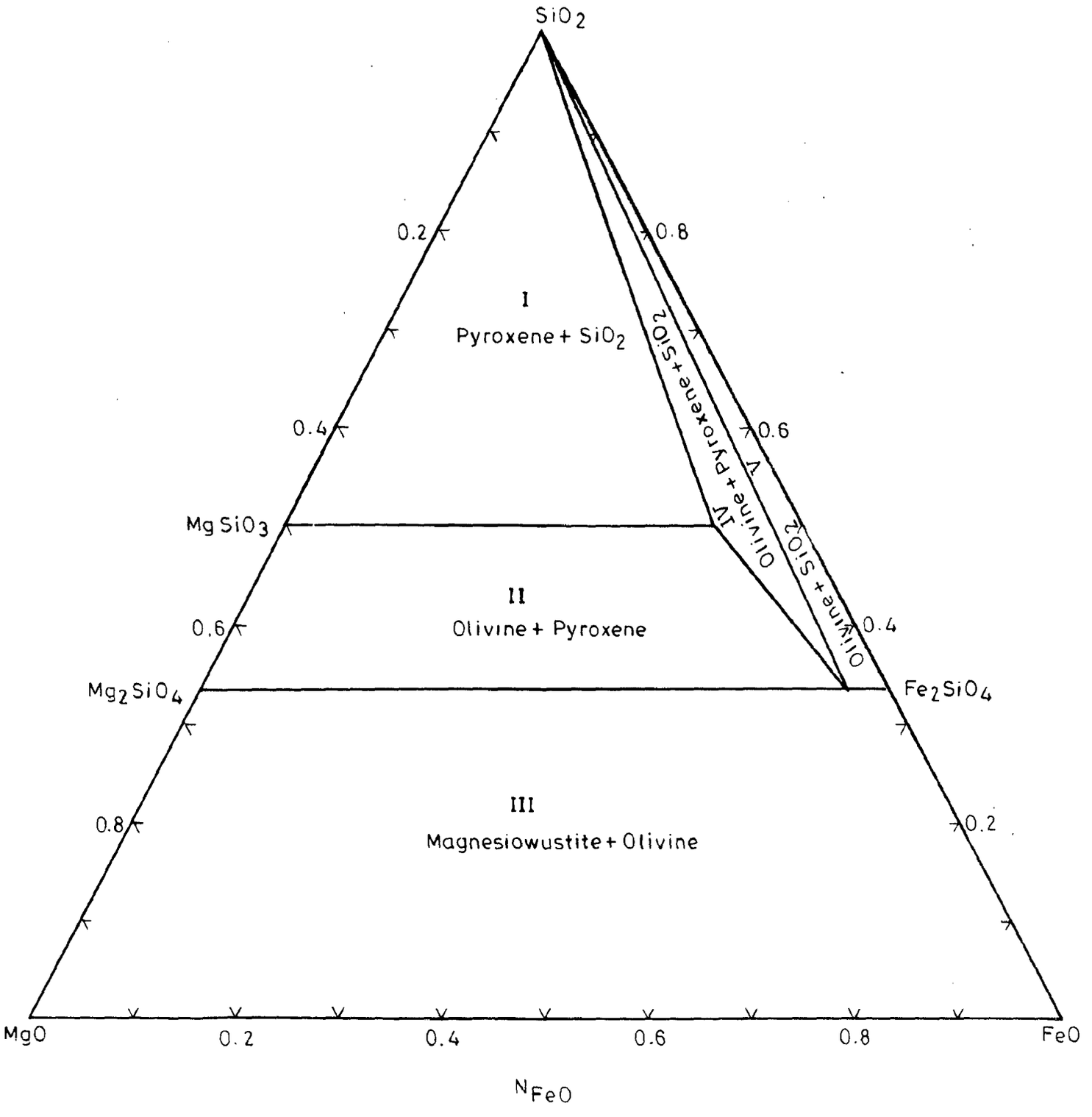

FIG.4.1. ISOTHERMAL SECTION AT 1000 K THROUGH THE SYSTEM $MgO - FeO - SiO_2$

A term N^{o}_{FeO} is defined to express the composition of the samples in the present system, such that

$$N^{o}_{FeO} = \frac{N_{FeO}}{N_{FeO}+N_{MgO}} \qquad ..(4.1)$$

If a straight line is drawn from the SiO_2 apex towards the MgO-FeO base, the value of N^{o}_{FeO} is constant along this line and is equal to the value of N_{FeO} at the point, where this line cuts MgO-FeO base line.

Compositions studied in the binary system FeO-MgO having N^{o}_{FeO} equal to 0.1, 0.23, 0.36, 0.5, 0.64, 0.77 and 0.9 were taken as base and varying amounts of third components SiO_2 were added to its to prepare the samples to study this system. Corresponding to each value of N^{o}_{FeO}, six samples having N_{SiO_2} equal to 0.1, 0.2, 0.3, 0.4, 0.47 and 0.6 were prepared. This choice of compositions of samples, practically covers all the important phase regions of this system at 1000K. We have - for each value of N^{o}_{FeO} - three different compositions in region III, two different compositions in region II and only one composition in region I. As the thermodynamic properties of the stable phases in region I shall not change along a line of constant N^{o}_{FeO}, experimental data on one composition for each value of N^{o}_{FeO} was considered to be sufficient for studying the properties of stable phases in this region.

Reversible emf values, measured on the cell represented by Eq. (3.1), at 1000K are given in Table-4.1. Variation of emf with N^{o}_{FeO} for different values of N_{SiO_2} is shown in

Fig. (4.2). Values of activity of FeO, calculated from emf data using Eq. (3.3), are given in Table-4.2. Variation of a_{FeO} with N^{o}_{FeO} is shown graphically in Figs. (4.3) and (4.4) for N_{SiO_2} equal to 0.1, 0.2 and 0.3, and N_{SiO_2} equal to 0.4, 0.47 and 0.6 respectively.

4.1.1 FeO Activity Lines

From a_{FeO} vs N^{o}_{FeO} plot at N_{SiO_2}=0.6(Fig.4.4) which is valid for all values of N_{SiO_2} in region I, values of N^{o}_{FeO} for a_{FeO} equal to 0.05, 0.1, 0.15, 0.2, 0.25, 0.3 and 0.35 were found and used to draw iso-a_{FeO} lines in region I.

Similarly a_{FeO} vs N^{o}_{FeO} plots at N_{SiO_2} equal to 0.4 and 0.47 were used to draw the iso-a_{FeO} lines in region II. Points of same a_{FeO} at N_{SiO_2} = 0.4 and 0.47 were found from Fig.(4.4) and two points for each value of a_{FeO} thus obtained were joined by a straight line. By this method iso-a_{FeO} lines for a_{FeO} equal to 0.1, 0.2, 0.3, 0.35, 0.37, 0.39 and 0.4 were drawn in region II.

Composition dependence of a_{FeO} along MgO-FeO binary and along N_{SiO_2} = 0.1, 0.2 and 0.3 in the present system was made use of to draw iso-activity lines for various values of a_{FeO} in region III. N^{o}_{FeO} values for selected values of a_{FeO} were read from Fig. (3.1) and Fig. (4.3) and on the basis of these points, iso-activity lines were drawn for a_{FeO} equal to 0.1, 0.3, 0.5, 0.6, 0.7, 0.8, 0.95. 0.98, 0.99 and 0.995. Activity of FeO in region IV, which is a three-phase region,

TABLE 4.1 : Emf values for the system MgO-FeO-SiO_2 at 1000 K

Cell : Pt/Fe, (FeO+MgO+SiO_2)//ZrO_2-CaO//Fe,FeO/Pt

N^{o}_{FeO}	Emf (mV)					
	N_{SiO_2}=0.1	N_{SiO_2}=0.2	N_{SiO_2}=0.3	N_{SiO_2}=0.4	N_{SiO_2}=0.47	N_{SiO_2}=0.6
0.10	41.5	28.0	7.5	52.9	50.8	101.0
0.23	20.5	12.5	2.0	51.2	51.3	69.0
0.36	14.5	7.0	0.5	46.0	42.3	57.9
0.50	9.0	1.5	0.5	40.8	38.1	52.2
0.64	4.5	0.5	0.4	38.3	37.7	48.0
0.77	1.0	0.3	0.2	37.9	38.6	42.0
0.90	0.9	-	-	39.8	40.4	41.0

TABLE 4.2 : Values of FeO-activity for the system MgO-FeO-SiO_2 at 1000 K

N^o_{FeO}	a_{FeO}					
	N_{SiO_2}=0.1	N_{SiO_2}=0.2	N_{SiO_2}=0.3	N_{SiO_2}=0.4	N_{SiO_2}=0.47	N_{SiO_2}=0.6
0.10	0.3818	0.5222	0.8403	0.2930	0.3077	0.0960
0.23	0.6215	0.7482	0.9547	0.3048	0.3041	0.2017
0.36	0.7143	0.8501	0.9885	0.3439	0.3748	0.2609
0.50	0.8115	0.9657	0.9885	0.3880	0.4131	0.2978
0.64	0.9008	0.9885	0.9908	0.4112	0.4170	0.3283
0.77	0.9771	0.9931	0.9954	0.4150	0.4084	0.3774
0.90	0.9793	-	-	0.3971	0.3916	0.3862

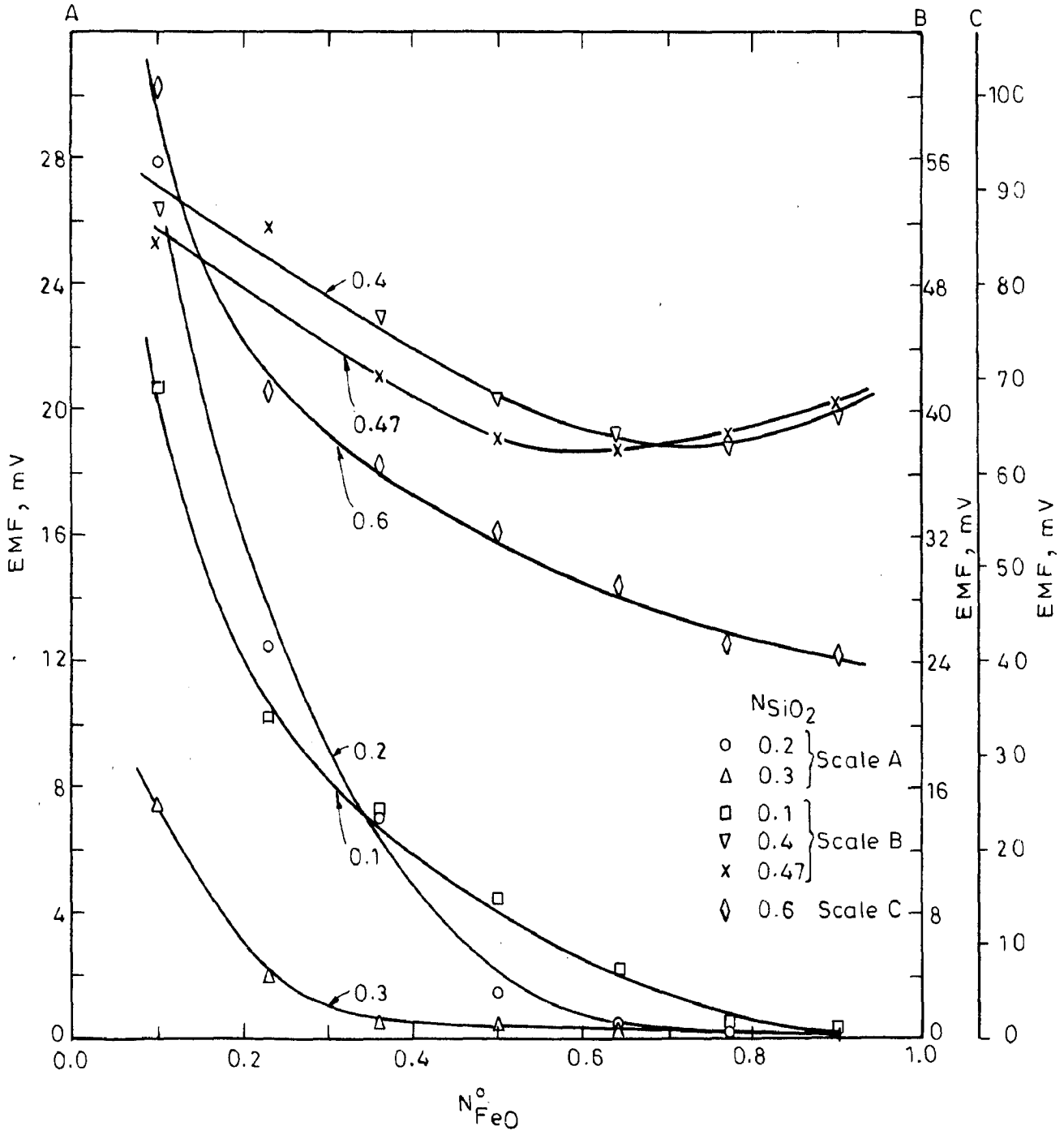

FIG.4.2. EMF Vs N°_{FeO} FOR THE SYSTEM $MgO-FeO-SiO_2$ AT 1000K.

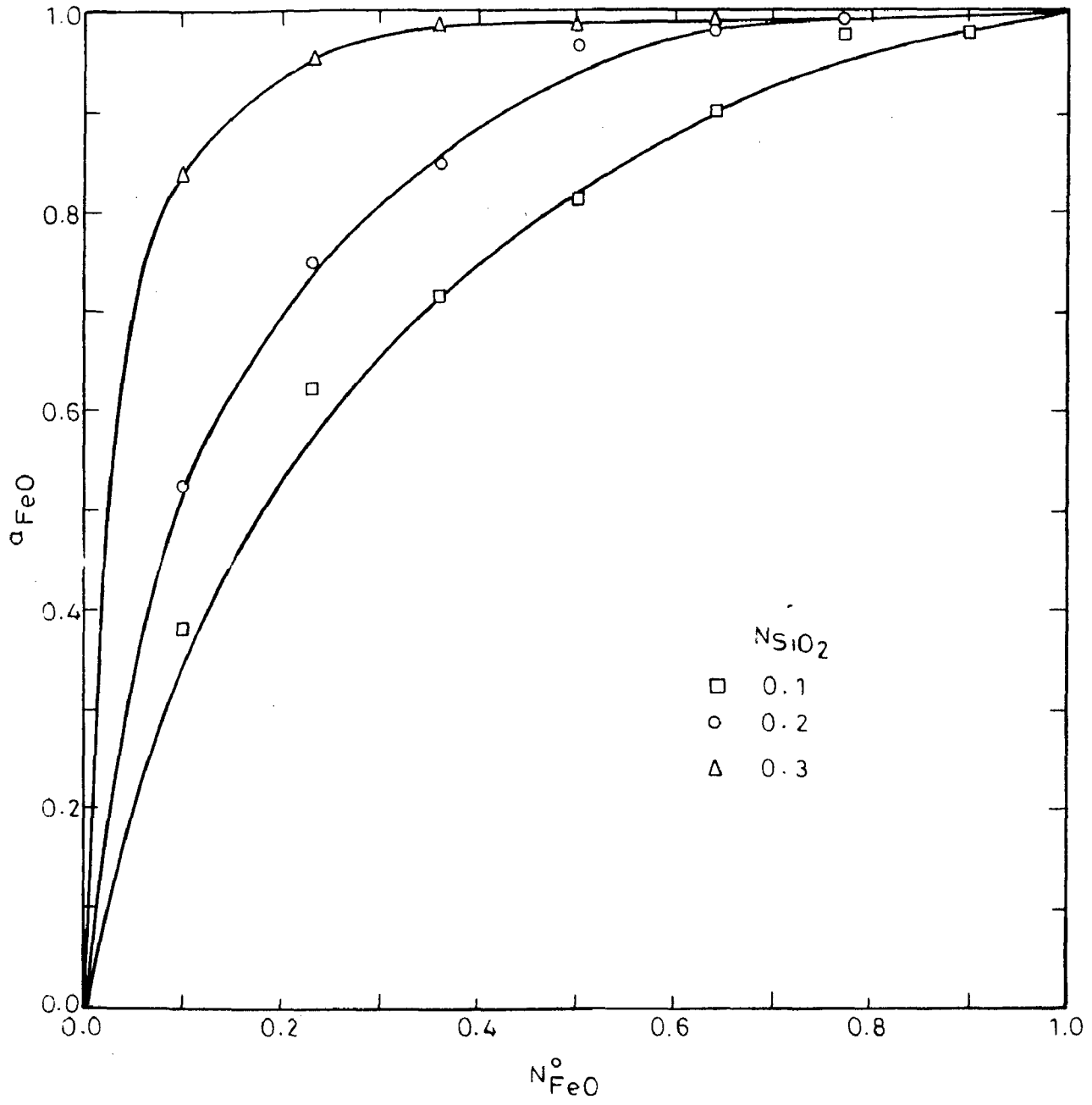

FIG.4.3. a_{FeO} Vs N°_{FeO} FOR THE SYSTEM MgO-FeO-SiO_2 AT 1000K
(N_{SiO_2} = 0.1, 0.2 AND 0.3)

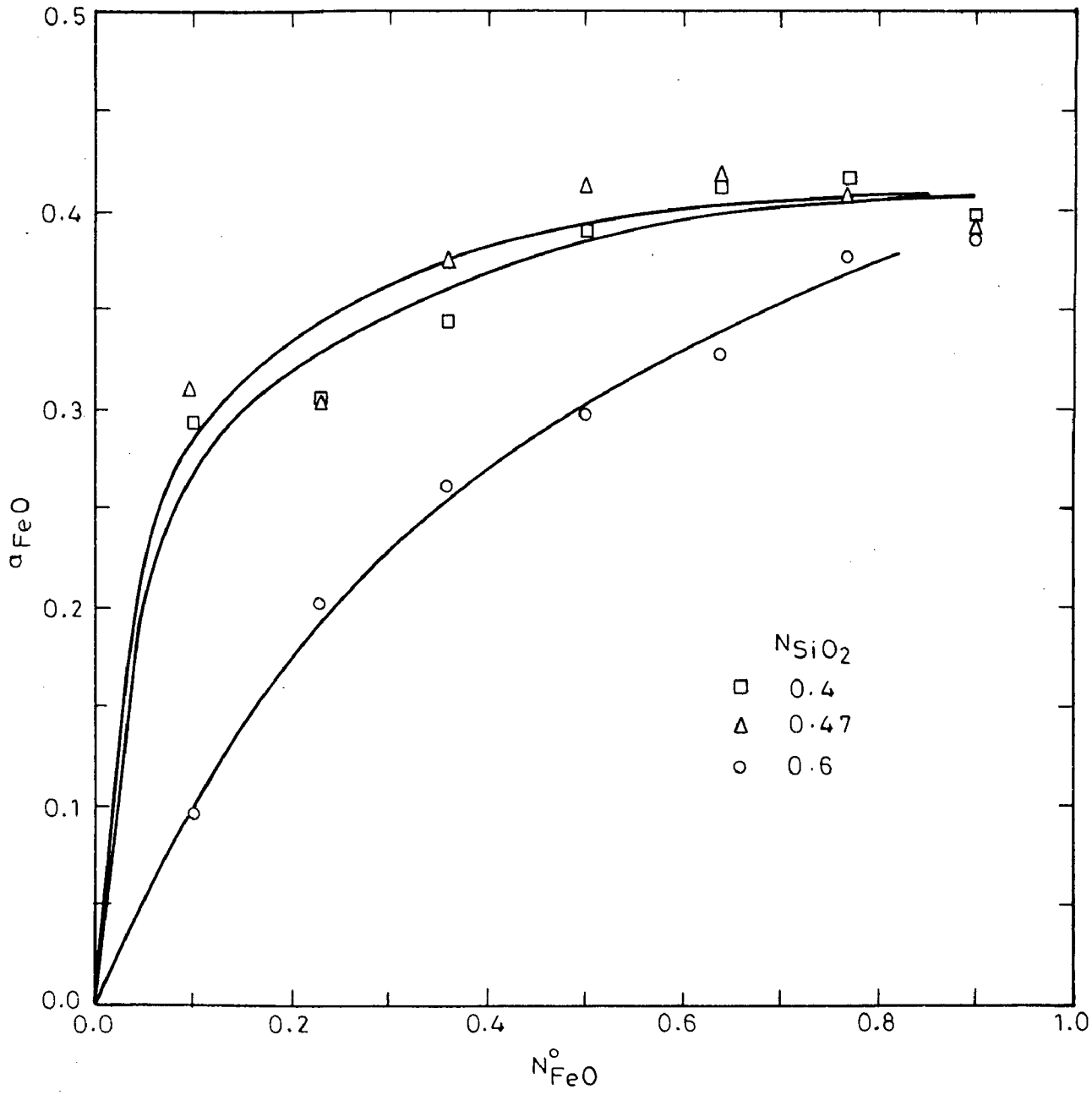

FIG.4.4. a_{FeO} Vs N°_{FeO} FOR THE SYSTEM MgO - FeO - SiO_2 AT 1000 K
(N_{SiO_2} = 0.4 , 0.47 AND 0.6)

should be constant and was calculated to be 0.41 on the basis of a_{FeO} vs. N^{o}_{FeO} plots for N_{SiO_2} equal to 0.4 and 0.47. Iso-activity lines for FeO in different regions are shown in Fig. (4.5).

4.1.2 System $FeSiO_3$-$MgSiO_3$

Stable phases in the region I at 1000 K are pure silica and pyroxene (solid solution of $FeSiO_3$ and $MgSiO_3$). Along the line $N_{SiO_2} = 0.5$, pyroxene is the only stable phase from $N^{o}_{FeO} = 0$ to $N^{o}_{FeO} = 0.823$.

Free energy of formation of $FeSiO_3$ was calculated from activity data as follows:

Consider the reaction,

$$FeO + SiO_2 = FeSiO_3 \qquad ..(4.2)$$

As silica exists as pure phase, equilibrium constant for the above reaction is given as

$$K_{(4.2)} = \frac{a_{FeSiO_3}}{a_{FeO}} \qquad ..(4.3)$$

Writing, activity of $FeSiO_3$, a_{FeSiO_3}, in terms of its activity coefficient and mole fraction, Eq. (4.3) yields

$$K_{(4.2)} = \frac{\gamma_{FeSiO_3}}{(a_{FeO}/N_{FeSiO_3})} \qquad ..(4.4)$$

In region I all the FeO and MgO present are consumed

in the formation of pyroxene, which implies that N_{FeSiO_3} is equal to N^{o}_{FeO}, therefore, Eq. (4.4) may be written as

$$K_{(4.2)} = \frac{\gamma_{FeSiO_3}}{(a_{FeO}/N^{o}_{FeO})} \qquad ..(4.5)$$

Taking logarithm and multiplying by RT gives

$$RT \ln K_{(4.2)} = RT \ln \gamma_{FeSiO_3} - RT \ln\left(\frac{a_{FeO}}{N^{o}_{FeO}}\right) \qquad ..(4.6)$$

Using the relation $\Delta G^{o}_{(4.2)} = -RT \ln K_{(4.2)}$ and re-arrangement of terms gives:

$$RT \ln\left(\frac{a_{FeO}}{N^{o}_{FeO}}\right) = \Delta G^{o}_{(4.2)} + RT \ln \gamma_{FeSiO_3} \qquad ..(4.7)$$

As $N^{o}_{FeO} \longrightarrow 1$, $\gamma_{FeSiO_3} \longrightarrow 1$ and $\ln \gamma_{FeSiO_3} \longrightarrow 0$, therefore,

$$\left[RT \ln\left(\frac{a_{FeO}}{N^{o}_{FeO}}\right) \longrightarrow \Delta G^{o}_{(4.2)} \right]_{N^{o}_{FeO} \longrightarrow 1} \qquad ..(4.8)$$

Plot of $RT \ln\left(\frac{a_{FeO}}{N^{o}_{FeO}}\right)$ vs N^{o}_{FeO} at N_{SiO_2} equal to 0.6, which is valid for all other values of N_{SiO_2} in region I, is given in Fig. (4.6). Standard free energy of formation, $\Delta G^{o}_{(4.2)}$, of $FeSiO_3$ from its component oxides was found to be -6.35 kJ/mole by extrapolating the curve in Fig. (4.6) to N^{o}_{FeO} equal to ~~zero~~ one. This value, derived from experimental values of activity of FeO, is in good agreement with the

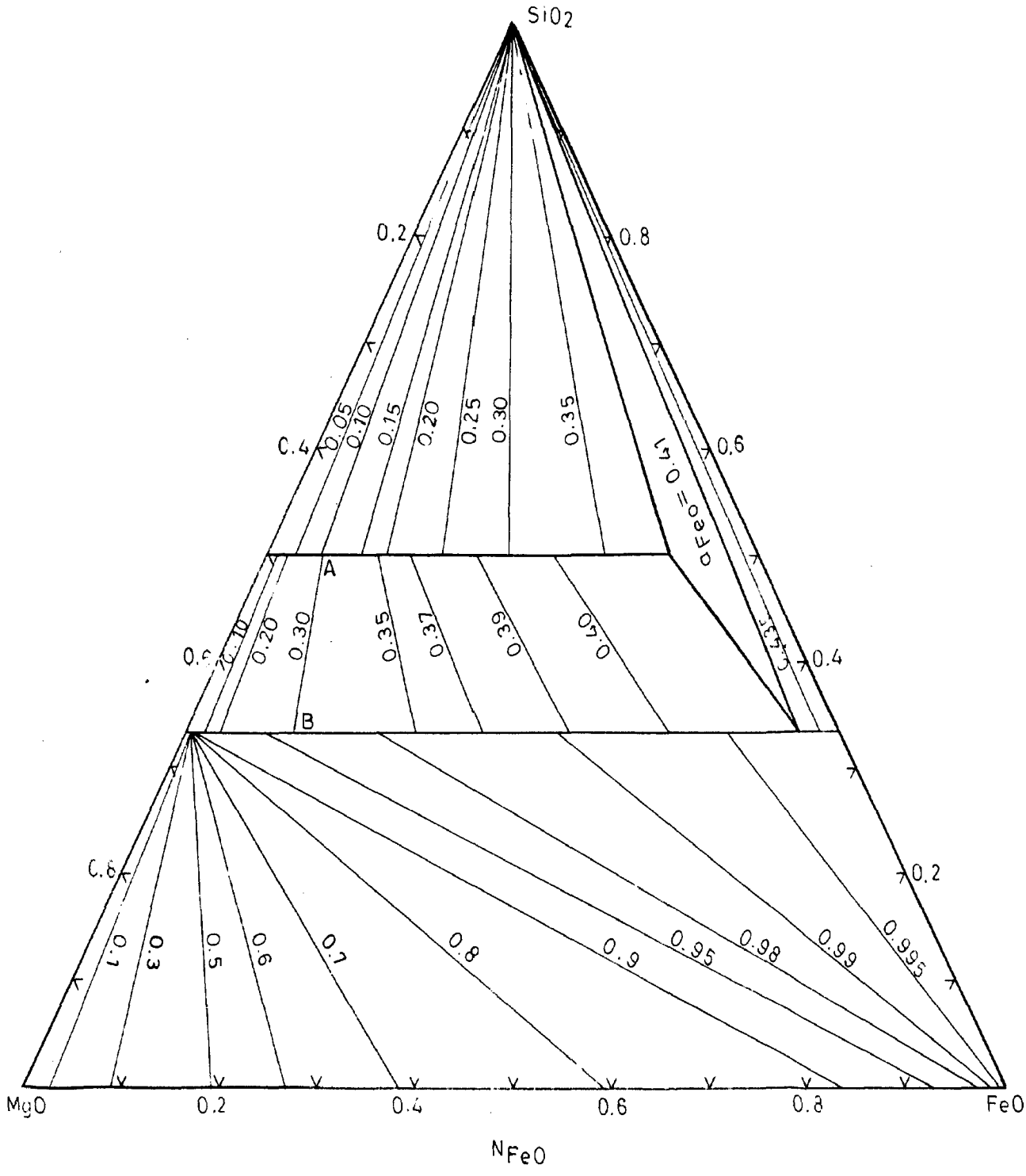

FIG.4.5. LINES OF FeO ACTIVITY AT 1000K IN THE SYSTEM MgO-FeO-SiO_2

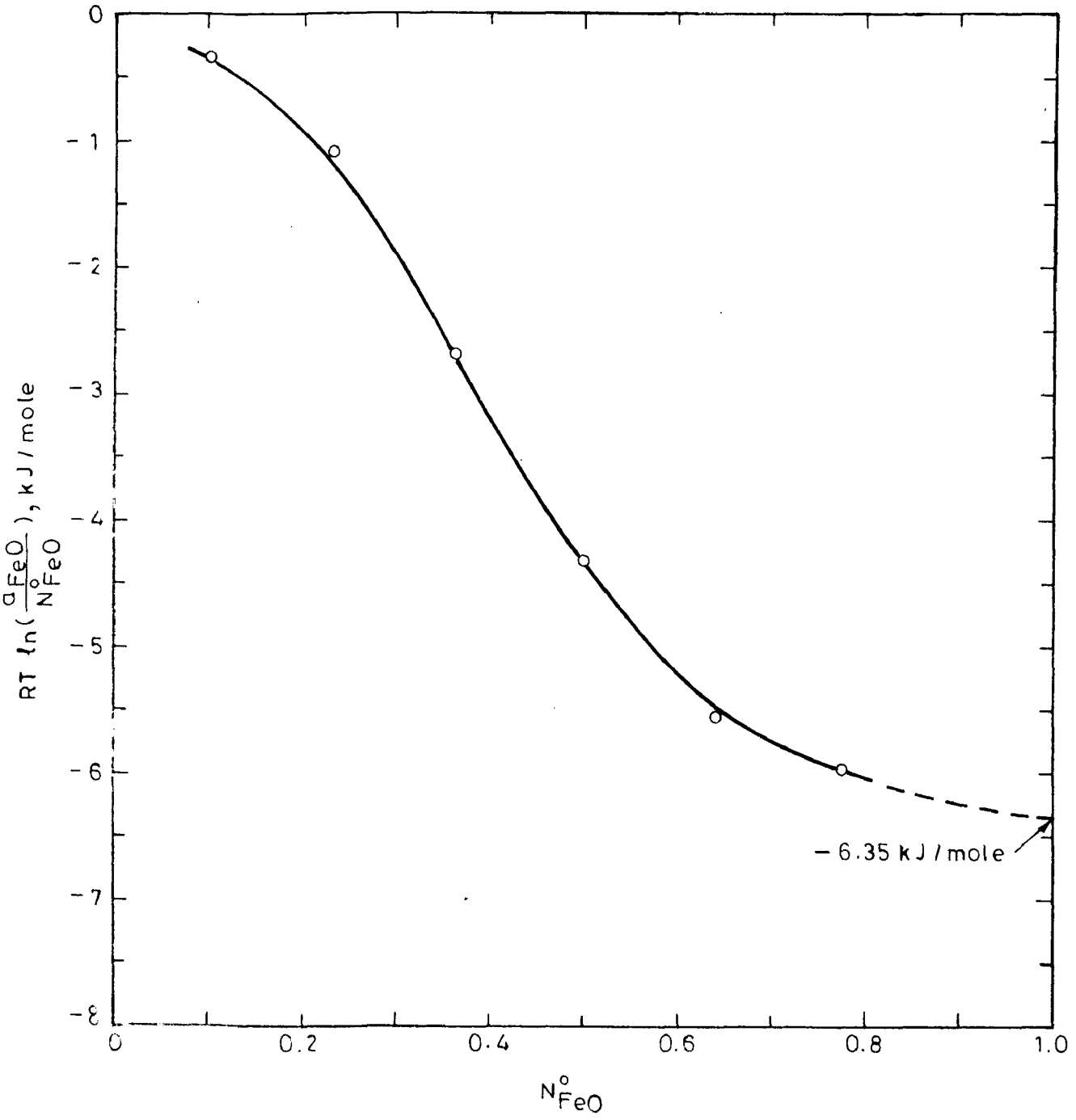

FIG.4.6. PLOT OF $RT\ ln(\frac{a_{FeO}}{N^{\circ}_{FeO}})$ Vs N°_{FeO} AT $N_{SiO_2}=0.6$ FOR THE SYSTEM $MgO-FeO-SiO_2$ AT 1000 K

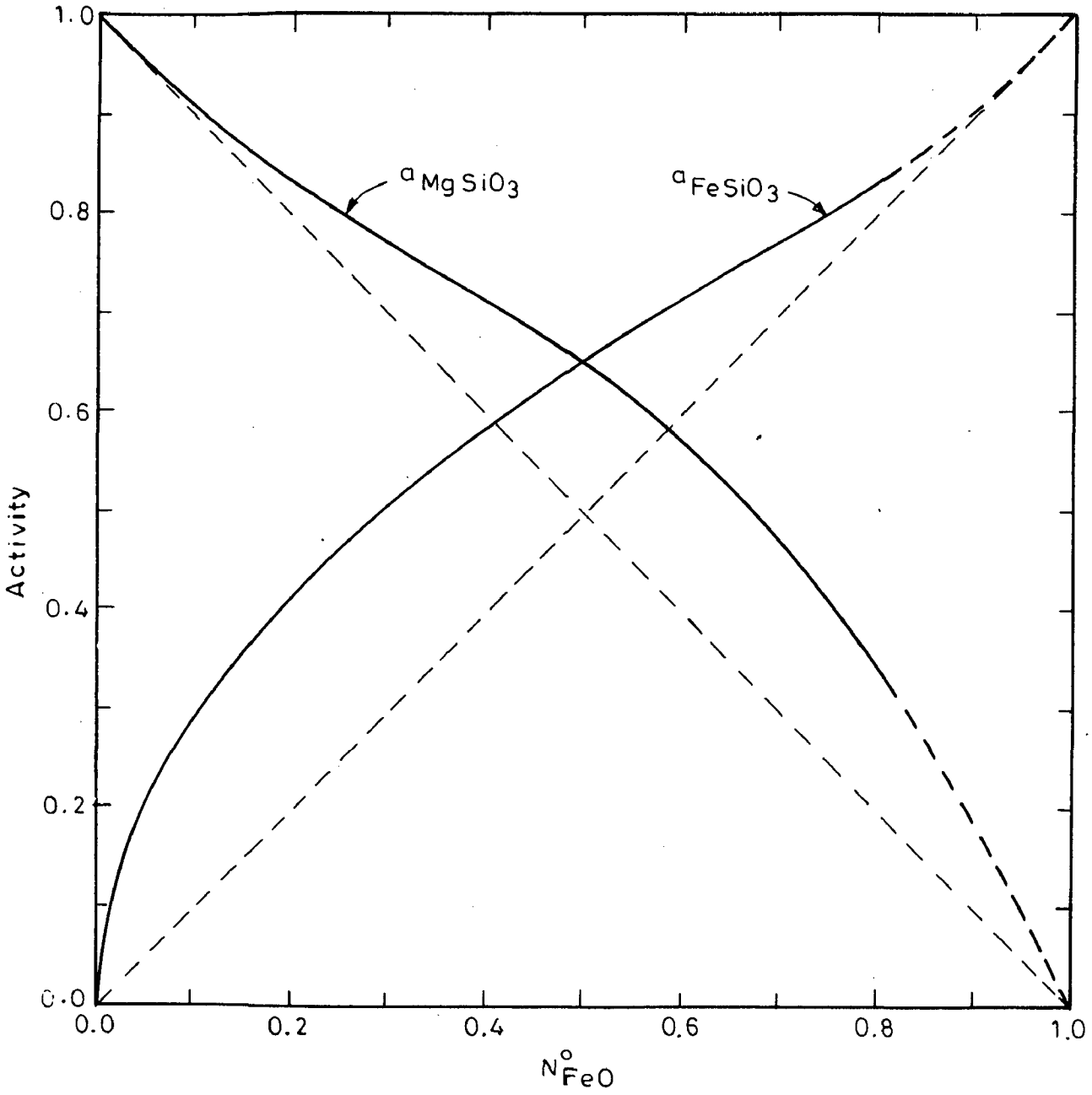

FIG.4.7. ACTIVITIES OF $FeSiO_3$ AND $MgSiO_3$ AT 1000K IN PYROXENE SOLID SOLUTIONS

value of standard free energy of formation of $FeSiO_3$ from its component oxides, determined by other workers, viz. -4.6 kJ/mole at 1353 K by Johnson and Muan [160], -3.8 kJ/mole at 1523 K by Nafziger and Muan [194], -5.4 KJ/mole at 1423 K by Schwerdtfeger and Muan [208], -4.6 kJ/mole at 1523K and 1573 K by Muan and Nafziger [193], and -10.5 kJ/mole at 800 K by Richardson, Jeffes and Withers [221].

Activity of $FeSiO_3$ as a function of N^{o}_{FeO} was calculated by making use of Eq. (4.3), which gives : $a_{FeSiO_3} = K_{(4.2)} \times a_{FeO}$. From the standard free energy of formation of $FeSiO_3$, equilibrium constant, $K_{(4.2)}$, for the reaction (4.2) was found to be equal to 2.15. Thus, a_{FeSiO_3} was calculated for various values of N^{o}_{FeO}, e.g. at $N^{o}_{FeO} = 0.36$, $a_{FeSiO_3} = 2.15 \times 0.26 = 0.56$. Activity of $MgSiO_3$ is calculated from Gibbs-Duhem equation using a relation similar to Eq. (3.4).

Variation of a_{FeSiO_3} and a_{MgSiO_3} with N^{o}_{FeO}, plotted in Fig. (4.7), shows that $FeSiO_3$-$MgSiO_3$ solid solution has considerable positive deviation from ideality. ΔG_{Mix} and ΔG^{Ex}_{Mix} calculated from activity values, are plotted as a function of N^{o}_{FeO} in Figs. (4.10) and (4.11) respectively.

4.1.3 System Fe_2SiO_4-Mg_2SiO_4

Standard free energy of formation, $\Delta G^{o}_{Fe_2SiO_4}$, of Fe_2SiO_4 from component oxides FeO and SiO_2 was calculated to be -13.7 kJ/mole, as reported in Section 3.3, from the reversible emf of the following cell,

$$Pt/Fe,(Fe_2SiO_4+SiO_2)//ZrO_2\text{-}CaO//Fe,FeO/Pt \qquad ..(4.9)$$

Value of $\Delta G^{o}_{Fe_2SiO_4}$ at 1000 K can also be determined by combining the values of standard free energy of reaction for the following reaction

$$FeSiO_3 + FeO = Fe_2SiO_4 \qquad ..(4.10)$$

and reaction (4.2). Standard free energy of reaction, $\Delta G^{o}_{(4.2)}$, for the reaction (4.2) at 1000 K is already known to be -6.35 kJ/mole, as determined in Section 4.1.2. As reaction (4.10) is valid in region II, experimental values of activity of FeO in this region were utilized to determine the value of $\Delta G^{o}_{(4.10)}$ as explained below.

Equilibrium constant, $K_{(4.10)}$ is expressed as

$$K_{(4.10)} = \frac{a_{Fe_2SiO_4}}{a_{FeSiO_3} \cdot a_{FeO}} \qquad ..(4.11)$$

Taking logarithm and multiplying by RT on both sides gives:

$$RT \ln K_{(4.10)} = RT \ln a_{Fe_2SiO_4} - RT \ln a_{FeSiO_3} - RT \ln a_{FeO} \qquad ..(4.12)$$

Use of relation $\Delta G^{o}_{(4.10)} = -RT \ln K_{(4.10)}$ and rearrangement of terms gives

$$RT \ln a_{FeO} = \Delta G^{o}_{(4.10)} + RT \ln a_{Fe_2SiO_4} - RT \ln a_{FeSiO_3} \qquad ..(4.13)$$

Now, as $N^{o}_{FeO} \longrightarrow 1$; $\begin{cases} \ln a_{Fe_2SiO_4} \longrightarrow 0 \\ \ln a_{FeSiO_3} \longrightarrow 0 \end{cases}$

Hence,

$$\left[RT \ln a_{FeO} \longrightarrow \Delta G^{\circ}_{(4.10)} \right]_{N^{\circ}_{FeO} \rightarrow 1} \qquad ..(4.14)$$

Equation (4.14) is valid in region II and therefore, applies to activity data for N_{SiO_2} equal to 0.4 and 0.47. Fig. (4.8) shows the variation of RT ln a_{FeO} with N°_{FeO} for N_{SiO_2} equal to 0.4 and 0.47. When both the curves are extrapolated to N°_{FeO} equal to 1, they cut the RT ln a_{FeO} axis at -7.25 kJ/mole, which is nothing but $\Delta G^{\circ}_{(4.10)}$ at 1000 K.

Addition of Eq. (4.2) and Eq. (4.10) gives

$$2FeO + SiO_2 = Fe_2SiO_4 \qquad ..(4.15)$$

Standard free energy of formation of Fe_2SiO_4 according to Eq. (4.15), therefore, is given by the relationship,

$$\Delta G^{\circ}_{(4.15)} = \Delta G^{\circ}_{(4.2)} + \Delta G^{\circ}_{(4.10)} \qquad ..(4.16)$$

Using the values -6.35 kJ/mole and -7.25 kJ/mole as determined earlier for $\Delta G^{\circ}_{(4.2)}$ and $\Delta G^{\circ}_{(4.10)}$ respectively, standard free energy of formation of Fe_2SiO_4, $\Delta G^{\circ}_{(4.15)}$ or $\Delta G^{\circ}_{Fe_2SiO_4}$, from its component oxides is found to be -13.6 kJ/mole.

Value of $\Delta G^{\circ}_{Fe_2SiO_4}$ equal to -13.7 kJ/mole, reported in Section (3.3) is based on a direct method and hence is more reliable. The agreement between the two values is excellent. Present value of $\Delta G^{\circ}_{Fe_2SiO_4}$ also compares well with the values of $\Delta G^{\circ}_{Fe_2SiO_4}$ reported by other workers [160,193,208,220-223] (see Section 3.3).

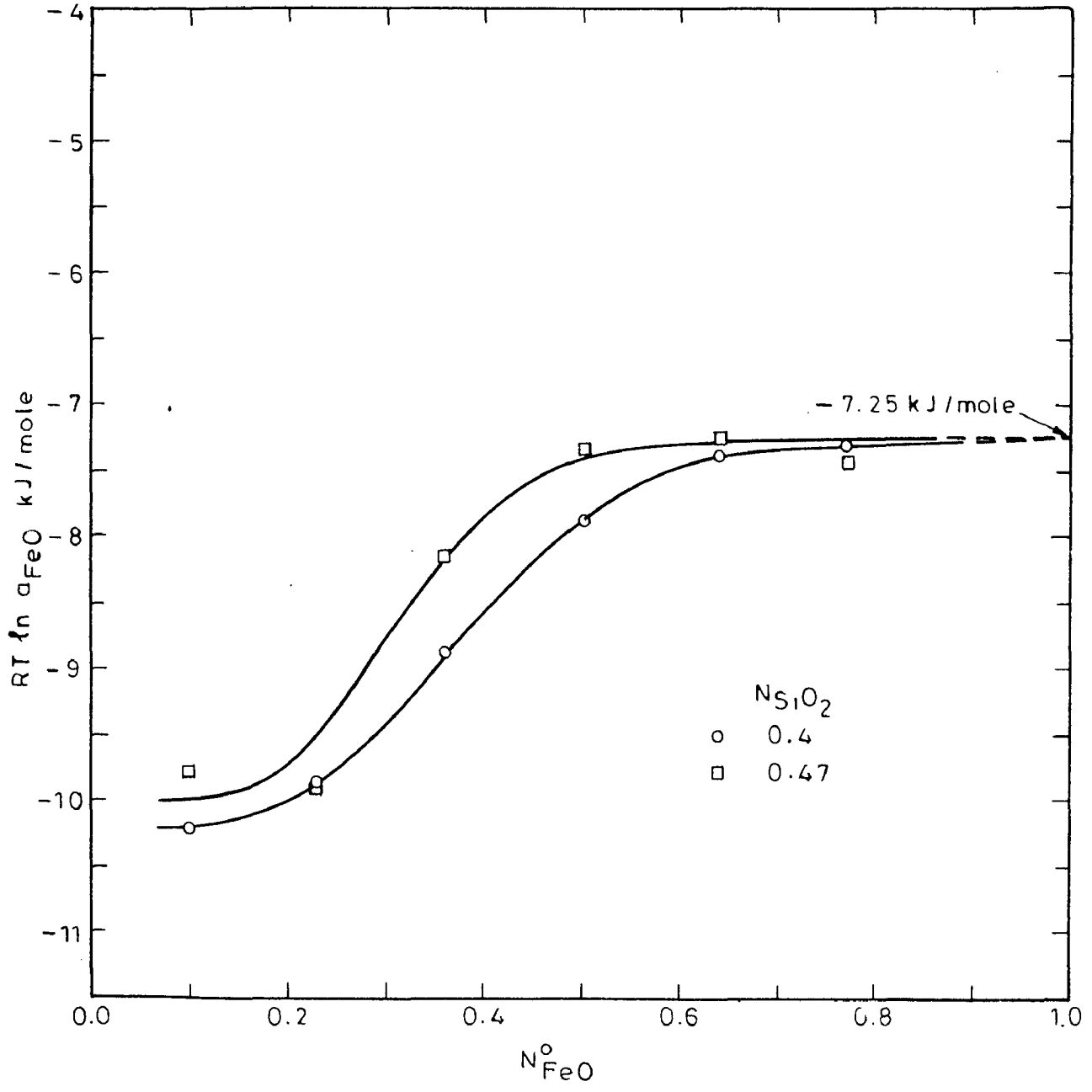

FIG.4.8. PLOT OF RT ln a_{FeO} Vs N^{o}_{FeO} AT N_{SiO_2} =0.4 AND 0.47 FOR THE SYSTEM MgO-FeO-SiO_2 AT 1000 K.

Values of activity of Fe_2SiO_4 were calculated from relation (4.11), which gives

$$a_{Fe_2SiO_4} = K_{(4.10)} \times a_{FeO} \times a_{FeSiO_3} \quad \ldots(4.17)$$

$K_{(4.10)}$, as calculated from $\Delta G^{o}_{(4.10)}$, which is equal to -7.25 kJ/mole, was found to be equal to 2.4. Activity of FeO along the line $N_{SiO_2} = 1/3$ is known from iso-a_{FeO} lines in region II. Activity of $FeSiO_3$ along the line $N_{SiO_2}=1/3$ was determined from the iso-a_{FeO} lines in region II and a_{FeSiO_3} vs N^{o}_{FeO} plot (Fig. 4.7) which is valid for $N_{SiO_2} \geq 0.5$.

As an example, consider iso-activity line for a_{FeO} equal to 0.3 in region II. All the compositions lying on this line have a_{FeO} equal to 0.3 and are in thermodynamic equilibrium. This line shows that point A defined by $N^{o}_{FeO} = 0.11$ and $N_{SiO_2} = 0.5$ is in thermodynamic equilibrium with point B, having $N^{o}_{FeO} = 0.168$ and $N_{SiO_2} = 1/3$ (see Fig. 4.7), which implies that a_{FeSiO_3} at point A and point B is same. a_{FeSiO_3} at point A, as read from Fig. (4.7), is equal to 0.305, therefore, activity of $FeSiO_3$ at $N^{o}_{FeO} = 0.168$ along the line $N_{SiO_2} = 1/3$ (point B) is also equal to 0.305. Hence the activity of Fe_2SiO_4 in olivine solid solution at point B is given by, $a_{Fe_2SiO_4} = 2.4 \times 0.3 \times 0.305 = 0.22$ at $N^{o}_{FeO} = 0.168$. Similarly activity of Fe_2SiO_4 was calculated at few other points. Values of activity of Mg_2SiO_4 were calculated from Gibbs Duhem equation, using a relation similar to Eq. (3.4).

Activity-composition relationships for Fe_2SiO_4 and Mg_2SiO_4 in the binary solid solution Fe_2SiO_4-Mg_2SiO_4 at 1000 K are plotted in Fig. (4.9). These plots show that olivine solid solution has moderate positive deviation from ideality. ΔG_{Mix} and ΔG^{Ex}_{Mix}, calculated from the values of activity of Fe_2SiO_4 and Mg_2SiO_4, for the olivine solid solution at 1000 K are plotted as a function of N^{o}_{FeO} in Figs. (4.10) and (4.11) respectively.

Values of $\Delta G^{o}_{Fe_2SiO_4}$, as determined earlier in this section to be -13.6 kJ/mole, was used to calculate the values of activity of FeO in region V.

Consider Eq. (4.15)

$$2FeO + SiO_2 = Fe_2\ SiO_4 \qquad ..(4.15)$$

As part of SiO_2 present exists as pure phase in region V, equilibrium constant for this reaction is given by

$$K_{(4.15)} = \frac{a_{Fe_2SiO_4}}{(a_{FeO})^2} \qquad ..(4.18)$$

Activity of Fe_2SiO_4 in region V is equal to its mole fraction as it follows Raoult's law in this region (Fig.4.9), and mole fraction of Fe_2SiO_4 is equal to N^{o}_{FeO}. Therefore, in region V, $a_{Fe_2SiO_4}$ is equal to N^{o}_{FeO}. Equilibrium constant, $K_{(4.15)}$ at 1000 K - calculated from $\Delta G^{o}_{Fe_2SiO_4}$ equal to -13.6 kJ/mole was found to be equal to 5.14. It was found from equation (4.18) that at N^{o}_{FeO} equal to 0.973, a_{FeO} is equal to 0.435 and an iso-activity line corresponding to this value

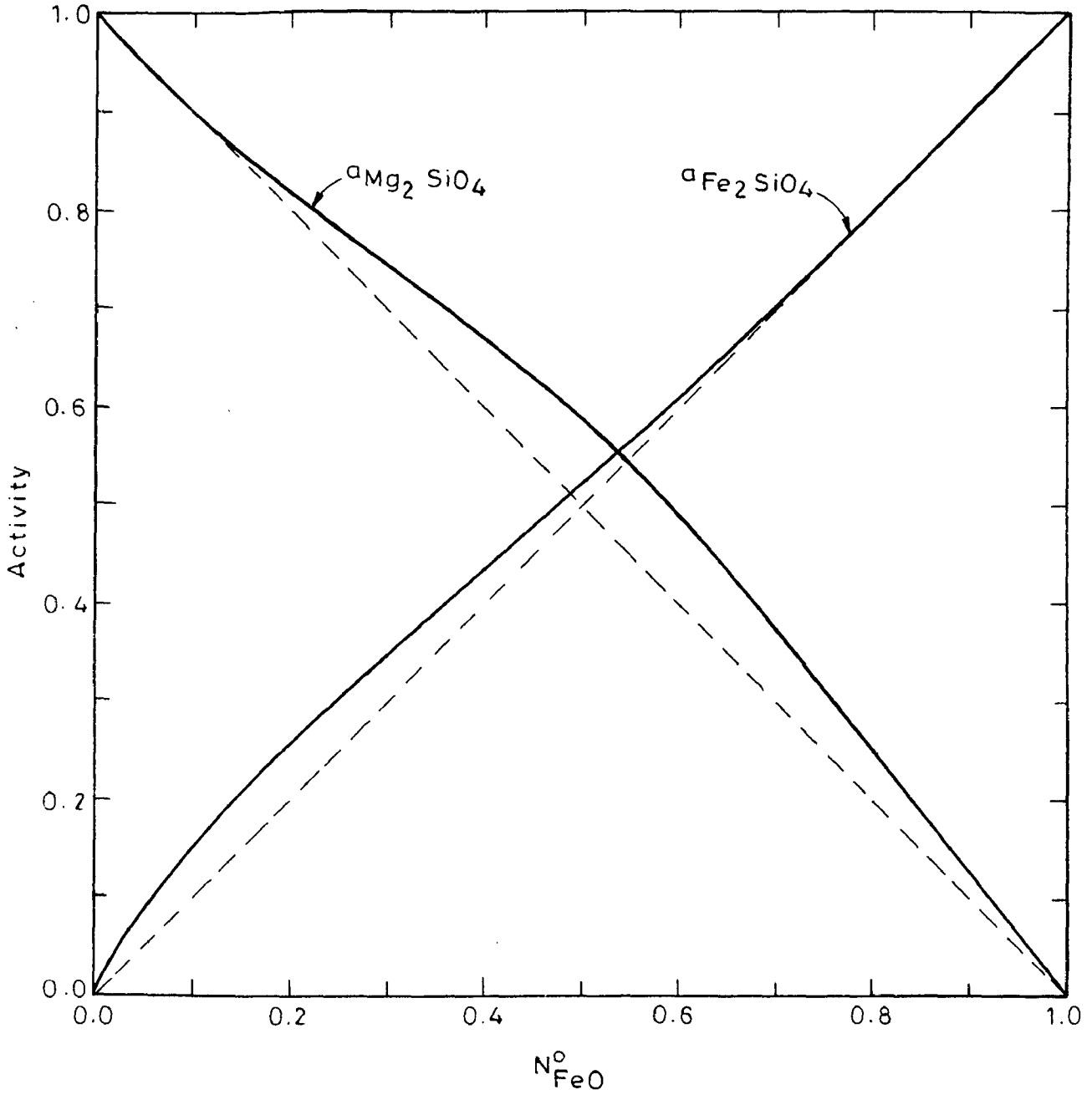

FIG.4.9. ACTIVITIES OF Fe_2SiO_4 AND Mg_2SiO_4 AT 1000 K IN OLIVINE SOLID SOLUTIONS

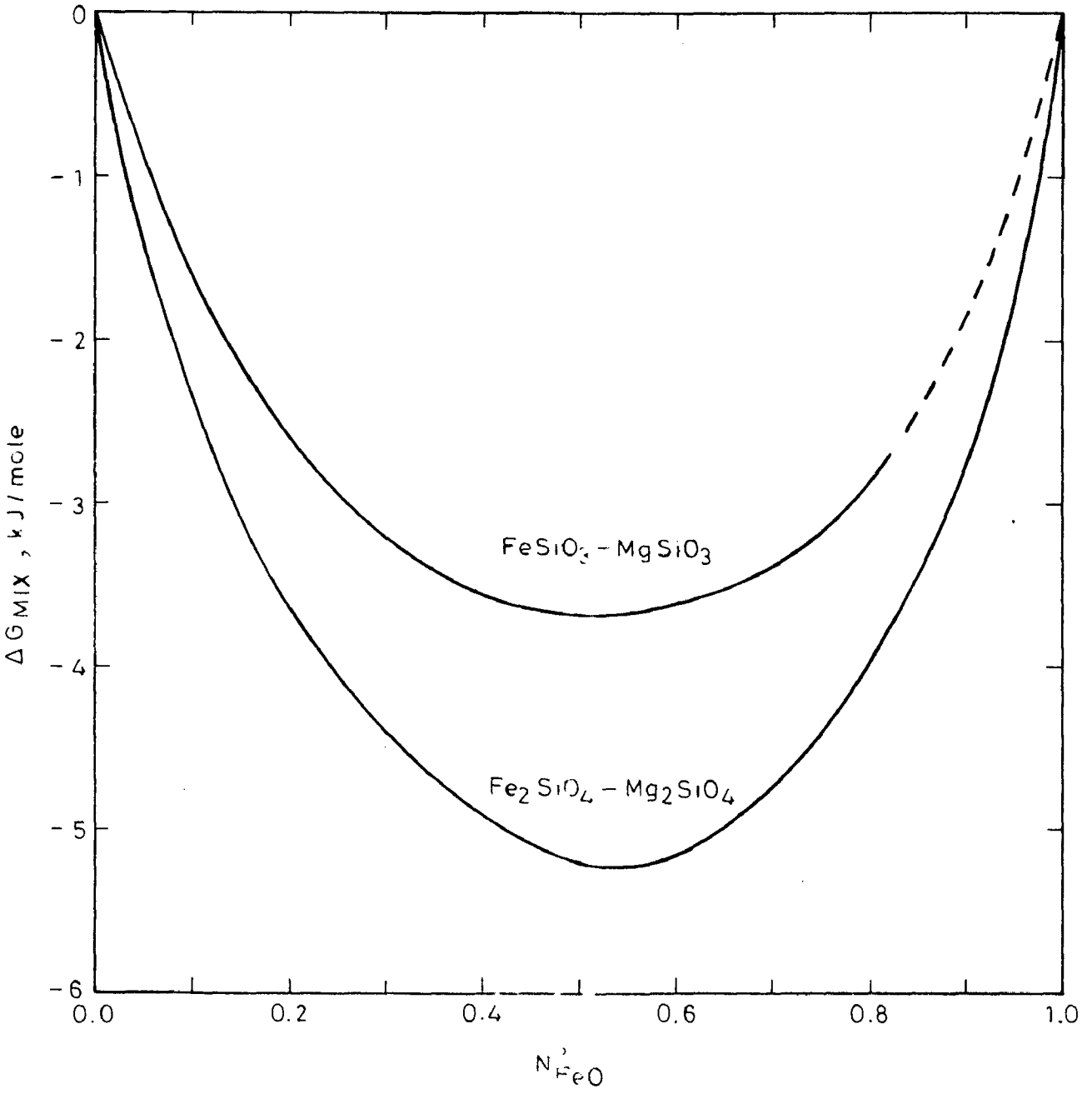

FIG.4.10. INTEGRAL FREE ENERGY OF MIXING FOR PYROXENE AND OLIVINE SOLID SOLUTIONS AT 1000 K

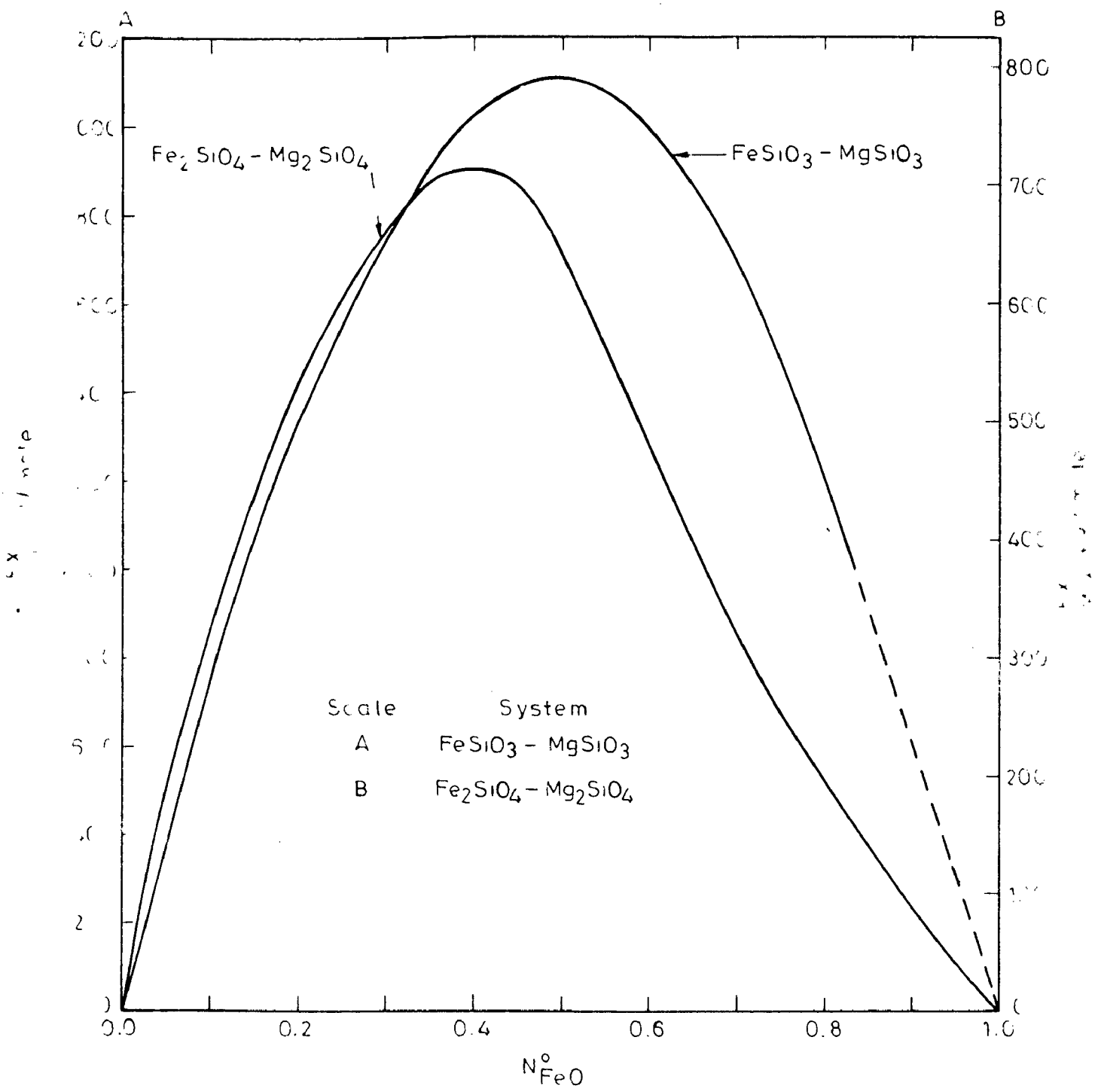

FIG.4.11. INTEGRAL EXCESS FREE ENERGY OF MIXING FOR PYROXENE AND OLIVINE SOLID SOLUTIONS AT 1000K

of a_{FeO} is drawn in region V of Fig. (4.5).

4.1.4 MgO Activity Lines

Iso-activity lines for MgO were drawn from the known values of a_{MgSiO_3} (section 4.1.3) and free energy of formation of $MgSiO_3$ taken from literature [220] on the basis of following reaction:

$$MgO + SiO_2 = MgSiO_3 \qquad ..(4.19)$$

Free energy of formation for this reaction is -33.5 kJ/mole at 1000 K and equilibrium constant, $K_{(4.19)}$, calculated from this value is equal to 56.3, which gives the following expression for the a_{MgO} in region I

$$a_{MgO} = \frac{a_{MgSiO_3}}{56.3} \qquad ..(4.20)$$

Using Eq. (4.20) , values of activity of MgO were calculated for certain values of N^o_{Feo} and were plotted as a function of N^o_{Feo}. From this plot N^o_{FeO} was found for selected values of a_{MgO} and iso-activity lines for a_{MgO} equal to 0.016, 0.014, 0.012, 0.01 and 0.008 were drawn in region I, as shown in Fig. (4.12).

Lines of MgO activity in region II were drawn from known values of activity of $MgSiO_3$ in pyroxene solid solution and that of Mg_2SiO_4 in olivine solid solution and from a knowledge of a_{FeO}-lines in region II as follows:

Consider the following reaction,

$$MgO + MgSiO_3 = Mg_2SiO_4 \qquad ..(4.21)$$

Equilibrium constant, $K_{(4.21)}$, for this reaction is given by the relationship,

$$K_{(4.21)} = \frac{a_{Mg_2SiO_4}}{a_{MgO} \cdot a_{MgSiO_3}} \qquad ..(4.22)$$

Standard free energy change, $\Delta G^o_{(4.21)}$, for the reaction (4.21) was calculated from the following relationship,

$$\Delta G^o_{(4.21)} = \Delta G^o_{Mg_2SiO_4} - \Delta G^o_{MgSiO_3} \qquad ..(4.23)$$

where,

$\Delta G^o_{Mg_2SiO_4}$ is the standard free energy of formation of Mg_2SiO_4 from its component oxides and $\Delta G^o_{MgSiO_3}$ is similarly defined. Taking $\Delta G^o_{Mg_2SiO_4}$ equal to -62.7 kJ/mole and $\Delta G^o_{MgSiO_3}$ equal to -33.5 kJ/mole at 1000 K, as determined from the data after Elliott, Gleiser and Ramakrishna [220], $\Delta G^o_{(4.21)}$ is computed to be -29.2 kJ/mole, which gives a value of 33.6 to equilibrium constant, $K_{(4.21)}$, for the reaction (4.21) at 1000 K. Substituting this value of $K_{(4.21)}$ in Eq. (4.22) and rearranging terms, we get

$$a_{MgO} = \frac{a_{Mg_2SiO_4}}{33.6 x a_{MgSiO_3}} \qquad ..(4.24)$$

Values of a_{MgO}, calculated from relation (4.24) were utilised to draw iso-a_{MgO} lines in region II. As an example consider iso-activity line for a_{FeO} equal to 0.3 in region II. All the points on this line are in thermodynamic equilibrium

with each other. End points of this line, as shown in Fig. (4.5) are : A(N^{o}_{FeO} = 0.11, N_{SiO_2} = 0.5) and B (N^{o}_{FeO} = 0.168, N_{SiO_2} = 1/3). Activity of $MgSiO_3$ at point A (Fig. 4.7) is 0.9 and activity of Mg_2SiO_4 at point B (Fig. 4.9) is 0.86,. Therefore, activity of MgO along this line, as calculated from Eq. (4.24), is 0.0284. Similarly activity of MgO along other a_{FeO}-lines was calculated. Two plots of a_{MgO} against N^{o}_{FeO} were then drawn, one for N_{SiO_2} = 0.5 and the other for N_{SiO_2} = 1/3. Corresponding end points for selected values of a_{MgO} were read from these plots, and on the basis of these points iso-activity lines were drawn for a_{MgO} equal to 0.029, 0.028, 0.026, 0.024, 0.022, 0.020, 0.018 and 0.014 in region II, as shown in Fig. (4.12).

Iso-a_{MgO} lines in region III were drawn on the basis of iso-a_{FeO} lines in region III and a_{MgO} vs N_{FeO} plot of the binary system FeO-MgO. Values of N^{o}_{FeO} corresponding to various values of a_{FeO} were read from Fig. (4.5) for N_{SiO_2} equal to 0.1, 0.2 and 0.3 and also the values of a_{MgO} were noted corresponding to these values of a_{FeO} from the activity-composition plot, Fig. (3.1), for the binary system FeO-MgO. Then, four curves showing the variation of a_{MgO} with N^{o}_{FeO} were drawn on the same graph paper, one for binary system FeO-MgO and the other three for the ternary system FeO-MgO-SiO_2 corresponding to N_{SiO_2} equal to 0.1, 0.2 and 0.3. On the basis of these curves, various iso-activity lines for MgO were drawn in region III. These lines are also shown in Fig. (4.12).

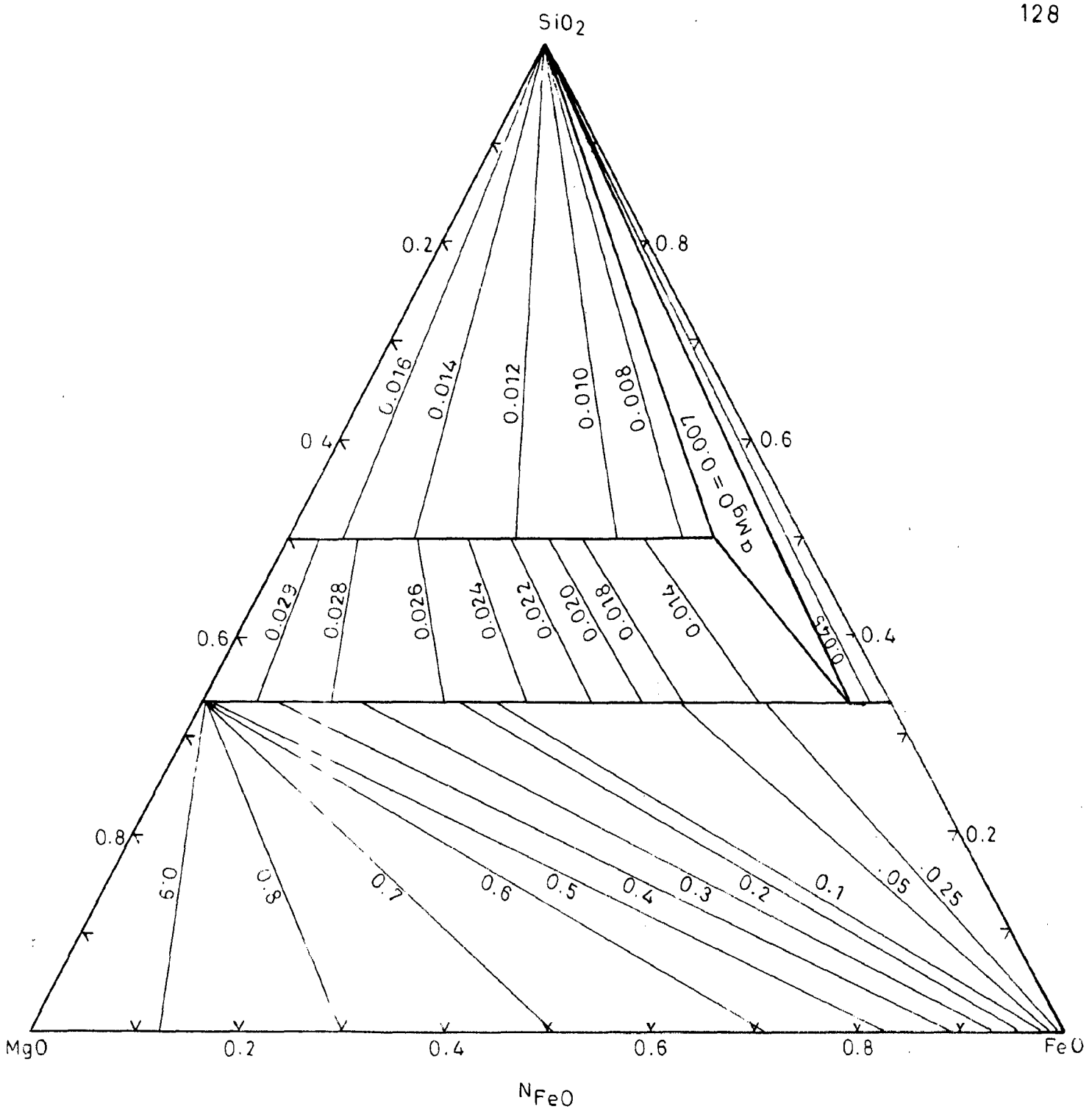

FIG.4.12. LINES OF MgO ACTIVITY AT 1000K IN THE SYSTEM $MgO-FeO-SiO_2$

Activity of MgO in region IV-a three-phase region - should be constant and was found to be equal to 0.007. This value was fixed on the basis of activity of MgO at the boundary of region II, as found from a_{MgO} vs N^{o}_{FeO} plots for N_{SiO_2} equal to 0.5 and 1/3.

Finally an iso-a_{MgO} line for a_{MgO} equal to 0.0045 was drawn in region V on the basis of following reaction:

$$2MgO + SiO_2 = Mg_2 SiO_4 \qquad ..(4.25)$$

Standard free energy change, $\Delta G^{o}_{(4.25)}$, for the above reaction, as found from the data reported in literature [220] is -62.7 kJ/mole, which gives a value of 1891.5 to the equilibrium constant, $K_{(4.25)}$, for the reaction (4.25). Using this value of $K_{(4.25)}$ and remembering that silica exists as pure phase in region V, we get the following expression for the activity of MgO.

$$a_{MgO} = \sqrt{\frac{a_{Mg_2SiO_4}}{1891.5}} \qquad ..(4.26)$$

Activity of MgO was found to be 0.0045 at N^{o}_{FeO} equal to 0.97 using relation (4.26). This line is also shown in Fig. (4.12).

4.1.5 SiO_2 Activity Lines

In regions I, IV and V, pure silica is one of the stable phase, therefore, activity of silica is equal to 1.

Values of activity of silica in region II were calculated from the following relation:

$$Fe_2SiO_4 + SiO_2 = 2FeSiO_3 \qquad ..(4.27)$$

This equation is obtained by subtracting Eq. (4.10) from Eq. (4.2) and therefore,

$$\Delta G^{\circ}_{(4.27)} = \Delta G^{\circ}_{(4.2)} - \Delta G^{\circ}_{(4.10)} \qquad ..(4.28)$$

Standard free energy change, $\Delta G^{\circ}_{(4.27)}$, for the reaction (4.27), as calculated from $\Delta G^{\circ}_{(4.2)}$ equal to -6.35 kJ/mole (section 4.1.2) and $\Delta G^{\circ}_{(4.10)}$ equal to -7.25 kJ/mole (section 4.1.3), was found to be 0.9 kJ/mole at 1000 K giving a value of 0.897 to $K_{(4.27)}$.

Equilibrium constant, $K_{(4.27)}$, for the reaction (4.27) is given as :

$$K_{(4.27)} = \frac{(a_{FeSiO_3})^2}{a_{Fe_2SiO_4} \cdot a_{SiO_2}} \qquad ..(4.29)$$

Rearrangement of terms and substitution of relevant value of $K_{(4.27)}$ give:

$$a_{SiO_2} = \frac{(a_{FeSiO_3})^2}{0.897 \times a_{Fe_2SiO_4}} \qquad ..(4.30)$$

Values of activity of silica were calculated using Eq. (4.30) along different a_{FeO} lines by a method similar to the method used to calculate the values of activity of MgO in this region. For example, values of activity of $FeSiO_3$

and Fe_2SiO_4 along the iso-a_{FeO} line for a_{FeO} equal to 0.3 are 0.305 and 0.22 respectively and thus a_{SiO_2} along this line and at end points A and B (see Fig. 4.5) is 0.471. Similarly, values of activity of silica along other iso-a_{FeO} lines were calculated. Then a_{SiO_2} lines for a_{SiO_2}=0.4,0.45, 0.5, 0.6, 0.7, 0.8, 0.85 and 0.9 were drawn in region II following the same procedure as was used to draw iso-a_{MgO} lines in region II(see section 4.1.4). These lines are shown in Fig. (4.13).

In region III, which consists of magnesiowustite and olivine, values of activity of silica were calculated from the following relationship:

$$2FeO + SiO_2 = Fe_2SiO_4 \qquad ..(4.15)$$

ΔG^o for this reaction is already known to be -13.6 kJ/mole and $K_{(4.15)}$ is equal to 5.14 (section 4.1.3). Hence activity of silica is given by the following relationship

$$a_{SiO_2} = \frac{a_{Fe_2SiO_4}}{5.14x(a_{FeO})^2} \qquad ..(4.31)$$

A plot of a_{FeO} vs N^o_{FeO} for N_{SiO_2} equal to 1/3 was drawn on the basis of iso-a_{FeO} lines in region III. Values of activity of FeO for selected values of N^o_{FeO} were read from this plot and values of activity of Fe_2SiO_4 were read from Fig. (4.9) at the same values of N^o_{FeO} and values of activity of silica were calculated using relation (4.31) at these points. These a_{SiO_2} values are valid only for N_{SiO_2} equal

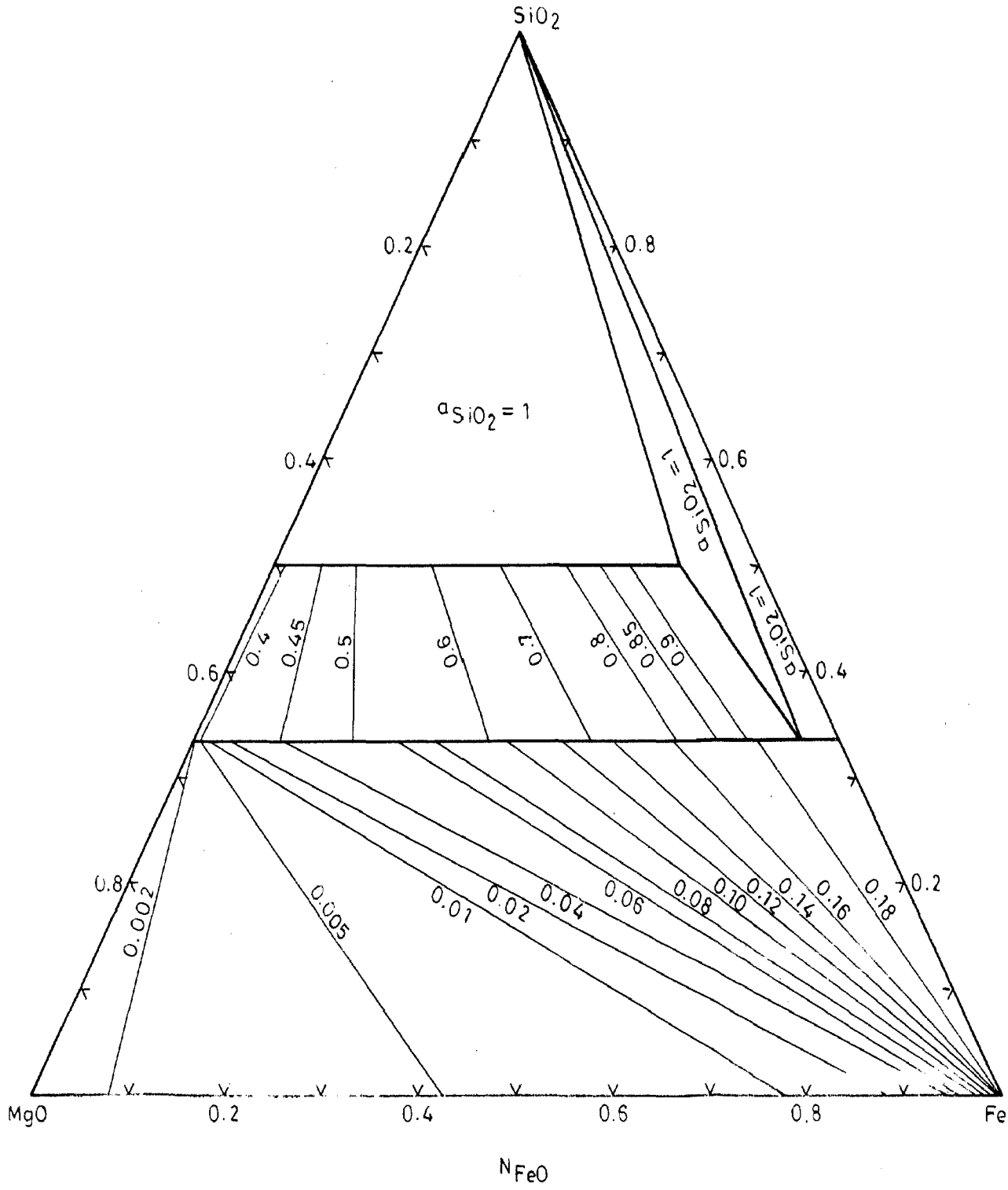

FIG.4.13. LINES OF SiO_2 ACTIVITY AT 1000 K IN THE SYSTEM MgO-FeO-SiO_2

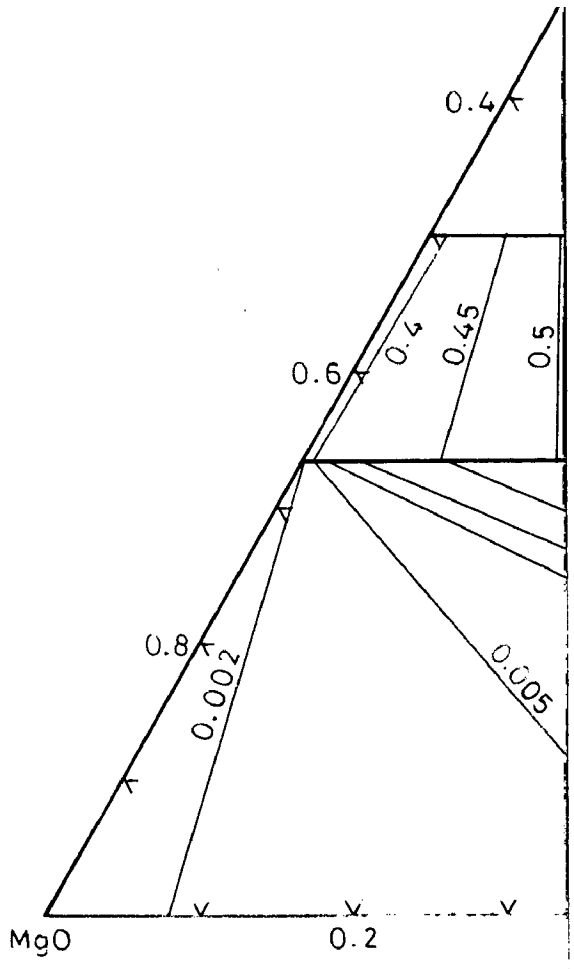

FIG.4.13. LINES OF SiO_2 A

to 1/3 in region III. A curve showing variation of a_{SiO_2} with N^{o}_{FeO} along the line N_{SiO_2} equal to 1/3 was drawn. On the basis of this plot and iso-a_{FeO} lines in region III, three other a_{SiO_2} vs. N^{o}_{FeO} plots for N_{SiO_2} equal to 0.1, 0.2 and 0.3 were drawn on the same graph paper. Making use of these plots iso-a_{SiO_2} lines for a_{SiO_2} = 0.18, 0.16, 0.14, 0.12, 0.10, 0.08, 0.06, 0.04, 0.02, 0.01, 0.005 and 0.002 were drawn in region III as shown in Fig. (4.13).

4.2 SYSTEM MgO-FeO-CaO

In literature, very little information is available about the phase relations in this system.Only the 1773 K isothermal section, studied in detail by Johnson and Muan [217] is reported for this system.

Although stable phases of the system MgO-FeO-CaO are not completely known at or near 1000 K, the phase stability relations for the three bounding binary systems are well studied and understood. FeO and MgO are completely soluble in each other in all proportions [151](Fig. 1.10),FeO and CaO have limited solubility for each other and an intermediate compound $Ca_2 Fe_2O_5$ is also present in this system (Fig. 1.11) and oxides MgO and CaO are practically insoluble in each other at 1000 K and form a simple eutectic system as shown in Fig. (4.14)[151]

Values of activity of FeO for various selected compositions were determined using a cell represented by Eq. (3.1)

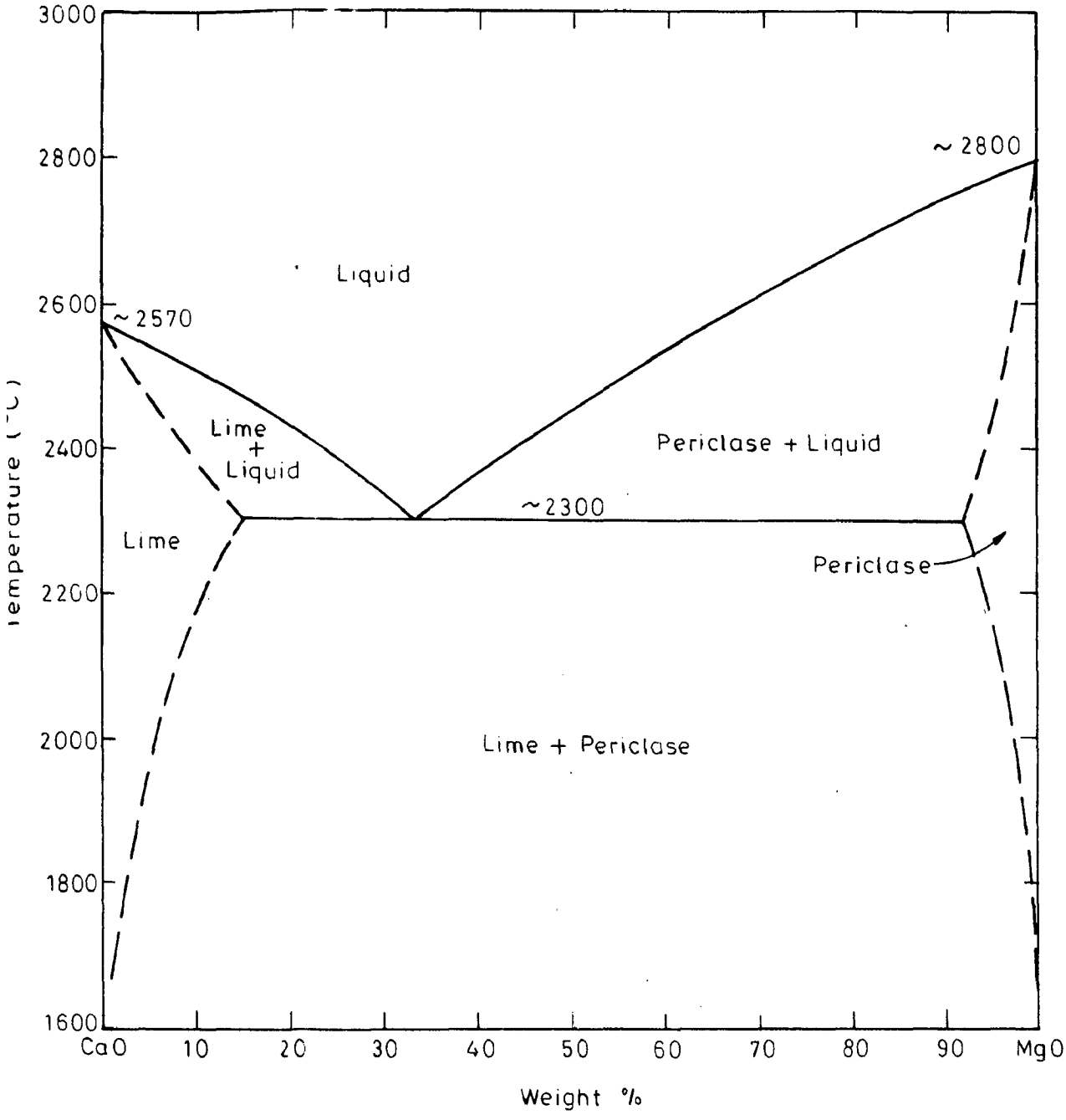

FIG.4.14. PHASE DIAGRAM FOR THE SYSTEM CaO-MgO [151]

with a hope that this information combined with the known phase relations in the three bounding binary systems will be helpful to arrive at possible phase boundaries leading to a step towards understanding of phase stability relations in this system at 1000 K.

Compositions studied in binary system FeO-MgO i.e. N_{FeO} equal to 0.1, 0.23, 0.36, 0.5, 0.64, 0.77 and 0.9 were taken as base and varying amounts of third component, CaO, were added to it to prepare the samples for studying this system. Corresponding to each value of N^{o}_{FeO} (defined by Eq. (4.1) in section 4.1), eight samples having N_{CaO} equal to 0.1, 0.2, 0.3, 0.4, 0.5, 0.6, 0.7 and 0.8 were prepared. Thus a total of fifty six samples of various compositions were prepared and studied by the cell represented by Eq.(3.1) at 1000 K.

Measured values of reversible emf for all the compositions are given in table 4.3. Plotted curves of emf vs. N^{o}_{FeO} for different values of N_{CaO} are shown in Figs. (4.15) and (4.16). Values of activity of FeO for all the samples studied in this system were calculated using Eq. (3.3) and are reported in Table 4.4. Calculated values of activity of FeO were plotted against N^{o}_{FeO} for various values of N_{CaO}. These curves are shown in Figs. (4.17 - 4.20) for N_{CaO} equal to 0.1 and 0.5, 0.2 and 0.6, 0.3 and 0.7, and 0.4 and 0.8 respectively.

TABLE 4.3 : Emf values for the system MgO-FeO-CaO at 1000 K

Cell : Pt/Fe,(FeO+MgO+CaO)//ZrO_2 - CaO//Fe,FeO/Pt

N^{o}_{FeO}	Emf (mV)							
	N_{CaO}=0.1	N_{CaO}=0.2	N_{CaO}=0.3	N_{CaO}=0.4	N_{CaO}=0.5	N_{CaO}=0.6	N_{CaO}=0.7	N_{CaO}=0.8
0.10	49.1	51.1	52.6	53.3	54.1	57.2	58.0	67.2
0.23	25.7	26.5	26.1	26.5	26.9	27.7	29.4	33.0
0.36	17.6	17.9	17.9	17.9	17.6	17.9	18.9	19.9
0.50	13.3	15.4	15.4	15.4	15.4	15.4	15.4	15.4
0.64	9.9	11.5	15.4	15.4	15.4	15.4	15.4	15.4
0.77	7.0	8.3	9.6	15.4	15.4	15.4	15.4	15.4
0,90	4.8	5.3	6.0	8.1	15.4	15.4	15.4	15.4

TABLE-4.4 Values of FeO-activity for the system MgO-FeO-CaO at 1000 K

N^{o}_{FeO}	a_{FeO}							
	$N_{CaO}=0.1$	$N_{CaO}=0.2$	$N_{CaO}=0.3$	$N_{CaO}=0.4$	$N_{CaO}=0.5$	$N_{CaO}=0.6$	$N_{CaO}=0.7$	$N_{CaO}=0.8$
0.10	0.3201	0.3055	0.2951	0.2903	0.2850	0.2652	0.2603	0.2103
0.23	0.5508	0.5407	0.5458	0.5407	0.5357	0.5259	0.5055	0.4650
0.36	0.6647	0.6601	0.6601	0.6601	0.6647	0.6601	0.6450	0.6302
0.50	0.7345	0.6995	0.6995	0.6995	0.6995	0.6995	0.6995	0.6995
0.64	0.7947	0.7658	0.6995	0.6995	0.6995	0.6995	0.6995	0.6995
0.77	0.8501	0.8248	0.8003	0.6995	0.6995	0.6995	0.6995	0.6995
0.90	0.8946	0.8843	0.8700	0.8287	0.6995	0.6995	0.6995	0.6995

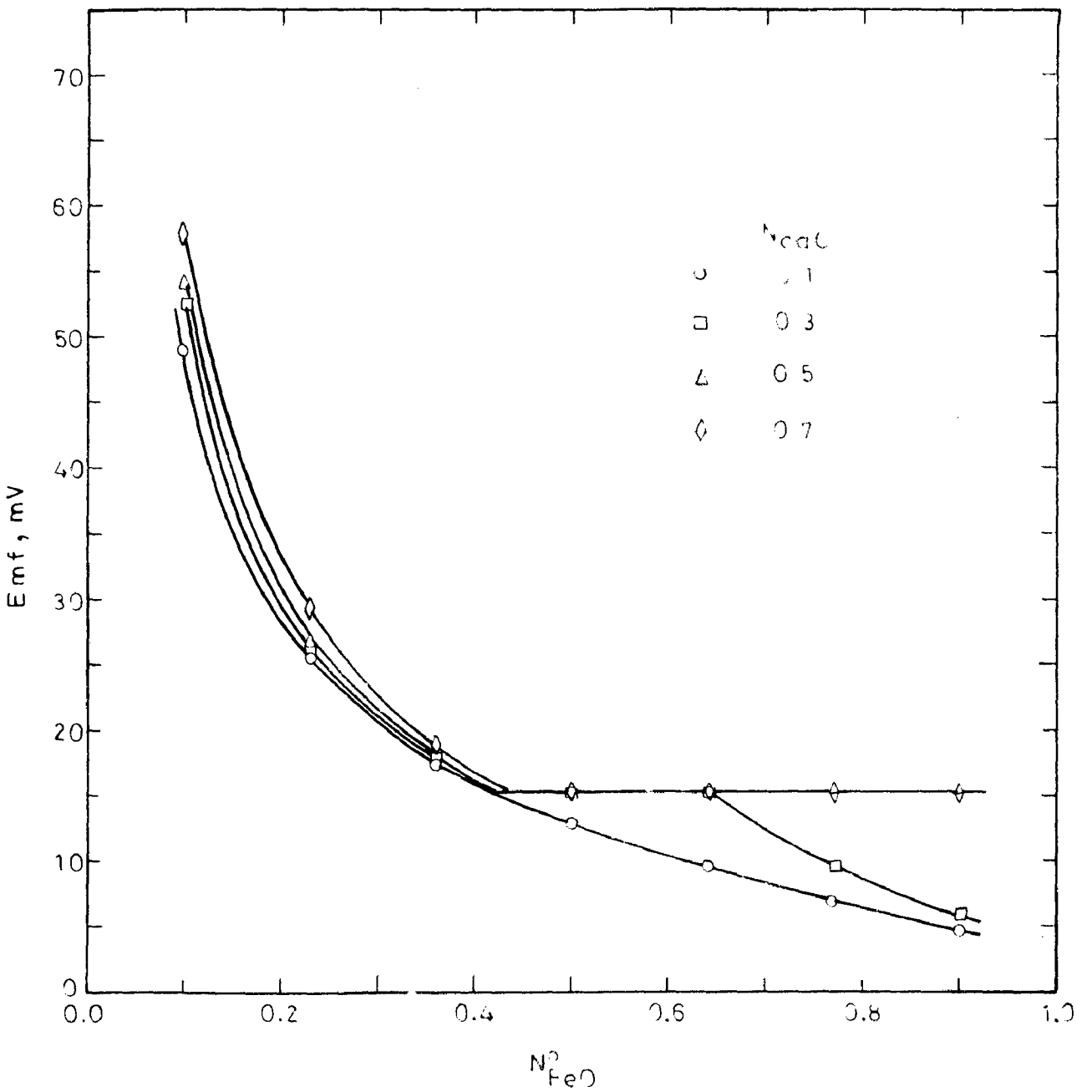

FIG.4.15. EMF Vs N°_{FeO} AT N_{CaO} = 0.1, 0.3, 0.5 AND 0.7 FOR THE SYSTEM MgO-FeO-CaO AT 1000 K

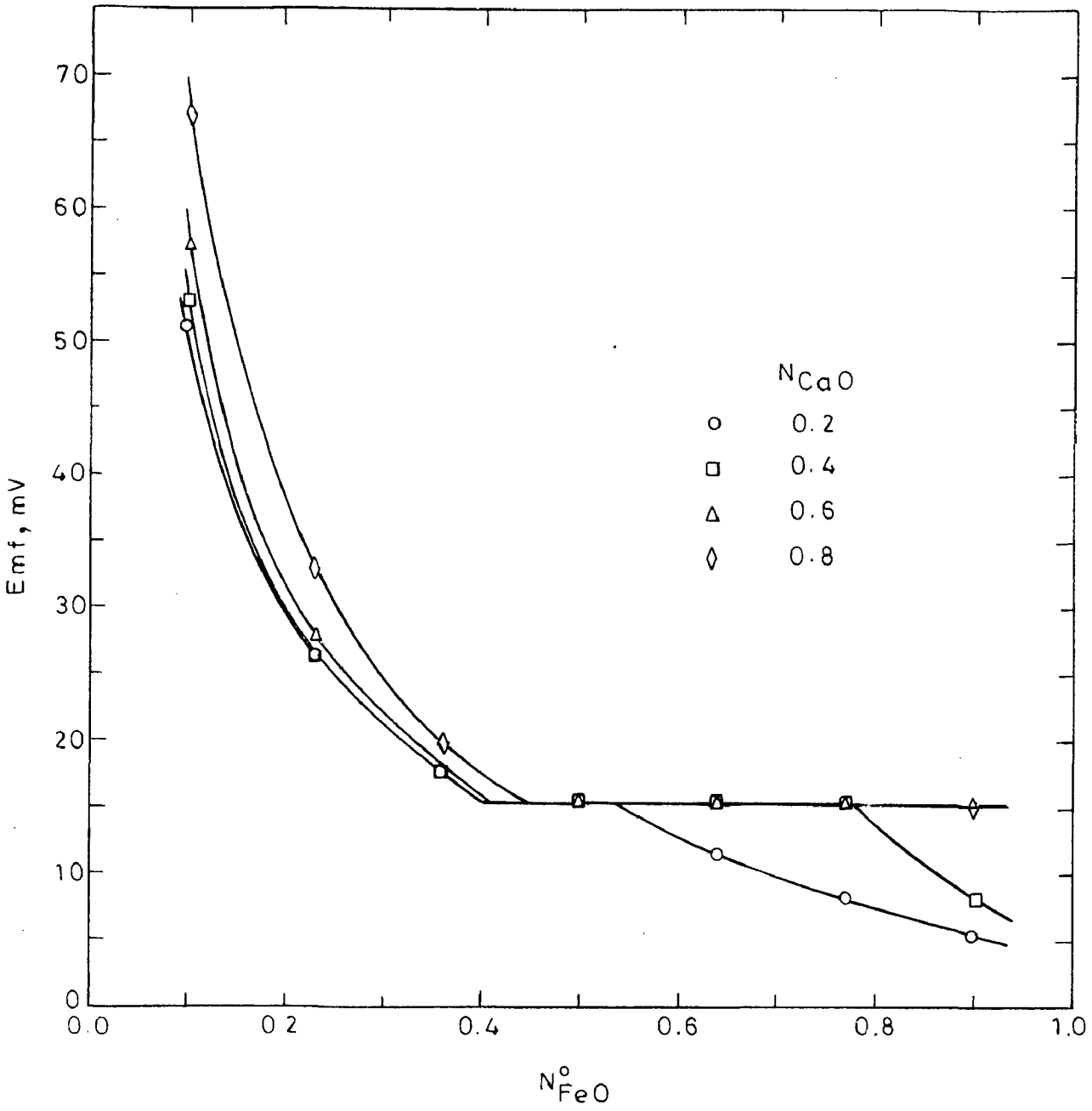

FIG.4.16. EMF Vs N°_{FeO} AT $N_{CaO} = 0.2, 0.4, 0.6$ AND 0.8 FOR THE SYSTEM MgO–FeO–CaO AT 1000 K

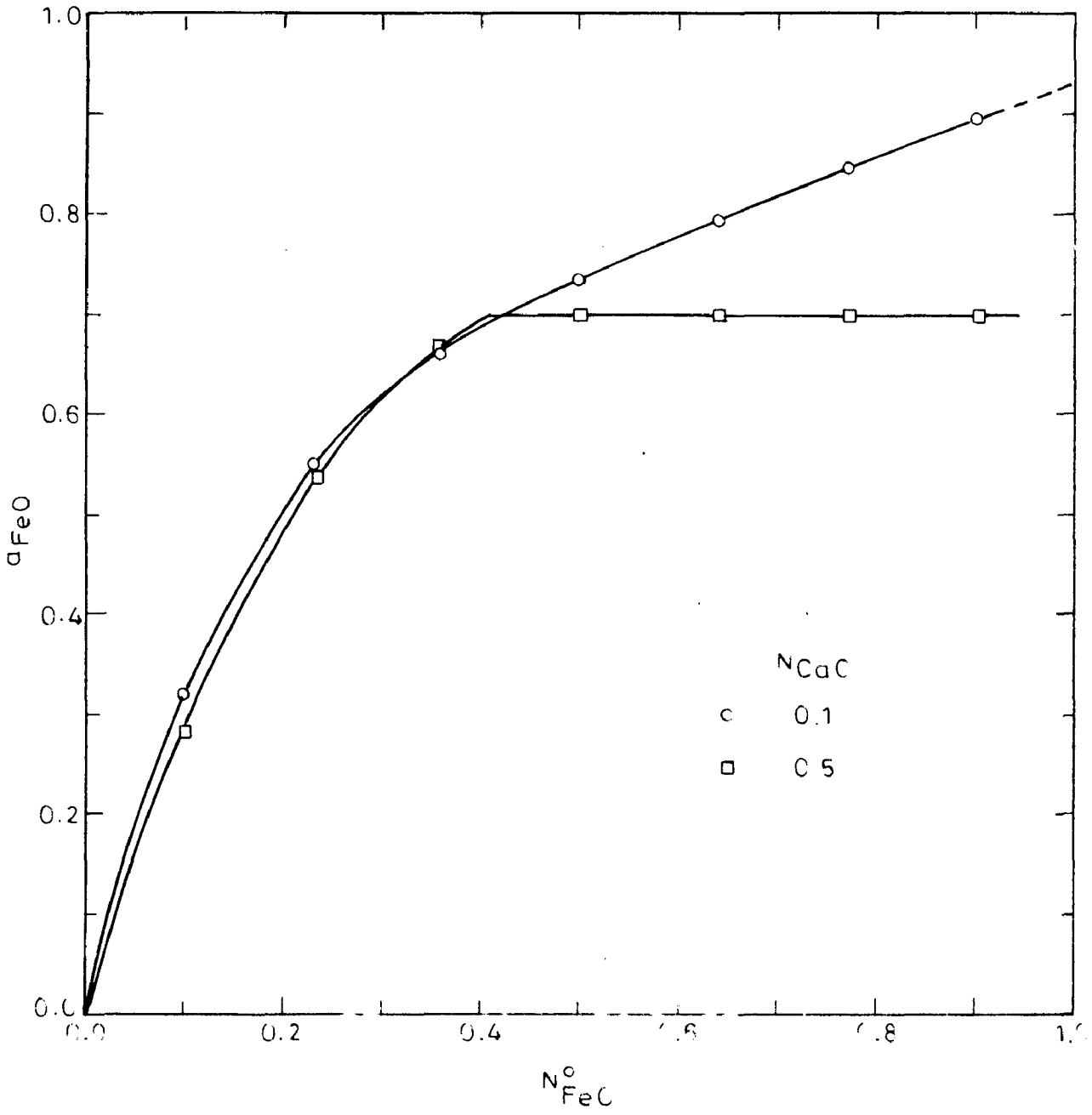

FIG.4.17. a_{FeO} Vs N°_{FeO} AT $N_{CaO} = 0.1$ AND 0.5 FOR THE SYSTEM MgO-FeO-CaO AT 1000 K

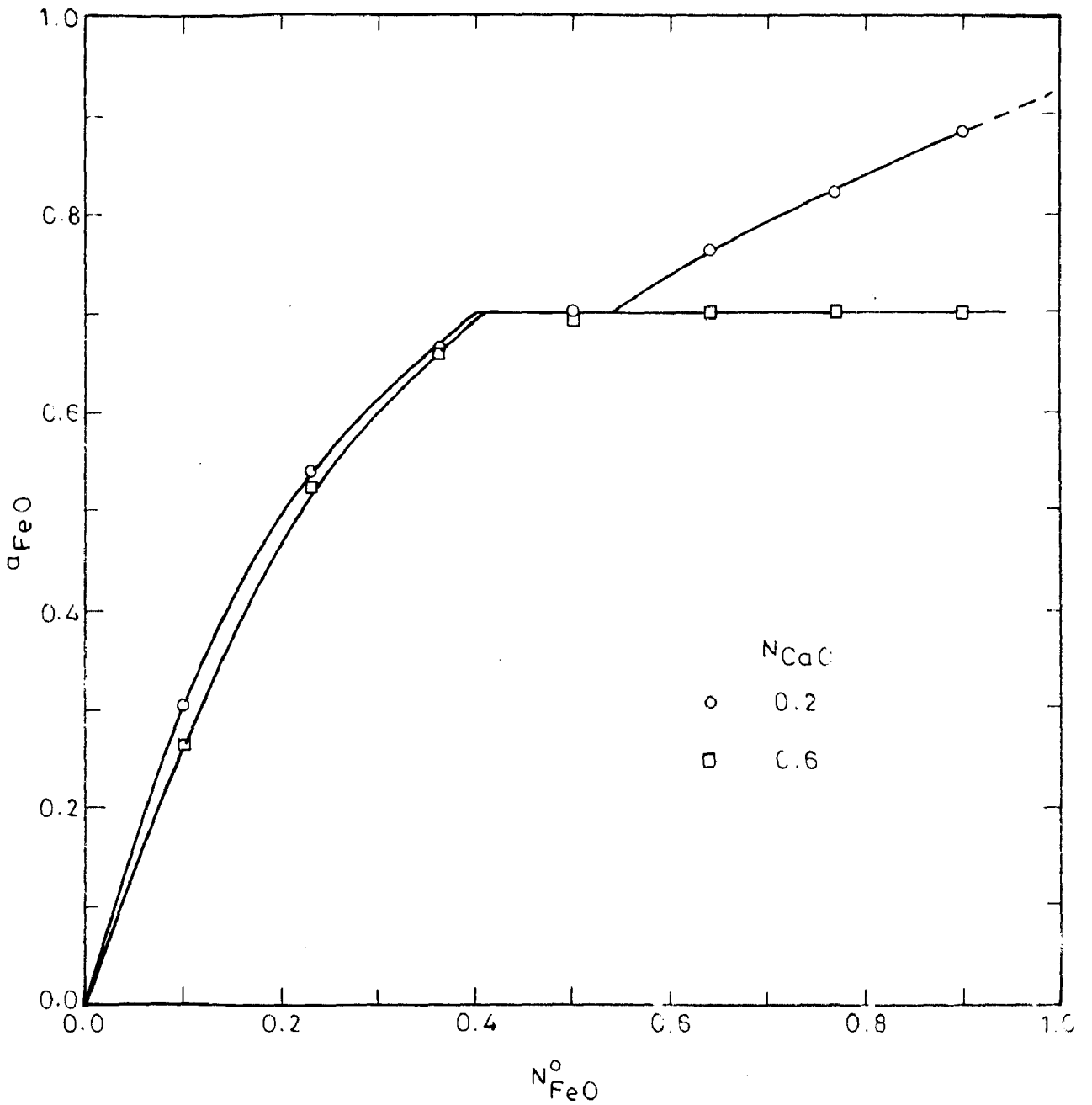

FIG.4.18. a_{FeO} Vs N^{o}_{FeO} AT $N_{CaO} = 0.2$ AND 0.6 FOR THE SYSTEM MgO - FeO - CaO AT 1000 K

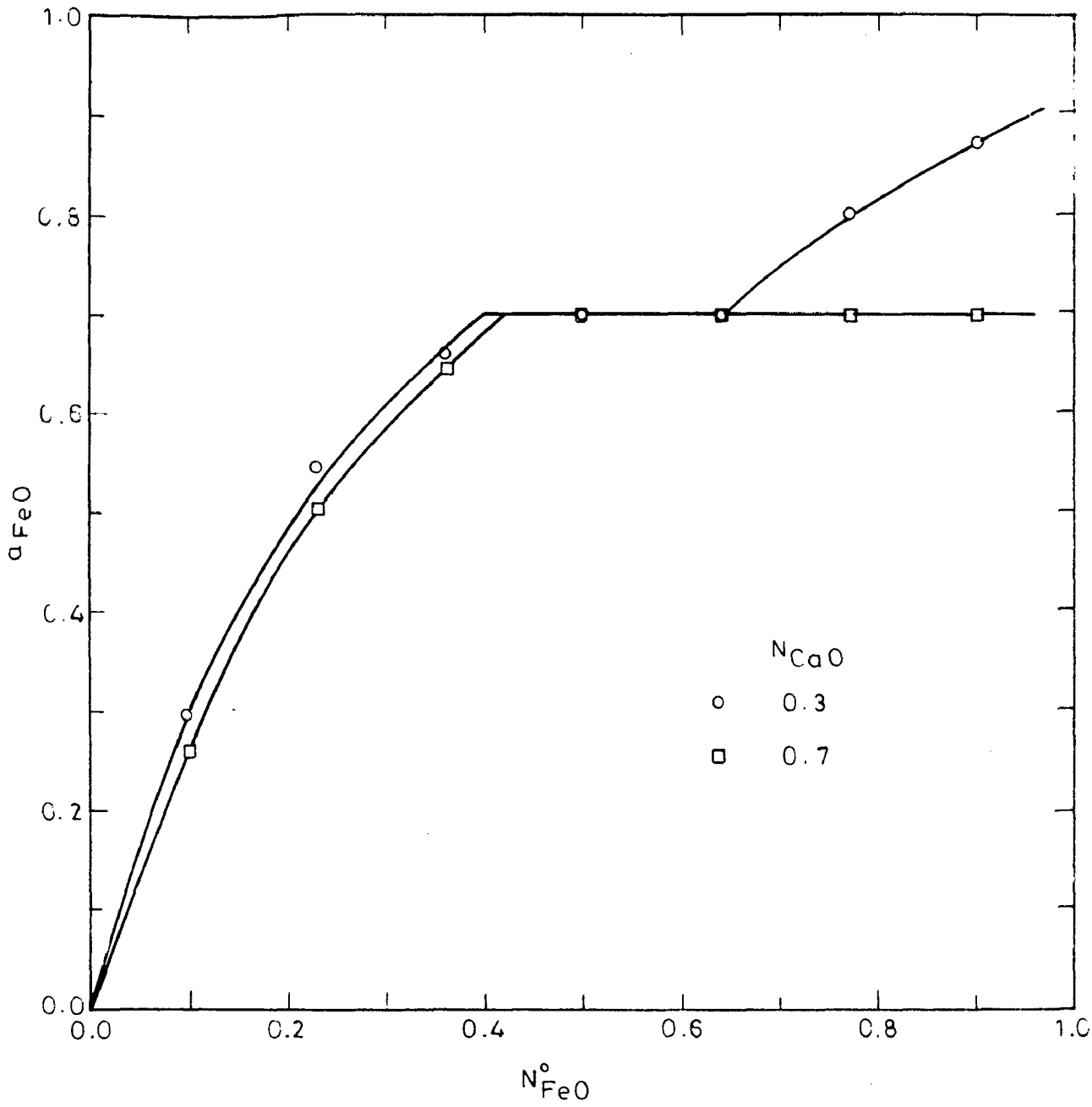

FIG.4.19. a_{FeO} Vs N°_{FeO} AT N_{CaO} = 0.3 AND 0.7 FOR THE SYSTEM MgO - FeO - CaO AT 1000 K

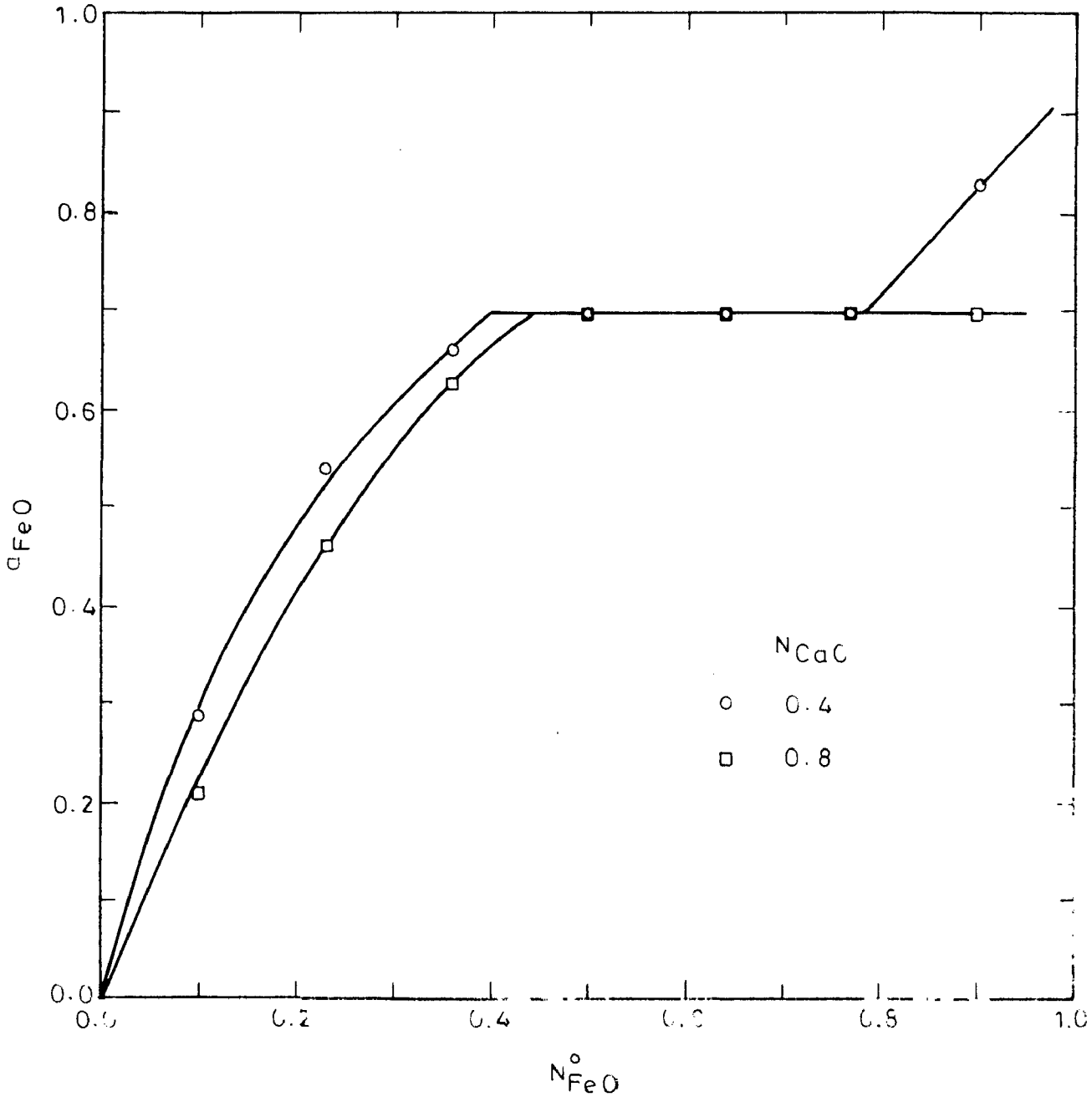

FIG.4.20. a_{FeO} Vs N°_{FeO} AT $N_{CaO} = 0.4$ AND 0.8 FOR THE SYSTEM MgO – FeO – CaO AT 1000 K.

4.2.1 FeO Activity Lines & Stability of Phases

In this section an attempt is made to understand phase stability relations for the system MgO-FeO-CaO at 1000 K by analysing experimental activity data on the basis of known thermodynamic laws relating to heterogeneous equilibria. One of the most important of the thermodynamic laws relating to phase equilibria is Gibbs' phase rule, which is concerned with the number of variables whose values are to be specified in order to define the thermodynamic state of a system uniquely. If temperature, pressure and composition are variables, which determine the state of a system, Gibbs' phase rule for n-component system is written as

$$p + f = n + 2 \qquad ..(4.32)$$

where,

p is the number of phases present in the system, n is the number of constituents, and f the number of possible independent changes of state of this system (usually, f is referred as number of degrees of freedom). If pressure and temperature are kept constant, Eq. (4.32) reduces to p+f = n. In the present case, where n is equal to 3 and pressure and temperature are maintained constant, phase rule is given by the following relationship:

$$p + f = 3 \qquad ..(4.33)$$

A close observation of Tables 4.3 and 4.4 indicates that for N_{CaO} = 0.5 to 0.8, values of activity of FeO have constant value of 0.6995 at N^{o}_{FeO} = 0.5 to 0.9. Similarly for lower

values of N_{CaO}, clearly there is a composition range where values of activity of FeO are constant. All these observations indicate that there is a composition range where activity of FeO is constant. In this region thermodynamic state of the system is fixed and cannot be changed by changing any of the variables (these variables are N^{o}_{FeO} and N_{CaO} in the present case), which amounts to saying that number of degrees of freedom, f, is zero in this region. Number of stable phases should, therefore, be equal to 3 in this region, according to Eq. (4.33). Three phases present in this region will be in thermodynamic equilibrium with each other and as the value of N^{o}_{FeO} and/or N_{CaO} is changed within this region, relative concentration of these phases will change, but their individual composition and thermodynamic properties will remain unchanged.

To locate the stability ranges of the phases, iso-activity lines for FeO were drawn for 1000 K - isothermal section through this system. Values of N^{o}_{FeO} for same activity of FeO for selected values of a_{FeO} were found from a_{FeO} vs N^{o}_{FeO} plots (Figs. 4.17-4.20) for various values of N_{CaO}. On the basis of these points iso-activity lines for FeO were drawn for a_{FeO} equal to 0.1, 0.2, 0.3, 0.4, 0.5, 0.6, 0.7, 0.75, 0.8, 0.85 and 0.9, as shown in Fig. (4.21). We know from the known phase diagrams that FeO dissolves to a maximum of 0.06 moles of CaO, and that FeO and MgO are miscible in all proportions, and MgO practically does not dissolve any CaO at 1000 K. Keeping these facts in mind,

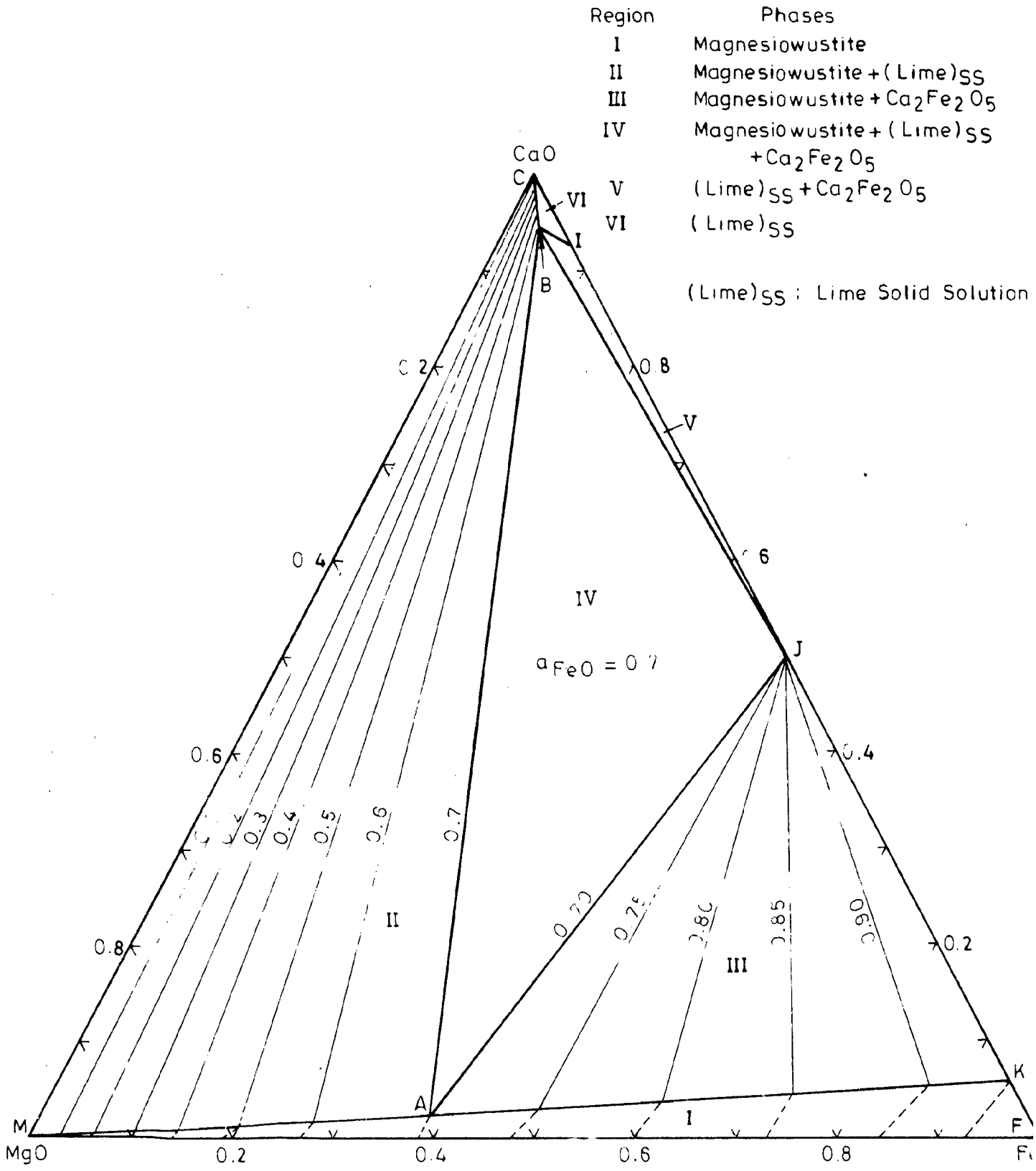

FIG.4.21. LINES OF FeO ACTIVITY AND PHASE STABILITY RELATIONS AT 1000K FOR THE SYSTEM MgO-FeO-CaO

MgO apex was joined with a point having N_{CaO} = 0·06 and lying on FeO-CaO join (line MK in Fig. 4.21). Region below this line (region MKF in Fig.4.21)designated as region I should be a single phase region consisting of magnesiowustite with some lime dissolved in it. There should be another single phase region near CaO apex as CaO dissolves upto 0.075 moles of FeO at 1000 K. On the basis of FeO-CaO and MgO-CaO phase diagrams and iso-a_{FeO} lines from 0.1 to 0.7, most probable boundaries for this region were drawn and this region is shown as region VI (region CBI) in Fig. (4.21). Obviously, the stable phase in this region is lime solid solution, which is nothing but CaO with small amounts of dissolved FeO and MgO.

Iso-activity lines for a_{FeO} equal to 0.7 - lines AB and AJ in Fig.(4.21) - give two of the phase boundaries of region IV. This region is a three-phase region (as discussed earlier in this section), where activity of FeO is equal to 0.7 and is constant throughout the region. Line BJ in Fig. (4.21), obtained by joining points B and J, separates the regions IV and V. Thus region IV is defined by the boundary lines AB, AJ and BJ. In an isothermal section of a ternary system, a three phase region meets single phase regions along its corners. In the present case, corners A,B and J of region IV meet regions of magnesiowustite , lime solid solution and compound $Ca_2Fe_2O_5$ respectively. Therefore, stable phases in region IV should be magnesiowustite of composition A, lime solid solution of composition B and compound $Ca_2Fe_2O_5$.

A three-phase region in a ternary system is always surrounded by two-phase regions along its phase boundaries and therefore, regions II, III and V, which surround region IV, should be two-phase regions. A careful observation of Fig. (4.21) indicates that equilibrium phases in region V should be lime solid solution and compound $Ca_2 Fe_2O_5$. As can be observed in Fig. (4.21) iso-a_{FeO} lines in regions II and III are practically straight lines.Iso-activity lines in a two-phase region of a three-component system are straight lines and are called tie lines. At any point on a given iso-activity line, there exists a mixture of two phases, whose compositions are given by two end points of the line and the relative proportions of the two phases may be determined from simple ratio proportion rule. Along any iso-activity line, if one of the composition variable, say N_{CaO}, is fixed, other variable, N^{o}_{FeO}, is automatically fixed and vice versa. Straight line-nature of iso-a_{FeO} lines in regions II and III confirms that these regions are two-phase regions. Regions I and VI are the single phase regions adjoining region II and therefore, stable phases in region II should be magnesio-wustite and lime solid solution. It is at once clear that magnesiowustite and compound $Ca_2Fe_2O_5$ are the phases stable in region III. In region II, composition of magnesiowustite and lime solid solution will change as the composition of the system is varied, except along an iso-activity line. Similarly composition of magnesiowustite in region III will change with a change in the composition of the system in any

direction other than that is followed by an iso-activity line.

All these possible phase regions, which are arrived at on the basis of experimentally known values of activity of FeO and known thermodynamic principles, are shown in Fig. (4.21). Also shown in this figure are iso-activity lines for selected values of a_{FeO} in regions II and III.

4.2.2 MgO Activity Lines

Iso-activity lines for magnesia in regions II and III were drawn from a knowledge of activity - composition relations in binary solid solution FeO-MgO (see section 3.1). As a first step activity of MgO corresponding to a_{FeO} equal to 0.7 was found to be 0.76 from Fig. (3.1). This is the activity of MgO in region IV. Therefore, activity of MgO in region II should vary from 1 to 0.76 whereas values of a_{MgO} in region III will be less than 0.76.

From Fig. (3.1), values of activity of FeO corresponding to activity of MgO equal to 0.95, 0.9, 0.85 and 0.8 were read to be 0.205, 0.37, 0.51 and 0.632 respectively. Next, values of N^{o}_{FeO} for these a_{FeO} values were read from a_{FeO} vs N^{o}_{FeO} plots (Figs. 4.17 - 4.20) for various values of N_{CaO}. On the basis of these points iso-activity lines for MgO were drawn for a_{MgO} equal to 0.95, 0.9, 0.85 and 0.8 in region II, as shown in Fig. (4.22). Similarly, from known properties of binary FeO-MgO solid solution and a_{FeO} vs N^{o}_{FeO} plots for the present system, iso-a_{MgO} lines

were drawn for a_{MgO} equal to 0.7, 0.65, 0.6 and 0.5 in region III. These lines are also shown in Fig. (4.22).

4.2.3 CaO Activity Lines

Lime solid solution is one of the two stable phases in region II. Iso-activity lines for a_{CaO} equal to 0.99, 0.98, 0.97, 0.96 and 0.95 as drawn in region II, are shown in Fig. (4.23). These lines were drawn following the same procedure as was used to draw iso-a_{MgO} lines in this region (see section 4.2.2).

Activity of lime in region IV was calculated from equilibrium constant of reaction (3.7).

$$3FeO + 2CaO = Ca_2Fe_2O_5 + Fe \qquad ..(3.7)$$

As iron and $Ca_2\ Fe_2\ O_5$ are pure, equilibrium constant, $K_{(3.7)}$, for the above reaction is given by

$$K_{(3.7)} = \frac{1}{(a_{FeO})^3\ (a_{CaO})^2} \qquad ..(3.8)$$

Equilibrium constant, $K_{(3.7)}$, for the reaction (3.7), as determined in section 3.2, is equal to 3.49 and activity of FeO in region IV is 0.7. Activity of lime in region IV, calculated from Eq. (3.8) was found to be equal to 0.915.

Values of activity of CaO in region III were determined from the known values of activity of FeO in this region and the known value of the equilibrium constant, $K_{(3.7)}$, for the

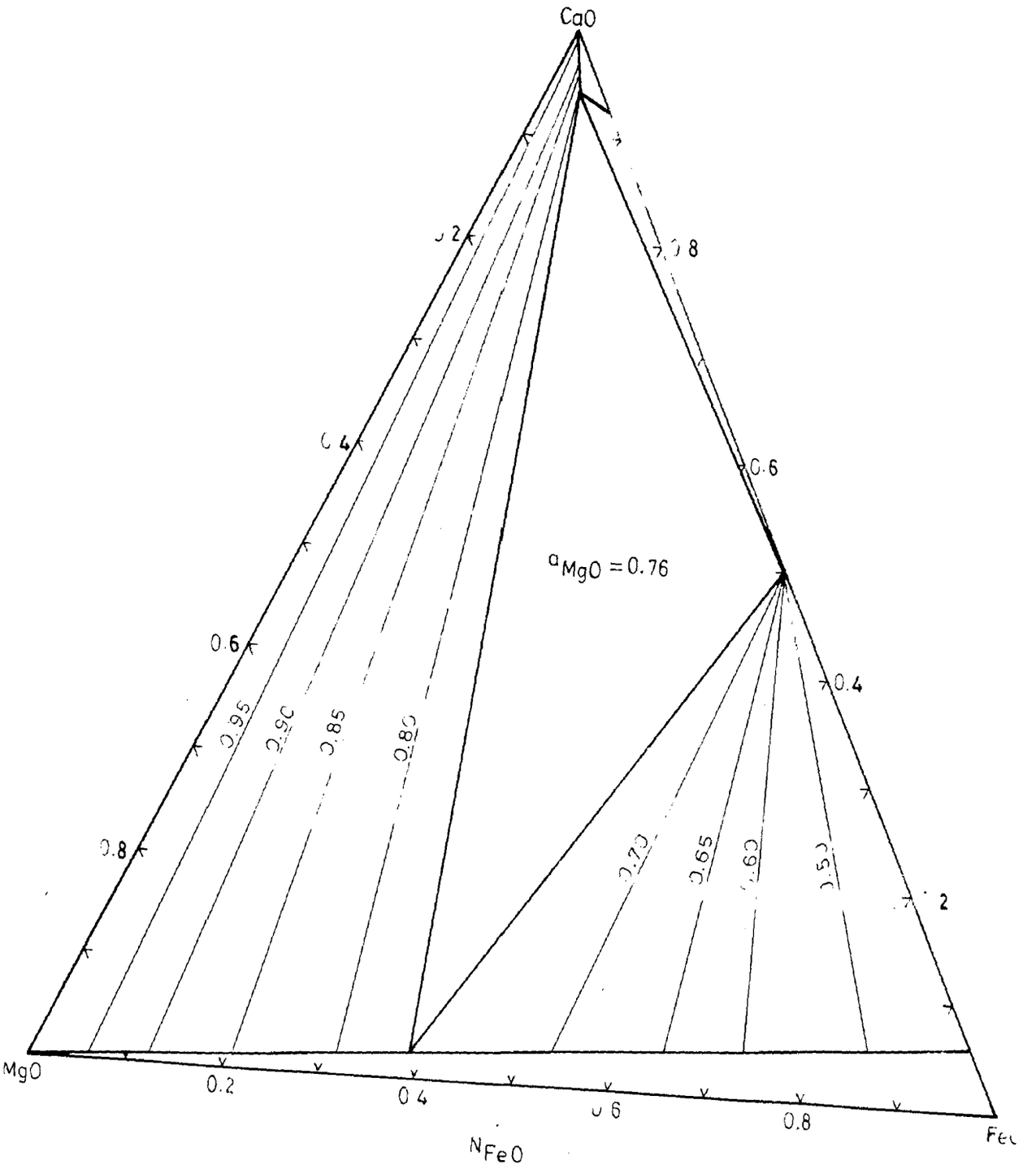

FIG.4.22. LINES OF MgO ACTIVITY AT 1000K IN THE SYSTEM MgO - FeO - CaO

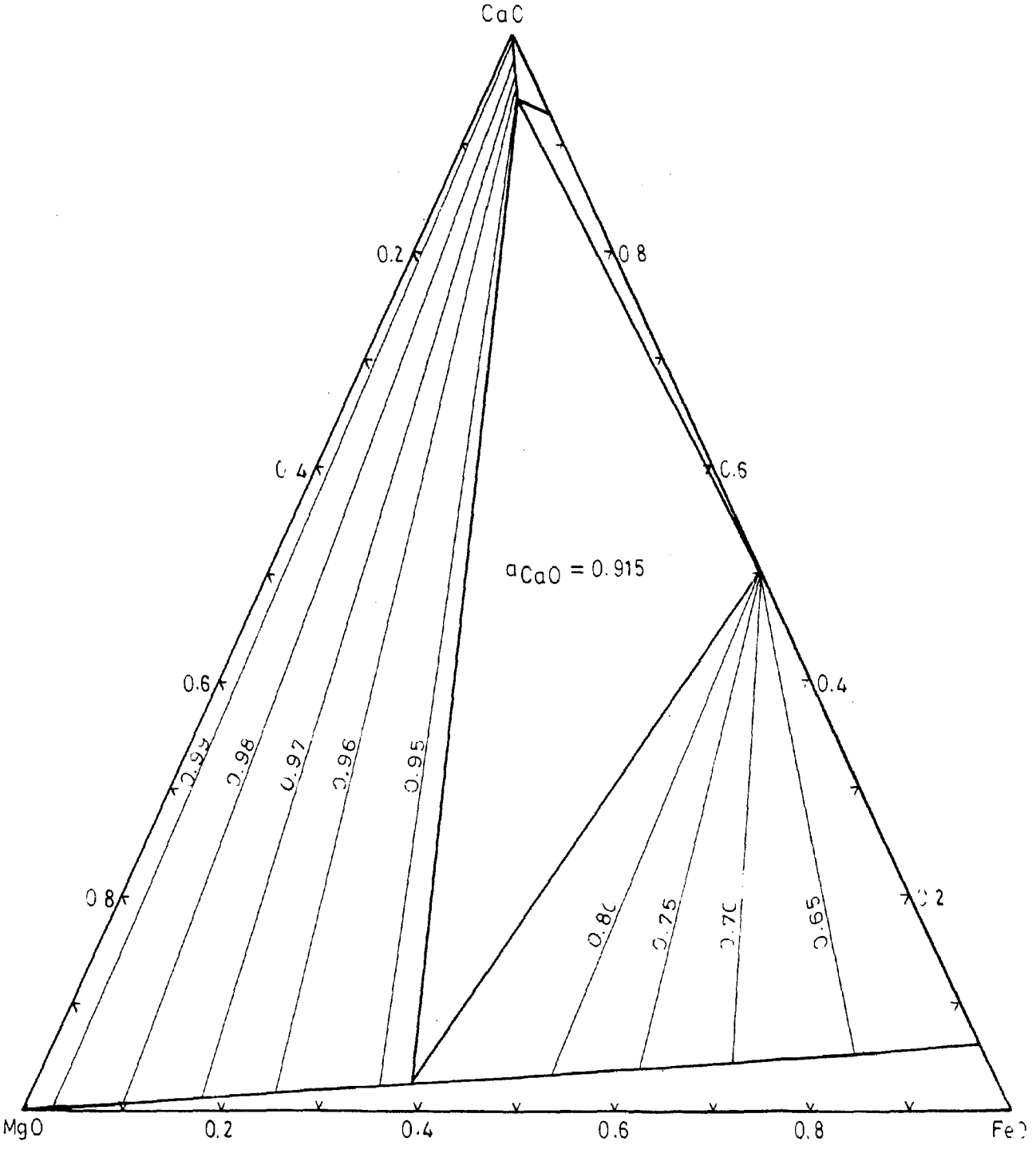

FIG.4.23.LINES OF CaO-ACTIVITY AT 1000K IN THE SYSTEM MgO - FeO - CaO

reaction (3.7). Values of activity of lime along N_{CaO} equal to 0.1, 0.2, 0.3, and 0.4 were, thus, calculated for different values of N^{o}_{FeO} . From these values variation of a_{CaO} with N^{o}_{FeO} was plotted for different values of N_{CaO}. On the basis of these plots, iso-activity lines for lime for a_{CaO} equal to 0.8, 0.75, 0.7, and 0.65 were drawn in region III, as shown in Fig. (4.23).

CHAPTER-5

DISCUSSION

5.1 SOLUTIONS OF OXIDES OF THE A_IO-$A_{II}O$ TYPE

An extensive literature is available to date on the thermodynamic properties of a large number of binary metal oxide systems which are of particular interest to chemical and process metallurgists. As a result, salient features of thermodynamic properties of important oxide solid solutions can be described fairly completely. However, there exists a serious gap regarding mathematical modelling of the thermodynamic properties in binary metal oxide systems. This is due primarily to several complications associated with the metal oxides, of which the most important ones are mentioned here. Formation of oxide solid solutions involving cations of different valencies is associated with the creation of extrinsic defects such as lattice vacancies, interstitials and electrons and holes in accordance with Hauffe-Wagner rules. More often than not, the disparity in the valency of cations is accompanied by a change in the crystal structure and cationic radii. As a consequence, the individual effects of these parameters on the thermodynamic properties cannot easily be resolved. Non-stoichiometric behaviour of the oxides further complicates

the analysis. In view of these considerations, Hume-Rothery's approach to metallic systems cannot be extended to oxide systems, in general. However, the analysis can be simplified to a greater extent by confining ourselves to the homovalent oxide systems of the $A_IO - A_{II}O$ type, where the valency effects are absent and therefore the solution behaviour of such systems can be rationalized in terms of size factor effect, difference in electronegativity, crystal structure and ionic field strength. Non-stoichimetry and crystal field effects are included wherever applicable.

The following points need to be mentioned: (i) the size factor of a solute oxide is defined as the difference between the cationic radii of solvent and solute oxides, (ii) the ionic field strength is expressed as the ratio of ionic charge to square of the ionic radius, (σ/r^2), (iii) the degree of non-stoichiometry of a given oxide is referred to its value in equilibrium with the respective metal. The effects of these factors on the thermodynamic properties have been analysed by many authors. For instance, disparity in size factor and difference in crystal structure give rise to positive deviation from Raoult's law, whereas a difference in electronegativity and ionic field strength lead to negative deviation from Raoult's law. Like in metallic systems, the parameters mentioned above are interelated in oxide systems also and the models developed to analyse their individual effects can at best be considered

as crude approximations. Nevertheless, it is possible to highlight their effects at least qualitatively.

It will be appropriate to consider here some of the theoretical models which are available for predicting the thermodynamic behaviour of the oxide solid solutions and to discuss the measured data on these oxide solid solutions in the light of these models.

Herasymenko [227] introduced the concept of mixing of ions. His model implicitly assumes random mixing between cations and anions. To obtain this, the thermal energy must be so high as to overcome the electrostatic bond between oppositely charged particles. The thermal energy requirement can be satisfied only at temperatures of the order of 100,000°C in case of sodium chloride as pointed out by Flood, Forland and Grjotheim [228]. Thus, Herasymenko's model is not considered to be reasonable. According to Temkin's model [229] the entropy in ionic melts is due to the random mixing of cations on the one hand and anions on the other. Thus a mixture of ionic compounds such as oxides or sulphides behave, according to Temkin, as a system with two "independent although inseparable solutions." In the binary solid solutions of oxides of the type A_IO and $A_{II}O$ used in the present work, the ideal activity of the component A_IO, according to this model is given by $a_{A_IO} = N_{A_IO}$, where N_{A_IO} is the mole fraction of

$A_I O$. Thus, this model is also applicable for explaining the behaviour of ideal solutions and is not applicable to the systems of the present work. Flood, Forland and Grjotheim [230] improved the Temkin model by introducing equivalent ionic fractions to deal with solutions with ions of different valencies. In the Regular Solution model developed by Hildebrandt and Scott [231], on the other hand, interactions between components are restricted to those between neighbouring atoms. In the development of this model it is assumed that molecules of the different species constituting the solution are of the same size, which is not true in most of the practical cases. Therefore, the thermodynamic behaviour of solutions predicted on the basis of this model deviates, in practice, from the real behaviour of such solutions. Also, according to this theory a plot of α- function against composition should be a horizontal line, independent of composition. The effect of preferential distribution of molecules of the different species constituting the solution has been taken into account in the Quasi-Chemical model developed by Guggenheim [232,233], but this theory treats only the chemical contribution to the energetics and ignores the contributions due to other effects. The changes in the interatomic distances due to changes in composition, are not considered. The bond energies between the like pairs in the solution are assumed to be the same as those existing in pure components. In the application

of this theory to oxide solid solutions with a common anion, as used in the present work, the next-nearest neighbour interactions are important since the nearest neighbour interactions cancel out. Also a plot of α-function against composition is expected to be a symmetrical one according to this model. Figs.[5.1] and [5.2] show that the results of the present investigation do not follow this relation and therefore this model does not hold good for the discussion of the results of the present work. Also, in solid solutions of oxides with appreciable differences in cationic radii, such as CaO- FeO solid solution of the present work, contributions to enthalpy of mixing due to local strain and changes in Born repulsive energy assume importance and therefore this model is not fully applicable to such solid solution.

The coulomb attractive and Born repulsive energies contributions to the enthalpy of mixing and the effects of the geometric mean displacement of ions caused by the differences in the ionic radii are taken into consideration in Wasatjerna's electrostatic theory [234] . This theory modified by Hovi [235] has successfully accounted for the observed enthalpies of mixing in various binary alkali halide systems having a common anion. In the binary metal oxide solid solutions of interest in the present investigation, the situation is quite analogous, as these oxides are essentially ionic in character. Friedel's elastic model [236]

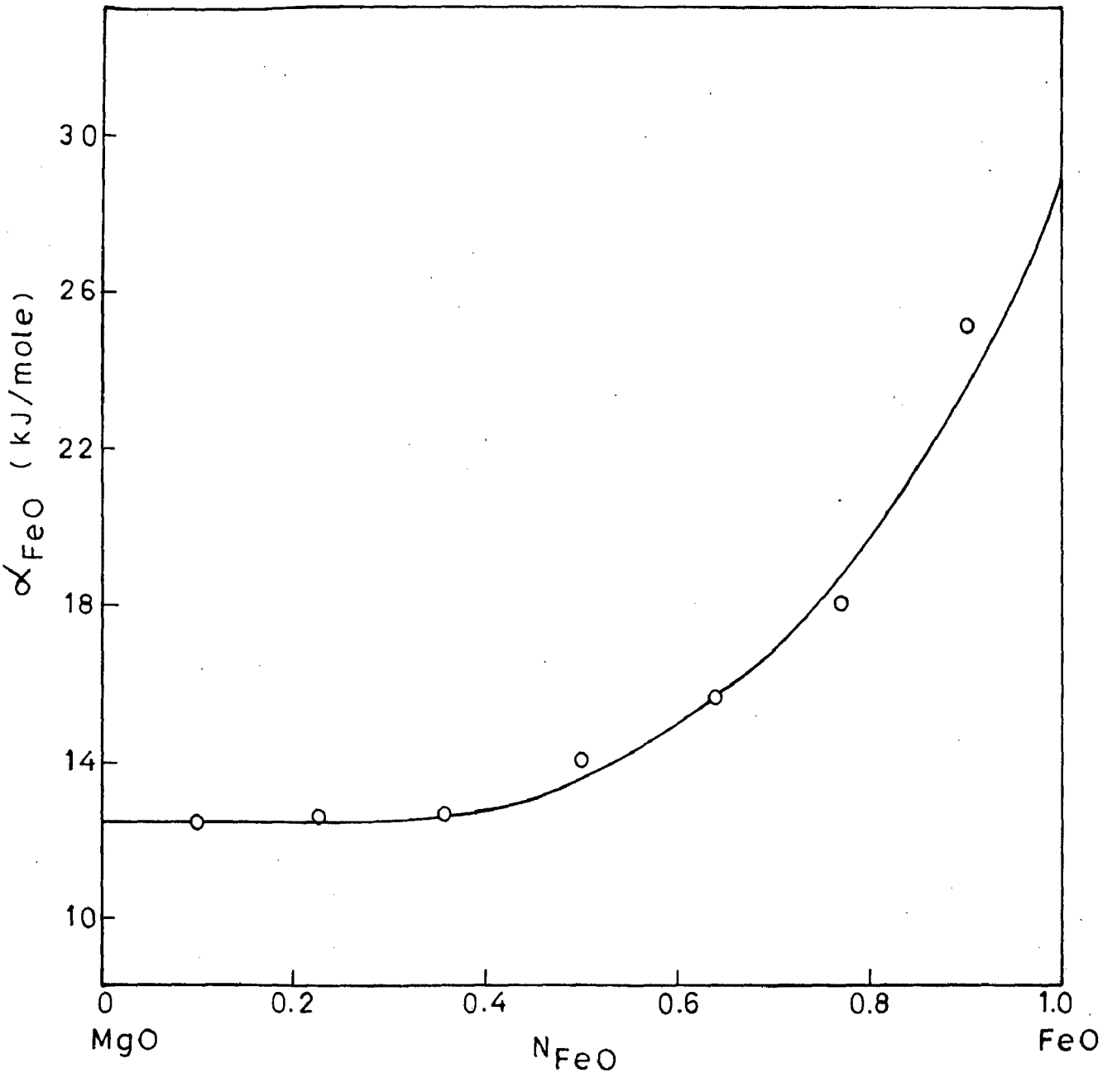

FIG. 5.1. α_{FeO} Vs. N_{FeO} FOR THE SYSTEM FeO-MgO AT 1000 K.

$$\alpha_{FeO} = \frac{RT \ln \gamma_{FeO}}{(1 - N_{FeO})^2}$$

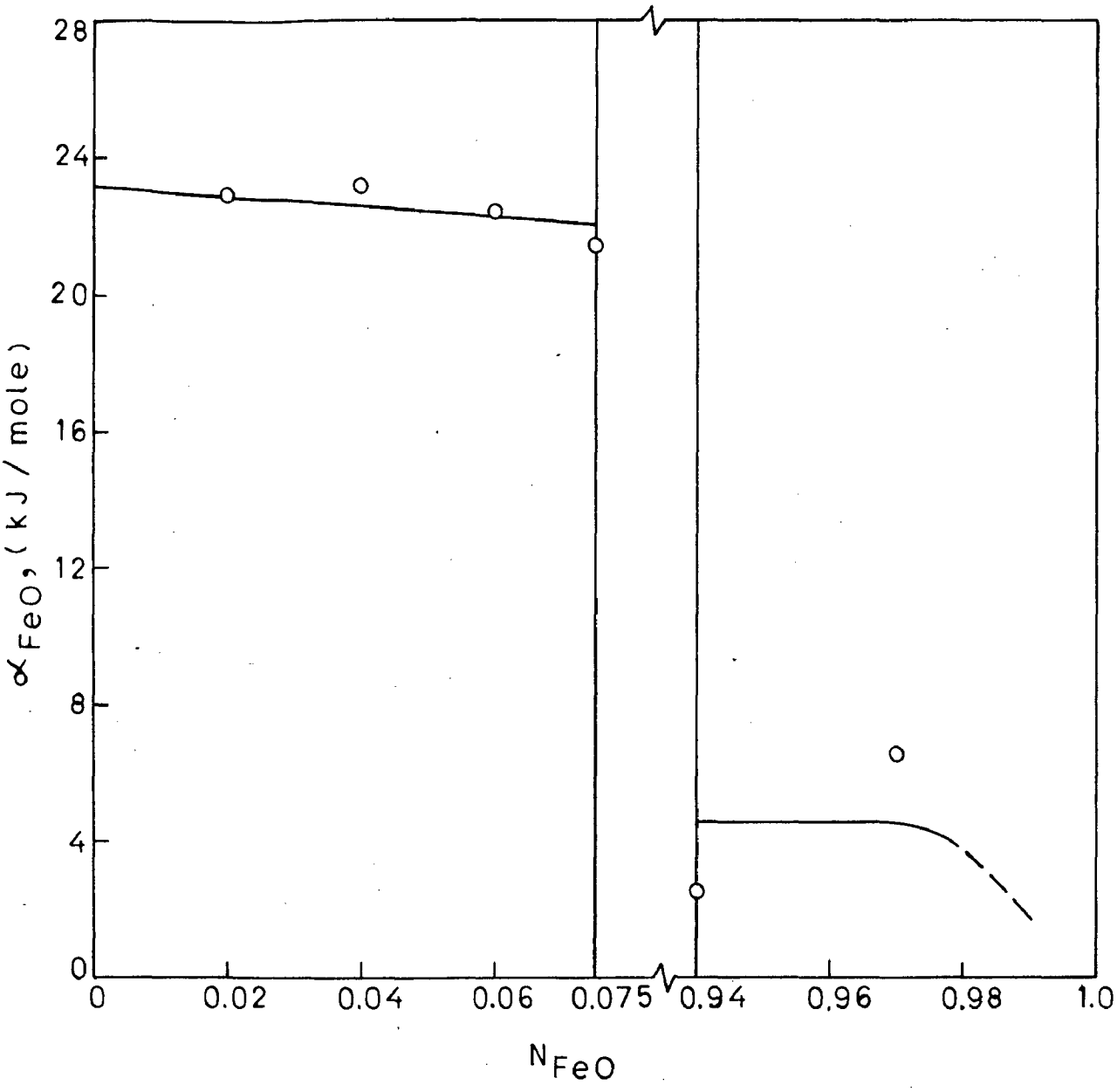

FIG. 5.2 α_{FeO} Vs. N_{FeO} FOR THE SYSTEM FeO-CaO AT 1000 K.

$$\alpha_{FeO} = \frac{RT \ln \gamma_{FeO}}{(1 - N_{FeO})^2}$$

on the other hand, highlights the influence of ionic size differences on the energetics of solution. He proposed a model to calculate the excess free energies of formation of substitutional solid solutions assuming that the introduction of an atom of different size introduces strain in the solvent matrix. This model can be applied to oxide systems if exact compressibility values are known. When oxides of transition metals are involved in the mixing process, there could be a definite contribution to the heat of mixing due to changes in the crystal field stabilization energies. The crystal field stabilization energies for various transition metal cations in octahedral and tetrahedral fields have been listed by Dunitz and Orgel [237]. From these data, Driessens [238] has calculated the contribution of this factor to the interaction parameter. Its contribution is added to the enthalpies calculated from the models proposed by Wasastjerna and Friedel to get the true enthalpies. However, the treatments of these models are not very rigorous for the quantitative explanations of the results of the binary oxide systems.

Therefore, it can be concluded that the results of the present investigation can be discussed only qualitatively on the basis of the factors affecting the properties of the solution of A_IO-$A_{II}O$ type. Cations Fe^{2+}, Mg^{2+} and Ca^{2+} have ionic radii equal to 0.76, 0.65 and 0.99 A^o respectively. A relatively small difference in the cationic sizes of Mg and Fe permits complete solid solubility in the

FeO-MgO system. There is no solid solution formation in the system CaO-MgO at lower temperatures. A relatively large cationic size difference between Ca and Fe permits compound formation in the CaO-FeO system. The high positive deviation from ideality in CaO-FeO and MgO-FeO systems appear to be reasonable due mainly to the ionic polarisation of oxygen and lattice distortion in view of the cationic size difference. A positive contribution to the energetics of mixing due to crystal-field stabilization (38 cals/mole) has been reported in the system MgO-FeO [175] which leads to a high positive deviation from ideality. In view of the cationic size differences, these systems are not expected to be ideal. Results of investigations by Shashkina and Gerasimov [152], Schmahl et al. [153], Hahn and Muan [154] using chemical equilibria technique and that of Gordeev et al. [157] and Engell [158] using emf technique support this view on MgO-FeO system and the results of investigations by Johnson and Muan [160] and Hahn [161] using chemical equilibria technique support this view for CaO-FeO system.

In view of the non-stoichiometry of FeO, the thermodynamics in these systems is likely to be influenced on that account in addition to the crystal-field stabilization effect. The effect of non-stoichiometry of component oxides on the thermodynamic properties of oxide solid solutions have been analysed by Seetharaman et al [239] and Muan and coworkers[240]. Seetharaman et al. [239] have shown that in binary metal oxide systems

involving FeO as one component marked positive deviation from ideality is exhibited by the component oxide activities and the measured enthalpies of mixing are abnormal, deviating considerably from the theoretical values calculated on the basis of size disparity of cations and changes in crystal field stabilization energies. It has been advanced that incorporation of MgO or CaO into the wustite lattice not only dilutes the cationic sublattice but also involves the removal of excess oxygen from the lattice during the solid solution formation. The enthalpy change associated with the removal of extra oxygen from the lattice for equimolar composition has been reported to be 1390 cals. for FeO-MgO system [239]. Another factor which can influence the thermodynamic properties of the system CaO-FeO can be inferred from the Fajan's rule according to which in the system CaO-FeO addition of CaO (which has lower field strength than FeO) to FeO increases field strength of FeO by pushing it to higher valency state as is imperative from the formation of the compound $2CaO.Fe_2O_3$ in equilibrium with Fe. This factor is not effective in the system MgO-FeO because there is little difference between the field strengths of FeO and MgO as is clear from the fact that there is no compound formation in this system.

A list of binary iso-structural oxide systems investigated is given in Table-5.1.

TABLE 5.1 BINARY ISOSTRUCTURAL METAL OXIDE SYSTEMS OF THE $A_I O - A_{II} O$ TYPE INVESTIGATED

No.	System	Ionic radius, A^o A_I	Ionic radius, A^o A_{II}	Investigator	Thermodynamic behaviour
1	FeO-MgO	0.76	0.65	(a) Shashkina and Gerasimov [152]	Positive deviation
				(b) Schmahl et al. [153]	-do-
				(c) Hahn and Muan [154]	-do-
				(d) Korneev et al. [155]	-do-
				(e) Gordeev et al. [157]	-do-
				(f) Engell [158]	-do-
				(g) Sakawa et al, [159]	-do-
				(h) Present work	-do-
2	FeO-CaO	0.76	0.99	(a) Hahn [161]	-do-
				(b) Johnson and Muan [160]	-do-
				(c) Lykasov et al. [115]	determined the solubility of CaO in wustite
				(d) Tare and Deo [114]	-do-
				(e) Shiro Ban-ya et al. [162]	
				(f) Present work	Positive deviation

Table-5.1 Contd.

No.	System	Ionic radius, A^{o} A_I	A_{II}	Investigator	Thermodynamic behaviour
3	FeO-MnO	0.76	0.80	(a) Foster and Welch [166]	Ideal
				(b) Schenck et al. [167]	Positive deviation
				(c) Schwerdtfeger and Muan [168]	-do-
				(d) Engell [158]	-do-
				(e) Takenov et al. [169]	-do-
				(f) Seetharaman [171]	-do-
4	FeO-CaO	0.76	0.74	(a) Aukrust and Muan [172]	-do-
				(b) Seetharaman and Abraham [173]	-do-
5	CaO-CdO	0.99	0.97	(a) Prasad [156]	Ideal
				(b) Raghavan [175]	-do-
6	NiO-MgO	0.72	0.65	(a) Hahn and Muan [178]	-do-
				(b) Seetharaman and Abraham [179]	Positive deviation
				(c) Petot et al. [150]	Ideal
				(d) Raghavan [175]	Positive deviation
7	MgO-MnO	0.65	0.80	(a) Woermann and Muan [180]	-do-
				(b) Hahn and Muan [181]	-do-
				(c) Raghavan [175]	-do-

Table-5.1 Contd.

No	System	Ionic radius, A^{O} A_I	A_{II}	Investigator	Thermodynamic behaviour
8	CaO-MnO	0.99	0.80	(a) Tiberg and Muan [183]	Positive deviation
				(b) Raghavan [175]	-do-
9	CoO-MgO	0.74	0.65	(a) Aukrust and Muan [172]	Ideal
				(b) Seetharaman and Abraham [184]	Positive deviation
				(c) Prasad [156]	
				(d) Rigand et al. [111]	-do-
10	CoO-MnO	0.74	0.80	(a) Aukrust and Muan [172]	Ideal
				(b) Seetharaman and Abraham [185]	Positive deviation
11	NiO-MnO	0.72	0.80	(a) Cameron and Unger [112]	-do-
				(b) Hahn and Muan [178]	-do-
				(c) Seetharaman and Abraham [186]	-do-
12	CaO-CoO	0.99	0.74	(a) Raghavan [175]	-do-

5.2 SOLUTIONS OF OXIDES OF THE TYPE A_IO-$A_{II}O$ -$A_{III}O$

A ternary oxide system is more complicated than a binary oxide system. However, ionic radii, crystal structures and ionic field strengths of component oxides affect the thermodynamic behaviour of a ternary oxide system. A knowledge of the phase stability relations and thermodynamic behaviour of the relevant binary systems can be a useful guide in qualitative and partial understanding of a ternary system. In the present case MgO does not dissolve CaO and FeO can dissolve upto 0.06 moles of CaO at 1000K. Therefore, it is reasonable to expect that an increase of FeO in magnesiowustite solid solution will increase the solubility of CaO in magnesiowustite. This fact is confirmed by the studies of Brisi and Burdese [216] who found that as the FeO content of magnesiowustite increases, it can dissolve more CaO at 1273 K. Present work indicates that addition of small amounts of CaO in magnesiowustite solid solution of a given composition tends to decrease the activity of FeO (Fig.4.21), which is probably due to the dilution effect of CaO.

As not much work is done on the study of the thermodynamic properties of ternary iso-structural oxide systems, comparison of present results with literature is not possible.

As the various models developed can not explain the results of binary oxide systems quantitatively to a good degree of approximation, they cannot be extended to explain the results of the ternary oxide systems. Therefore, the results of the studies on ternary oxide systems can be explained qualitatively.

5.3 PYROXENES

Pyroxenes are the crystalline solutions of two or more components of composition $RSiO_3$, where R may be magnesium, iron, manganese, cobalt, calcium etc. The basic structure of pyroxene group is silica tetrahedra that share two of their corners with neighbouring tetrahedra so as to produce infinite chains with the composition $(SiO_3)_n^{2-}$. These parallel chains have two nonequivalent structural sites with the cations distributed between these two sites. Depending upon the sizes of cations and their distribution between the two structural sites, pyroxenes may have either orthorhombic symmetry or monoclinic symmetry, giving rise to orthopyroxenes and clinopyroxenes respectively. Pyroxenes belonging to both the groups have been studied experimentally by various workers. Activity-composition relations as determined in the present study at 1000K along with the results of other workers at various temperatures are presented in Fig. 5.3. Curves 1 to 5 show the activity-composition relation for Fe-Mg

pyroxenes. Except for curve 2 all other curves show positive deviation from ideality. Positive deviation exhibited by Fe-Mg pyroxene solid solutions is attributed to the volume effect which is caused by the distortion when smaller Mg ions are replaced by larger Fe ions. This effect increases with a decrease in temperature and thus explains the higher positive deviation at lower temperatures. This effect is insignificant at higher temperatures leading to ideal or near-ideal behaviour as reported by Nafziger and Muan [194] at 1523 K (curve 2 in Fig. 5.3). Results on other pyroxenes incorporating the cations Fe and Mn, Mn and Co, Fe and Ca at 1423, 1573 and 1353 K are shown by curves 6,7 and 8 respectively in Fig. [5.3]. These curves show that these pyroxenes mix ideally at the indicated temperatures, because of good structural compatibility.

5.4 OLIVINES

Olivines are crystalline solutions of two or more components of composition R_2SiO_4 where R may be magnesium, iron, manganese, calcium etc. In olivines, the separate SiO_4 tetrahedra are stacked together only through the medium of other cations which lie between them and the structure has orthorhombic symmetry. The olivine structure may be visualised as based on HCP of O^{2-} ions, where R^{2+} ions occupy octahedral voids and the Si^{4+} ions occupy tetrahedral voids.

Olivines of different compositions have been studied by various workers. Fig.[5.4] shows the activity-composition relationship for Fe-Mg olivines solid solution at 1000K based on the present study along with the results of other workers as reported in literature for olivines of different compositions. In olivines also, thermodynamic behaviour depends upon distortion caused in the lattice due to the mixing of cations of different sizes. As an example Mg ions occupy octahedral voids in the SiO_4-tetrahedra network in the structure of Mg_2SiO_4. When Fe_2SiO_4 is mixed with Mg_2SiO_4, both the cations mix among octahedral voids. The higher the distortion caused by the mixing of cations, the more the system will deviate from ideality. Most of the curves in Fig.[5.4] show slight to moderate deviation from ideality In the system $(Fe,Mg)_2SiO_4$, small difference in the ionic radii of Fe and Mg ions does not cause much distortion in the lattice and therefore leads to only slight positive deviation from ideal behaviour. Positive deviation exhibited by the Fe-Mg olivines in the present study is in good agreement with the results of Nafziger and Muan [194] and Kitayama and Katsura [192].

1 & 1A	$FeSiO_3$-$MgSiO_3$	AT 1000 K, PRESENT WORK
2 & 2A	"	" AT 1523 K, NAFZIGER & MUAN [194]
3	"	" AT 1477 K, KITAYAMA & KATSURA [192]
4	"	" AT 873 K, SAXENA [226]
5	"	" AT 1073 K, SAXENA [226]
6 & 6A	$FeSiO_3$-$MnSiO_3$	AT 1423 K, SCHWERDTFEGER & MUAN [208]
7	$CoSiO_3$-$MnSiO_3$	AT 1473 & 1523 K, BIGGER & MUAN [224]
8 & 8A	$FeSiO_3$-$CaSiO_3$	AT 1353 K, JOHNSON & MUAN [160]

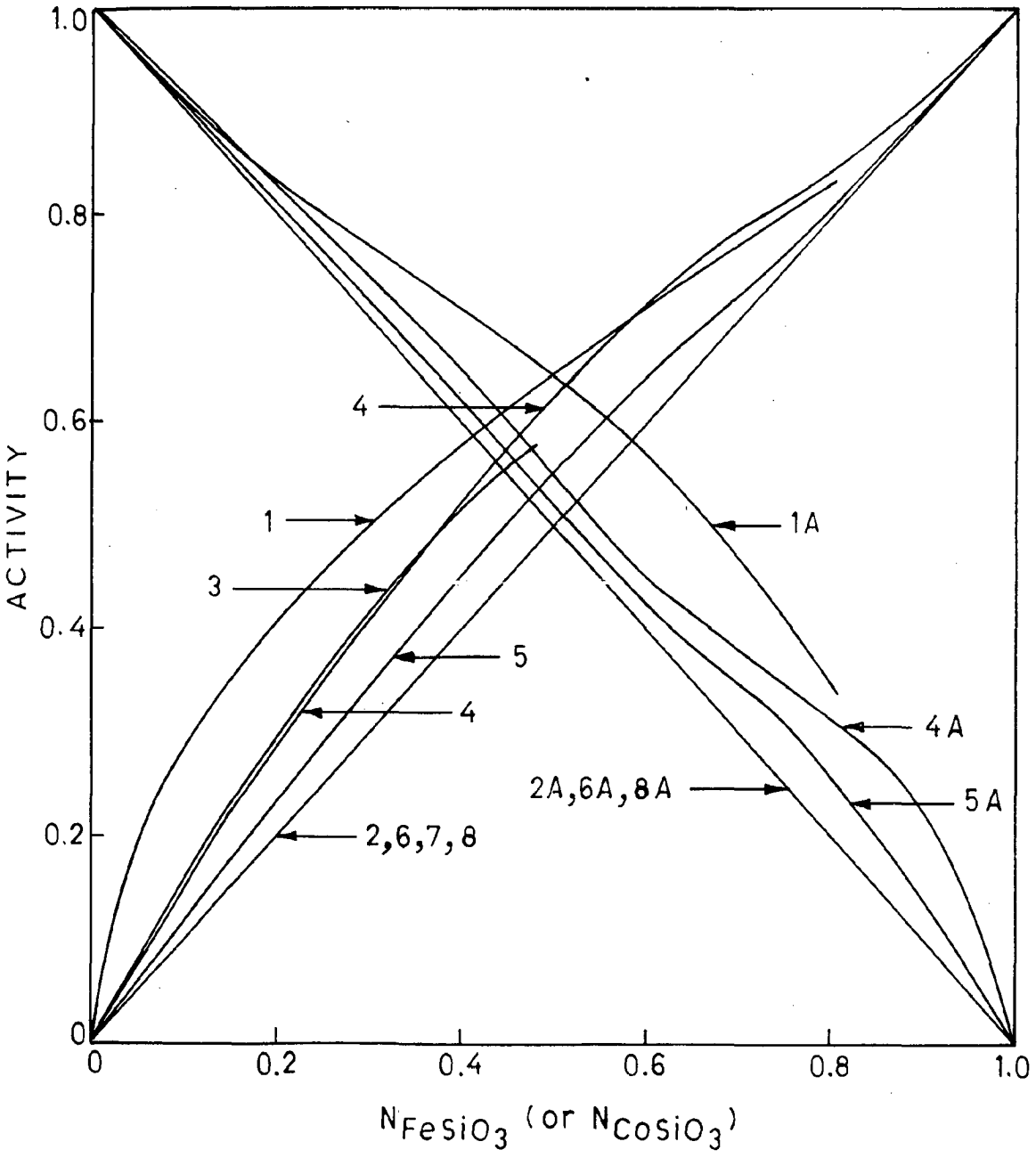

FIG. 5.3 ACTIVITY-COMPOSITION RELATIONS IN PYROXENE SOLID SOLUTIONS.

1 & 1A	$Fe_2SiO_4 - Mg_2SiO_4$	AT 1000 K, PRESENT WORK
2 & 2A	,, ,,	AT 1523 K, NAFZIGER & MUAN [194]
3	,, ,,	AT 1477 K, KITAYAMA & KATSURA [192]
6 & 6A	$Fe_2SiO_4 - Mn_2SiO_4$	AT 1423 K, SCHWERDTFEGER & MUAN [208]
7	$Co_2SiO_4 - Mn_2SiO_4$	AT 1523 K, BIGGERS & MUAN [224]
8 & 8A	$Fe_2SiO_4 - Ca_2SiO_4$	AT 1353 K, JOHNSON & MUAN [160]
9	$Co_2SiO_4 - Fe_2SiO_4$	AT 1453 K, MASSE, ROSEN & MUAN [225]

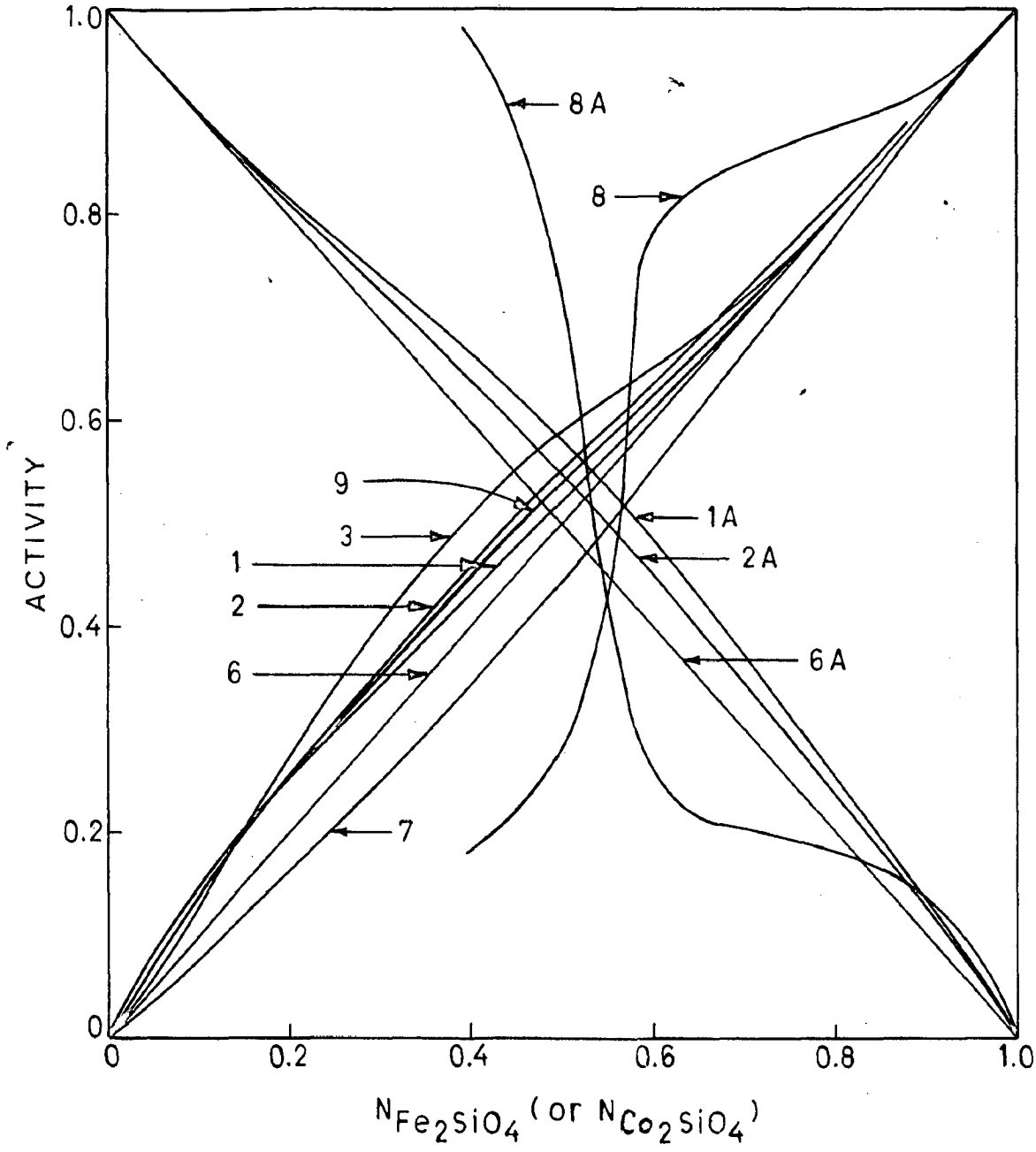

FIG. 5.4 ACTIVITY-COMPOSITION RELATIONS IN OLIVINE SOLID SOLUTIONS.

CHAPTER-6

CONCLUSIONS

From emf studies on the binary systems FeO-MgO, FeO-CaO and FeO-SiO_2 and ternary systems MgO-FeO-SiO_2 and MgO-FeO-CaO at 1000K, following conclusions are drawn

(1) FeO and MgO are miscible over the whole composition range and magnesiowustite solid solution exhibits considerable positive deviation from ideality at 1000K.

(2) FeO and CaO have limited solubility for each other and the system has a high positive deviation from ideality.

(3) Standard free energy of formation of $Ca_2Fe_2O_5$ from the component oxides CaO and FeO according to the reaction

$$2CaO + 3FeO = Ca_2Fe_2O_5 + Fe \qquad ----(6.1)$$

is -10.4 KJ/mole at 1000 K.

(4) Standard free energy of formation of Fe_2SiO_4 from its oxide components as determined from the emf studies on the binary system FeO-SiO_2 is -13.7 KJ/mole at 1000K.

(5) Nature of tie lines or lines of constant activity of FeO in different phase regions of the ternary system $MgO-FeO-SiO_2$ is revealed in Fig. 4.5.

(6) Standard free energies of formation of compounds "Fe SiO_3" and Fe_2SiO_4 from their component oxides, as calculated from the activity data on the ternary system $MgO-FeO-SiO_2$ at 1000K, are -6.35 KJ/ mole and -13.6 KJ/mole respectively.

(7) $(Fe,Mg)SiO_3$ and $(Fe,Mg)_2SiO_4$ solid solutions exhibit positive deviation from ideality at 1000K.

(8) Phase boundaries for the ternary system MgO-FeO -CaO at 1000K, as determined from the activity data on this system, are shown in Fig.4.21 .

(9) Nature of lines of constant activity for FeO, MgO and CaO (or tie lines) in different phase regions is shown in Figs. 4.21 -4.23 respectively for the ternary system MgO-FeO-CaO.

SUGGESTIONS FOR FURTHER WORK

Present study was conducted at 1000 K on binary and ternary oxide systems involving oxides FeO, MgO, CaO and SiO_2. Studies on these systems may be carried out at four or five different temperatures, in different suitable ranges, to get an information on the temperature dependence of activities of different components and to derive additional thermodynamic data on these systems. As the systems encountered in actual practice are complex, the experimental studies may be extended to quaternary system FeO-MgO-CaO-SiO_2. Pyroxene and olivine solid solutions involving three or four different cations may also be studied.

REFERENCES

1. O.Kubaschewski, E.L.Evans and C.B.Alcock, 'Metallurgical Thermochemistry', (1967), Pergamon Press, Oxford.

2. J.O'M. Bockris, J.L.White and J.D.Mackenzie, Eds., 'Physico-Chemical Measurements at High Temperatures', (1959), Butterworths, London.

3. R.F.Bunshah, Chief Ed., 'Techniques in Metal Research', Vol. IV, Pt. I and II, 'Physico-Chemical Measurements in Metal Research', R.A.Rapp, Ed., (1970), Interscience Publishers.

4. C.Wagner and A.Werner, J.Electrochem. Soc., Vol. 110, 1963, p 326.

5. G.N.Lewis and C.A.Kraus, J.Am. Chem. Soc., Vol. 32, 1910, p 1459.

6. James L.Broadhead, 'Zinc in the 1980's', in 'Lead-Zinc-Tin 80', (Proc. Conf.), T.M.S./A.I.M.E., 'World Symp. on Metallurgy and Environmental Control', Eds.-John. F. Cigan, Thomas S.Mackey and Thomas J. O'Keefe, Feb. 1980, p 13.

7. A.Olander, J.Am. Chem. Soc., Vol. 54, 1932, p 3819.

8. J.A.Yanko, A.E.Drake and F.Hovorka, Trans. Electrochem. Soc., Vol. 89, 1946, p 357.

9. J.F.Elliot and J.Chipman, Trans. Faraday Soc., Vol. 47, 1951, p 138.

10. J.J.Egan, Acta Met., Vol. 7, 1959, p 560.

11. H.S.Stricler and H.Seltz, J.Am. Chem. Soc., Vol. 58, 1936, p 2084.

12. H.Seltz and F.J.Dunkerley, J.Am. Chem. Soc., Vol. 64, 1942, p 1392.

13. O.J.Kleppa, J.Am. Chem. Soc., Vol. 74, 1952, p 6052.

14. N.W.Taylor, J.Am. Chem. Soc., Vol. 45, 1923, p 2865.

15. H.Seltz and B.J.Dewitt, J.Am. Chem. Soc., Vol. 60, 1938, p 1305.

16. R.A.Oriani, Acta Met., Vol. 1, 1953, p 144.

17. J.F.Elliot and J.Chipman, J.Am. Chem. Soc., Vol. 73, 1951, p 2862.

18. H.Seltz and B.J.Dewitt, J.Am. Chem. Soc., Vol. 61, 1939, p 2594.

19. C.S.Sivarama Krishna and M.L.Kapoor, N.M.L. Tech. Jl., Vol. 20, 1978, p 20.

20. J.V.Gluck and R.D.Pehlke, Trans. Met. Soc. AIME, Vol.233, 1965, p 233.

21. R.L.Louvet, J.V.Gluck and R.D.Pehlke, Trans. Met. Soc., AIME, Vol. 242, 1968, p 2369.

22. S.T.Cleveland, K.O. Kajima and R.D.Pehlke, J.Phys. Chem., Vol. 69(12), 1965, p 4085.

23. W.Ptak and Z.Moser, Trans. Met. Soc. AIME, Vol. 242, 1968, p 558.

24. R.A.Oriani, Acta Met., Vol. 4, 1956, p 15.

25. A.Watcher, J.Am. Chem. Soc., Vol. 54, 1932, p 4609.

26. J.N.Pratt, Trans. Faraday Soc., Vol. 56, 1960, p 975.

27. T.C.Wilder, Trans. Met. Soc. AIME, Vol. 233, 1965, p 1202.

28. T.C.Wilder and J.F.Elliot, J.Electrochem. Soc., Vol. 107(7), 1960, p 628.

29. V.N.Eremenko, Zhur. Fiz. Khim., Vol. 34(7), 1960, p 1495 (Met. A., 1961, 28, 575).

30. T.S.Nozaki, M.Shimoji and K.Niwa, Ber. Busenges, Vol. 70(2), 1966, p 207 (Met.A., 1966, 1, 1343).

31. A.Yazawa and Y.K.Lee, Nippon Kinzoku Gakkai-Si, Vol.33(3), 1969, p 318 (Met. A., 6910-151066).

32. A.V.Klibus et al., Trudy. Inst. Met. Sverdlovsk, Vol. 55, 1969, p 1183 (Met. A., 7002-150080).

33. M.M.Tsyplakova et al., Zhur. Priklad. Khim., Vol.42(11), 1969, p 2498 (Met. A., 7007-150617).

34. Hideoki Hoshino et al., Ber. Bunsenges, Vol. 69(2), 1965, p 114(Met. A., 1966, 1, 516).

35. R.A.Vecher et al., Doklady Akad. Nauk. SSSR, Vol.164(4), 1965, p 835, (Met. A., 1966, 1, 517).

36. T.Nozaki, M. Shimoji and K.Niwa, Nippon Kinzoku Gakkai-Si, Vol. 30(1), 1966, p 7(Met. A., Nov. 1966, p 1848).

37. S.P.Yatsenko et al., Zhur, Priklad Khim., Vol. 42(3), 1969, p 605 (Met. A., 7001-150012).

38. A.G.Morachevsky et al., Izvest V.U.Z. Tsventnaya Met., 1970(2), p 97(Met. A., 7008-150919).

39. G.I.Batalin and V.S.Sudavtsova, Urkain. Khim.Zhur., Vol. 40(5), 1974, p 542, (Met. A. 7409-152000).

40. H.Sako and J.F.Elliot, Met. Trans., Sept. 1974(5),p 2063.

41. A.S.Abbasov and K.N.Mamedov, Izvest. Akad. Nauk, Azerb, SSR (Fiz-Tekhn), 1970(3), p 86 (Met. A., 7108-151070).

42. L.F.Kozin, R.Sh. Nigmetova and A.M.Dairova, Izvest. Akad. Nauk.SSSR Metally, Mar-Apr 1971(2), p 191 (Met.A. 7108-151090).

43. Y.K.Lee and A.Yazawa, Nippon Kinzoku Gakkai-Si, Vol.33 (3), 1969, p 323 (Met. A., 6910-151067).

44. J.F.Hillard, B.L.Averbach and M.Cohen, Acta Met., Vol. 2, 1954, p 621.

45. T.A.Trumbore, W.E.Wallace and R.S.Craig, J.Am. Chem. Soc., Vol. 74, 1952, p 132.

46. ibid, Vol. 76, 1954, p 6417.

47. F.Haber and A.Moser, Z.Elektrochem., Vol. 11, 1905,p 593.

48. M.Katayama, Z.Phys. Chem., Vol. 61(5), 1908, p 566.

49. W.D.Treadwell, Z.Elektrochem., Vol. 22, 1916, p 414.

50. R.W.Ure, J.Chem.Phys., Vol. 26(6), 1957, p 1363.

51. R.W.Taylor and H.Schmalzried, J.Phys. Chem., Vol.68(9), 1964, p 2444.

52. E.H.Dewing, Met. Trans., Vol.1(8), 1970, p 2211.

53. W.D.Treadwell and L.Terebesi, Helv. Chim. Acta, Vol.16, 1933, p 922.

54. K.Hauffe, Z.Elektrochem., Vol. 46, 1940, p 348.

55. M.F.Lantratov, Zhur. Fiz. Khim., Vol. 34(4), 1960, p 782 (Met. A., 1961 ,8, p 575).

56. S.Aronson and S.Lemont, J.Chem. Thermodynamics Vol.5(2), 1973, p 155 (Met A., 7306-151114).

57. O.Kubaschewski and O.Huchler, Z.Elektrochem. Vol.52(4), 1948, p 170.

58. A.L.Virek, ibid, Vol. 54(6), 1950, p 436.

59. M.Ohtani and K.Sanbongi, Tetsu-to-Hagane, Vol.49(1), 1963, p 22(Chem. Abs., 61, 15928).

60. S.P.Mitoff, J.Chem. Phys. Vol. 16(1), 1962, p 1383.

61. S.F.Pal'guev and A.D.Neuimin, Sov. Phys.-Solid State, Vol. 4(4), 1962, p 629.

62. C.B.Alcock,in Proc. Symp., 'Electromotive Force Measurements in High Temperature Systems', (Ed., C.B.Alcock), Instn. Mining Met.,London, 1968, p 109.

63. K.Kiukkola and C.Wagner, J.Electrochem. Soc., Vol.104, 1957, p 379; ibid, p 308.

64. H.Schmalzried, Z.Elektrochem., Vol. 66, 1962, p 572.

65. H.Schmalzried, Z.Phys. Chem.(Frankfurt), Vol. 38(12), 1963, p 87.

66. C.M.Sellars and F.Maak, Trans. Met.Soc. AIME, Vol. 236(4), 1966, p 457.

67. R.J.Fruehan, Met. Trans., Vol. 1(4), 1970, p 865.

68. J.Deleet and J.J.Egan, J.Less Common Metals, Vol. 59(2), 1978, p 229.

69. H.Fischbach, Z. Metallkd., Vol. 71(7), 1980, p 448.

70. M.Rievier and A.D.Pelton, J.Electrochem. Soc., Vol. 125(9), 1978, p 1377.

71. N.S.Choudhury, NASA Tech. Note 1973, NASA TN D-7322, 16 pp.

72. B.C.H.Steele, in Proc. Symp., 'Electromotive Force Measurements in High Temperature Systems', (Ed., C.B.Alcock) Instn. Mining Met., London, 1968, p 3.

73. L.Heyne, in 'Fast Ion Transport in Solids', (Ed., W.van Gool) p 123, North-Holland, Amsterdam (1973).

74. B.C.H.Steele and C.B.Alcock, Trans. Met. Soc. AIME, Vol. 233 (7), 1965, p 1359.

75. T.H.Etsell and S.N.Flengas, Chem. Rev., Vol. 70, 1970, p 339.

76. J.Stocker, Ann. Chim. (Paris), Vol. 5, 1960, p 1459.

77. W.D.Kingery, J.Pappis, M.E.Doty and D.C.Hill, J.Amer. Ceram. Soc., Vol. 42, 1959, p 393.

78. F.Hund, Z. Phys. Chem. (Leipzig), Vol. 199, 1952,p 142.

79. T.Y.Tien and E.C.Subbarao, J.Chem. Phys., Vol 39, 1963, p 1041.

80. A.M.Diness and R.Roy, Solid State Commun., Vol. 3, 1965, p 123.

81. J.B.Wachtman Jr. and W.C.Corwin, J.Res. Nat. Bur.Std., Vol. 69A, 1965, p 457.

82. F.A.Kroger, J.Amer.Ceram. Soc., Vol.49, 1966, p 215.

83. R.E.Carter and W.L.Roth, in Proc. Symp. 'Electromotive Force Measurements in High Temperature Systems', (Ed., C.B.Alcock), Instn. Mining, Met., London (1968). p 125.

84. Z.S.Volchenkova and S.F.Pal'guev, 'Electrochemistry of Molten and Solid Electrolytes', Vol. 1, Consultants Bureau, New York, N.Y. (1961), p 97.

85. A.Cocco and M.Danelon, Ann. Chim.(Rome), Vol. 55, 1965, p 1313.

86. T.Takahashi and Y.Suzuki, Denki Kagaku, Vol. 34, 1966, p 887.

87. T.Y.Tien, J.Appl. Phys., Vol. 35, 1964, p 122.

88. L.A.Simpson and R.E.Carter, J.Amer Ceram. Soc., Vol. 49, 1966, p 139.

89. W.H.Rhodes andR.E.Carter, ibid, Vol. 49, 1966, p 44.

90. H.H.Mobius, H.Witzmann and D.Gerlach, Z.Chem., Vol 4, 1964, p 154.

91. J.W.Patterson, E.C.Bogren,and R.A.Rapp, J.Electrochem. Soc., Vol. 114, 1967, p 752.

92. D.Yuan and F.A.Kroger, ibid, Vol. 116, 1969, p 594.

93. Y.D.Tretyakov, Izv. Akad. Nauk. SSSR, Neorg. Mater., Vol. 2, 1966, p 501; Inorg. Mater., Vol. 2, 1966, p 432.

94. H.Schmalzried, Z. Physik. Chem. N.F., Vol. 25, 1960,p178.

95. R.W.Vest and J.W.Patterson, 'Physics of Electronic Ceramics', Part A, (Ed., L.L.Hench and D.B.Dove), Marcel Dekker, Inc., New York (1972).

96. J.W.Patterson, J.Electrochem. Soc., Vol. 118(7),1971,p1033.

97. F.Hund and R.Mezger, Z. Phys. Chem. (Leipzig), Vol. 201, 1952, p 268.

98. H.Peters and H.H.Mobius, Z. Phys. Chem. (Leipzig), Vol. 209, 1958, p 298.

99. A.V.Ramana Rao and V.B.Tare, Scripta Met., Vol. 5, 1971, p 813.

100. G.G.Charette and S.N.Flengas, J.Electrochem. Soc., Vol. 115, 1968, p 796.

101. F.N.Mazandarany and R.D.Pehlke, J.Electrochem. Soc., Vol. 121(5), 1974, p 711.

102. E.S.Ramakrishnan, O.M.Sreedharan and M.S.Chandrasekharaiah, J.Electrochem. Soc., Vol. 122, 1975, p 328.

103. G.Rog, B.Langanke, G.Borchardt and H.Schmalzried, J.Chem. Thermodyn., Vol. 6(12), 1974,p 1113.

104. J.C.Cahn, C.B.Alcock and K.T.Jacob, Can. Met. Quart., Vol. 12, 1973, p 439.

105. K.T.Jacob and J.C.Cahn, J.Electrochem. Soc., Vol. 121 (4), 1974, p 534.

106. K.T.Jacob and C.B.Alcock, Met. Trans. B., Vol. 6B(2), 1975, p 215.

107. H.B.Bell, J.P.Hajra, F.H.Putland and P.J.Spencer, Met. Sci. J., Vol. 7, 1973, p 185.

108. K.P.Jagannathan and A.Ghosh, Met. Trans., Vol. 4, 1973, p 1577.

109. A.Kubik and C.B.Alcock, Met. Sci. J., Vol. 1,1967,p 19.

110. L.A.Pugliese and G.R.Fitterer, Met. Trans., Vol. 1, 1970, p 1997.

111. M.Rigaud, G.Giovannetti and M.Hone, J.Chem. Thermodyn., Vol. 6, 1974, p 993.

112. D.J.Cameron and A.E.Unger, Met. Trans., Vol. 1(9), 1970, p 2615.

113. J.S.Kachhwaha, M.P.Ganu and V.B.Tare, Scripta Met., Vol. 7, 1973, p 311.

114. V.B.Tare and B.Deo, Conf. Int. Thermodyn. Chim. (C.R.) 4^{th} , 1973, 3, p 104.

115. A.A.Lykasov and N.V.Kozheurova, Izv. V.U.Z.Chernaya Metall., 1980(4), p 10 (Met. A., 8104-440095).

116. B.Indyk and H.B.Bell,J.Iron Steel Inst., Vol. 208, 1970, p 1015.

117. C.Wagner, in 'Progress in Solid State Chemistry', Vol. 6, (Ed., H.Reiss and J.O.McCaldin), Pergamon Press, London, 1971, p 1.

118. T.Oishi, Z.Kozuka and J.Moriyama, Trans. Japan Inst. Metals, Vol. 12(6), 1971, p 410.

119. T.C.Wilder, Trans. Met. Soc. AIME, Vol. 236(7), 1966, p 1035.

120. R.J.Fruehan, L.J.Martonik and E.T.Turkdogan, Trans. Met. Soc. AIME, Vol. 245, 1969, p 1501.

121. R.A.Rapp, Trans. Met. Soc. AIME, Vol. 245(8), 1969, p 1711.

122. V.B.Tare and H.Schmalzried, Trans. Met. Soc. AIME, Vol. 236(4), 1966, p 444.

123. J.Weissbart and R.Ruka, J.Electrochem. Soc., Vol.109 (8), 1962, p 723.

124. E.Zintle and A.Udgard, Z.Anorg. Allg. Chemie, Vol.290, 1939, p 150.

125. J.Short and R.Roy, J.Chem. Phys., Vol.67, 1963,p 1860.

126. E.Barsis and A.Taylor, J.Chem. Phys., 1966, p 1154.

127. C.Wagner, J.Electrochem. Soc., Vol. 115, 1968, p 933.

128. H.Matzke, J.Mater. Sci., Vol. 5(10), 1970, p 831.

129. H.S.Ray, C.Roy, R.S.Sharma and G.N.K.Iyengar, J.Electrochem. Soc. India, Vol. 22,(4), 1973, p 315.

130. M.F.Berard, J.Amer.Ceram. Soc., Vol. 54(5), 1971, p 144.

131. J.M.Short and R.Roy, J.Phys. Chem., Vol. 68(10), 1964, p 3077.

132. M.E.Baker and A.Taylor, J.Phys. Chem. Solids, Vol. 30(4), 1969, p 1003.

133. H.Matzke and R.Lindner, Z.Naturforsch., Vol. 19a, 1964, p 1178.

134. R.J.Hawkins and C.B.Alcock, in Proc. Symp. on 'Thermodynamics: Vol. II', Atomic Energy Agency, Vienna, 1965.

135. J.W.Hinze and J.W.Patterson, J.Electrochem. Soc., Vol. 120(1), 1973, p 96.

136. U.Croatto and M.Bruno, Gazz. Chim. Ital., Vol. 78, 1948, p 95.

137. C.Tubandt, H.Reinhold and G.Leibold, Z.Anorg. Allg. Chemie, Vol. 197, 1931, p 225.

138. A.B.Mireille,L.Carlo, B.Pierre and D.Monique, C.R. Acad. Sci, Paris, Ser. A., B, Vol. 264B(11),1967,p 875.

139. F.K.Volynets and G.N.Dronova, Fiz. Tverd. Tela., Vol. 11, 1969, p 1867.

140. A.Barriere, Y.Danto and J.Salardenna, Thin Solid Films, Vol. 16(2), 1973, p S13.

141. V.V.Gorlach and V.M.Lisitsyn, Fiz. Tverd, Tela (Leningrad), Vol. 16(7), 1974, p 1988.

142. E.Zintle and U.Croatto, Z.Anorg. Allg. Chemie, Vol. 242, 1939, p 79.

143. Ya. I.Gerasimov, I.A.Vasil'eva, T.P.Chusova, V.A.Geiderikh and M.A.Timofuva, Russ.J. Phy.Chem., Vol. 36, 1962, p 180.

144. H.Schmalzried, Z.Phy. Chem., Vol. 25, 1960, p 178.

145. R.Benz and H.Schmalzried, Z.Phy. Chem., Vol.29, 1961, p 77.

146. R.A.Rapp, Trans. Met. Soc. AIME, Vol. 227, 1963 p 371.

147. W.G.Bugden and J.N.Pratt, Instn. Min. Met., Trans., Sect. C., Vol. 79, 1970, p C221.

148. Discussion on the 'EMF Measurements', Session 'Thermodynamics', Vienna, IREA (1965).

149. K.Goto and Y.Matsushita, J.Electrochem. Soc. Japan, Vol. 35, 1967, p 1.

150. C.Petot, E.G.Petot and M.Rigaud, Can. Met. Quart, Vol. 10, 1971, p 203.

151. A.Muan and E.F.Osborn, 'Phase Equilibria among Oxides in Steelmaking' Addison - Wesley Publishing Co., Inc., Reading, Mass., 1965.

152. A.V.Shashkina and Ya.I.Gerasimov, Zhur. Fiz. Khim., Vol. 27, 1953, p 399.

153. N.G.Schmahl, B.Frisch and G.Stock, Arch. Eisenhuttenw., Vol. 32, 1961, p 297.

154. W.C.Hahn and A.Muan, Trans. Met. Soc. AIME, Vol. 224, 1962, p 416.

155. Yu.A.Korneev, V.F.Balakirev, A.N.Men and G.I.Chufarov, Zhur. Fiz. Khim., Vol. 39(10), 1965, p 2625.

156. K.K.Prasad, Ph.D.Thesis, Indian Institute of Science, Bangalore (1971).

157. I.V.Gordeev, Yu.D.Tretyakov and K.G.Khomyakov, Vestn. Mosk. Univ., Ser.II, Khim., Vol.18(6), 1963, p 59.

158. H.J.Engell, Z.Physik, Chem.(Frankfurt), Vol. 35, 1962, p 192.

159. M.Sakawa, S.G.Whiteway and C.R.Masson, Trans. Iron Steel Inst. Japan, Vol. 18, 1978, p 173.

160. R.E.Johnson and A.Muan, Trans. Met. Soc. AIME, Vol. 239, 1967, p 1931.

161. W.C.Hahn, Jr., Ph.D.Thesis, Pennsylvania State University, 1960 (Diss. Abs., 21, 163).

162. Shiro Ban-ya, A.Chiba and A.Hilosaka, Tetsu to Hagane, Vol. 66(10), 1980, p 1493, (Chem. Abs., 93: 156609 m).

163. J.H.Andrews et al., J.Iron Steel Inst., Vol. 124(2), 1931, p 283.

164. A.H.Jay and K.W.Andrews, J.Iron Steel Inst., Vol.152 (2), 1945, p 15.

165. P.K.Foster and A.F.E.Welch, Trans. Faraday Soc., Vol. 52, 1956, p 1626.

166. ibid, p 1636.

167. R.Schenck et al., Anorg. Allg. Chemie, Vol. 184, 1929, p 1.

168. K.Schwerdtfeger and A.Muan, Trans. Met. Soc. AIME, Vol. 239(8), 1967, p 1114.

169. T.D.Takenov et al., Dokl. Akad. Nauk SSSR, Vol.165(6), 1965, p 1325.

170. B.D.Averbukh et al., Russ. J.Phys. Chem., Vol.36(11), p 1320.

171. S.Seetharaman, Ph.D.Thesis, Indian Institute of Science, Bangalore (1971).

172. E.Aukrust and A.Muan, Trans. Met. Soc. AIME, Vol. 227(12), 1963, p 1378.

173. S.Seetharaman and K.P.Abraham, Trans. Indian Inst. Metals, Vol. 25(2), 1972, p 16.

174. Natta and L.Passerini, Gazz. Chim. Ital., Vol. 59, 1929, p 139 (Chem. Abs., 23:4124[8]).

175. S.Raghavan, Ph.D.Thesis, Indian Institute of Science, Bangalore (1977).

176. L.Passerini, Gazz. Chim. Ital., Vol. 59, 1929, p 144.

177. S.Holgersson and A.Karlsson, Z. Anorg. Allg.Chemie, Vol. 182, 1929, p 255.

178. W.C.Hahn and A.Muan, J.Phys. Chem. Solids, Vol. 19, 1961, p 338.

179. S.Seetharaman and K.P.Abraham, Indian J.Technology, Vol. 5, 1968, p 123.

180. E.Woermann and A.Muan; Mater. Res. Bull., Vol. 5(10), 1970, p 779.

181. W.C.Hahn and A.Muan, Mater. Res. Bull., Vol. 5(11), 1970, p 955.

182. F.P.Glasser, J.Amer. Ceram. Soc., Vol. 45, 1962, p 242.

183. N.Tiberg and A.Muan, Met. Trans., Vol.1, 1970, p 435.

184. S.Seetharaman and K.P.Abraham, J.Electrochem. Soc. India, Vol. 20, 1971, p 54.

185. S.Seetharaman and K.P.Abraham, Scripta Met., Vol. 3, 1969, p 911.

186. S.Seetharaman and K.P.Abraham, Trans. Instn. Min. Met., Sect. C., Vol. 77, 1968, p C209.

187. N.L.Bowen and O.Andersen, Amer.J. Sci., Vol.187, 1914, p 487.

188. J.W.Greig, Amer. J.Sci.,Vol. 213, 1927, p 1; p 133.

189. N.L.Bowen and J.F.Schairer, Amer. J.Sci., Vol. 229, 1935, p 151.

190. F.D.Richardson, Trans. Faraday Soc., Vol. 52,1956.p 1312.

191. Th.G.Sahama and D.R.Torgeson, U.S.Bur. Mines Rep. Invest. 4408.

192. K.Kitayama and T.Katsura, Bull.Chem.Soc. Japan, Vol. 41(5), 1968, p 1146.

193. A.Muan, R.H.Nafziger and P.L.Roeder, Nature, Vol. 202, 1964, p 688.

194. R.H.Nafziger and A.Muan, Amer.Mineralogist, Vol. 52, 1967, p 1364.

195. Y.Kojima et al., Arch. Eisenhuttenw., Vol. 40(1),1969, p 37(Met. A., 6908-440185).

196. N.L.Bowen, J.F.Schairer and E.Posnjak, Amer. J.Sci., Vol. 26, 1933, p 193.

197. W.C.Allen and R.B.Snow, J.Amer. Cer. Soc., Vol. 38, 1955, p 264.

198. K.L.Fetters and J.Chipman, Trans. Met. Soc. AIME, Vol. 145, 1941, p 95.

199. C.R.Taylor and J.Chipman, Trans. Met. Soc. AIME, Vol. 154, 1943, p 228.

200. F.D.Richardson, 'Physical Chemistry of Melts in Metallurgy', Vol. 1, Academic Press, London, 1974.

201. H.Flood and J.M.Toguri, Trans. Met. Soc. AIME, Vol. 227, 1963, p 525.

202. J.F.Elliott, J.Metals, Vol. 7, 1955. p 485

203. H.V.Ende et al., Stahl Eisen, Vol. 82, 1962, p 1027.

204. L.G.Lavrov and M.M.Lakermik, Sbornik Nauchn. Trudy Gos. Nauchn.-issled. Inst. Tsvetn. Met., 1965,(23), p 5(Met. A., 1966, p 1260).

205. T.P.Floridis and W.S.Moser, Met. Trans., Vol. 3(3), 1972, p 738.

206. Y.Wanibe et al., Arch. Eisenhuttenw., Vol. 44(9), 1973, p 711.

207. P.V.Riboud and A.Muan, Trans. Met. Soc., AIME, Vol. 224, 1962, p 27.

208. K.Schwerdtfeger and A.Muan, Trans. Met. Soc. AIME, Vol. 236, 1966, p 201.

209. H.Fujita and S.Maruhashi, Tetsu to Hagane, Vol. 56, 1970, p 830 (Met. A., 7101-440029).

210. M.R.Kalyanram, T.G.Macfarlane and H.B.Bell, J.Iron and Steel Inst., Vol. 195, May 1960, p 58.

211. D.Henderson and J.Taylor, J.Iron and Steel Inst. Vol. 204(1), 1966, p 39.

212. K.Sawamura, Tetsu to Hagane, Vol. 48, 1962, p 8 (Chem. Abs., 58: 2198 h).

213. K.P.Abraham, M.W.Davies and F.D.Richardson, J.Iron Steel Inst., Vol. 196, 1960, p 82.

214. T.C.M.Pillay and F.D.Richardson, Trans. Instn. Min. Met., Vol. 66, 1956-57, p 309.

215. M.L.Kapoor and M.G.Frohberg, Met. Trans. B, Vol.8B, 1977, p 15.

216. C.Brisi and A.Burdese, Ricerca Sci., Vol. 22(3), 1952, p 348(Chem. Abs., 48:11173 d).

217. R.E.Johnson and A.Muan, J.Amer. Ceram. Soc., Vol.48(7), 1965, p 359.

218. O.Valla, K.Grjotheim and A.Muan, Trans. Met. Soc. AIME, Vol. 242, 1968, p 2389.

219. L.S.Darken and R.W.Gurry, 'Physical Chemistry of Metals', (1953), McGraw-Hill Book Co., Inc.,New York, p 264.

220. J.F.Elliott, M.Gleiser and V.Ramakrishna, 'Thermochemistry for Steelmaking', Vol. II, (1963), Addison-Wesley Publishing Co., Inc., Massachusetts.

221. F.D.Richardson, J.H.E.Jeffes and G.Withers, J.Iron Steel Inst, Vol. 166, 1950, p 213.

222. R.W.Taylor and H.Schmalzried, J.Phys. Chem., Vol.68(9), 1964, p 2244.

223. K.Kitayama and T.Katsura, Bull. Chem.Soc. Japan, Vol. 41(2), 1968, p 525.

224. J.V.Biggers and A.Muan, J.Amer. Ceram. Soc., Vol. 50, 1967, p 230.

225. D.P.Masse, E.Rosen and A.Muan, J.Amer. Ceram. Soc., Vol. 49, 1966, p 328.

226. S.K.Saxena, 'Thermodynamics of Rock-Forming Crystalline Solutions', Springer-Verlag, Berlin, 1973, p 98.

227. P.Herasymenko, Trans. Faraday Soc., Vol. 35,1938,p 1245.

228. H.Flood, T.Forland and K.Grjotheim, Phys.Chem. Melts Symp. Molten Slags and Salts. Instn.Mining Met., London, 1953, p 46.

229. M.Temkin, Acta Physicochimica USSR, Vol.20(4), 1945, p 411.

230. H.Flood, T.Forland and K.Grjotheim, Z.Anorg. Allg. Chemie, Vol. 276, 1954, p 289.

231. M.L.Kapoor, International Metallurgical Reviews, Vol. 20, 1975, p 150.

232. E.A.Guggenheim, Proc. Roy.Soc., Ser.A, Vol. 148, 1935, p 304.

233. R.H.Fowler and E.A.Guggenheim, Proc. Roy. Soc., Ser.A, Vol. 174, 1940, p 189.

234. J.A.Wasastjerna, Soc. Sci., Fenn., Comment. Phys.-Math., Vol. 15(3), 1949, p 1.

235. V.Hovi, Soc. Sci. Fenn., Comment. Phys.-Math., Vol. 15(12), 1950, p1.

236. J.Friedel, Advan. Phy., Vol. 3, 1954, p 446.

237. J.D.Dunitz and L.E.Orgel, J.Phys. Chem. Solids, Vol. 3, 1957, p 318.

238. F.C.M.Driessens, Ber. Bunsenges, Phys. Chem., Vol. 72(7), 1968, p 764.

. S.Seetharaman, K.K.Prasad and K.P.Abraham, Indian J. Technology, Vol. 11(11), 1973, p 585.

. E.Aukrust and A.Muan, Trans. Met. Soc. AIME, Vol.230, 1964, p 1395.